COLLAGEN AND FIBRIN BIOPOLYMER MICROTHREADS FOR BIOENGINEERED LIGAMENT REGNERATION

A Dissertation
Submitted to the Faculty
of the
WORCESTER POLYTECHNIC INSTITUTE
and
THE UNIVERSITY OF MASSACHUSETTS MEDICAL SCHOOL
in partial fulfillment of the requirements for the
Degree of Doctor of Philosophy
in
Biomedical Engineering and Medical Physics
May 2007
by

Kevin G. Cornwell

APPROVED:

George D. Pins, Ph.D
Associate Professor, Advisor
Biomedical Engineering Department
Worcester Polytechnic Institute

Paul Fanning, Ph.D.
Research Assistant Professor
Orthopedics and Cell Biology
University of Massachusetts Medical School

Kristen L. Billiar, Ph.D.
Assistant Professor
Biomedical Engineering Department
Worcester Polytechnic Institute

Peter Grigg, Ph.D.
Research Assistant Professor
Department of Physiology, Chair
University of Massachusetts Medical School

Glenn R. Gaudette, Ph.D.
Assistant Professor
Biomedical Engineering Department
Worcester Polytechnic Institute

Karl Helmer, Ph.D.
Athinoula A Martinos Center
for Biomedical Imaging
Massachusetts General Hospital

Acknowledgments

I would like to thank my advisor, George Pins, who has continually encouraged me to explore and grow as a researcher. His door has always been open, even when we both knew it probably should have stayed closed. Thank you for your support and guidance. You've been both a mentor and a friend.

I would also like to thank my committee members for their guidance and help in directing this dissertation. And a special thanks to a couple of you for keeping the errant elbows to a minimum, and for improving my shot blocking ability.

I'd like to thank the many undergraduates who contributed to this research during work study, summer research, and REU, especially Jason Robinson, Erica Levorson, Shawn Carey, Kirsten Kinneberg, and Gharam Han.

I would like to thank my fellow graduate students, Katie Bush, Brett Downing, and Angie Throm. I wouldn't have made it through the endless hours in the lab without your help and friendship.

Last but not least, I'd like to thank wife, Shannon, and soon to be born son, Conor. Without your endless support and understanding, none of this would have been possible. Without you I'd be lost. Figuratively and literally.

Abstract

Rupture of the anterior cruciate ligament (ACL) of the knee leads to chronic joint instability and reduced range of motion while the long term results are marred by a high prevalence of degenerative joint disease especially osteoarthritis. Bundles of collagen threads have been widely investigated for the repair of torn ACL, but are limited by insufficient tissue ingrowth to repopulate and completely regenerate these grafts. We have developed a novel *in vitro* method of characterizing fiber-based thread matrices by probing their ability to promote tissue ingrowth from a wound margin as a measure of their ability to promote repopulation and regeneration. This method is useful in the optimization of thread scaffolds, and is sensitive enough to distinguish between subtle variations in biopolymer chemistry and organization. Furthermore, this method was used to characterize the effects of crosslinking on the cell outgrowth and correlated the findings with the mechanical properties of collagen threads. The results suggest that crosslinking is required to achieve sufficient mechanical properties for high stress applications such as ACL replacement, but regardless of technique, crosslinking attenuated the cell outgrowth properties of the threads. To improve the regenerative capacity of these scaffolds, novel fibrin microthread matrices were developed with a similar morphology to collagen threads and sufficient mechanical strength to be incorporated in composite thread scaffold systems. These fibrin microthreads were loaded with FGF-2, a potent mitogen and chemotactic agent that works synergistically with fibrin in regulating cell signaling and gene expression. Increases in fibroblast migration and proliferation in FGF-2-loaded fibrin threads were successfully demonstrated with the concomitant promotion of oriented, aligned, spindle-like fibroblast morphology. These results suggest that fibrin-FGF-2 microthreads have distinct advantages as a biomaterial for the rapid regeneration of injured tissues such as the ACL.

TABLE OF CONTENTS

Chapter 1: Overview....1
Chapter 2: Background....7
2.1 Anterior Cruciate Ligament (ACL)....7
2.1.1 Healthy ACL....7
2.1.1.1 ACL Composition....9
Matrix....9
Cells....11
2.1.1.2 ACL Injury and Repair....11
Clinical Significance....11
Surgical Repair....12
2.1.1.3 ACL Healing....13
Stages of Ligament Wound Healing....14
2.1.1.4 ACL Regeneration....15
2.2 Thread Scaffolds for ACL Repair....16
2.2.1 Synthetic Polymers....16
2.2.2 Biopolymer Threads....17
2.2.2.1 Collagen Threads....17
Self-Assembly of Type I Collagen Threads....18
Collagen Crosslinking....19
2.2.2.2 Other Novel Biopolymer Threads....22
2.3 Extracellular Matrix (ECM)....22
2.3.1 Integrins and Matrix Signaling....23
2.3.2 ECM in Wound Healing....24
2.4 Fibrin, FGF-2, and the Provisional Matrix....24
2.4.1 Fibrin Provisional Matrix....24
2.4.2 Fibrin....25
2.4.2.1 Fibrin Biomaterials....25
2.4.3 FGF-2....26
2.4.3.1 ECM and FGF-2 Combinatorial Signaling....27
2.4.3.2 FGF-2 In Tendon/Ligament....28
2.5 Migration in Wound Healing....29
2.5.1 Mechanics of Cell Migration....29
2.5.2 Stimuli of Cell Migration....30
2.5.3 In Vitro Models of Cell Migration....31
Chapter 3: Cell Outgrowth Bioassay:
Development of an in vitro method of characterizing tissue ingrowth on discrete threads.
....41
3.1 Introduction....41
3.2 Materials and Methods....43
3.2.1 Preparation of Collagen Solutions....43

3.2.2 Collagen Thread Extrusion 43
3.2.3 Fibroblast Culture....44
3.2.4 Genetically Modified Fibroblasts....45
3.2.4.1 Retrovirus production and cell culture....45
3.2.4.2 Retroviral Transduction....45
3.2.5 Cell Outgrowth Bioassay....46
3.2.5.1 Construction....46
3.2.5.2 Cell Seeding....47
3.2.5.3 Measurement....47
3.2.6 Inhibition of Proliferation....47
3.2.7 Statistical Analyses....48
3.3 Results....48
3.3.1 Imaging....48
3.3.2 Metric Development....49
3.3.3 Additional Model Considerations....50
3.3.4 Effect of Collagen Source and Crosslinking....51
3.4 Discussion....52
Chapter 4: Optimized Self-Assembled Collagen Microthreads:
Effect of crosslinking on collagen microthread strength and cell outgrowth....59
4.1 Introduction....59
4.2 Materials and Methods....61
4.2.1 Production of Self-Assembled Collagen Threads....61
4.2.1.1 Preparation of acid soluble collagen 61
4.2.1.2 Collagen thread extrusion....61
4.2.1.3 Collagen Thread Crosslinking....62
4.2.2 Swelling Ratio and Crosslink Density Calculations....62
4.2.3 Mechanical Testing of Collagen Threads....63
4.2.4 Enzymatic Degradation of Crosslinked Collagen Threads....64
4.2.5 Cell Outgrowth Bioassay....65
4.2.6 Fibronectin Adsorption on Collagen Threads....66
4.2.7 Statistical Analyses....66
4.3 Results....67
4.3.1 The Mechanical Properties of Self-Assembled Collagen Threads are Enhanced by Crosslinking....67
4.3.2 Crosslink Densities Correlate with Ultimate Tensile Strengths of Threads....68
4.3.3 Crosslinking Affects the In Vitro Enzymatic Stability of the Collagen Threads 69
4.3.4 Cell Outgrowth Is Decreased On Crosslinked Threads....70
4.3.5 Fibronectin Adsorption to Collagen Threads is Dependent on Crosslinking Technique 71
4.4 Discussion....71
Chapter 5: Fibrin Microthreads:
Development of novel fibrin microthreads with comparable properties to collagen threads 77

5.1 Introduction....77
5.2 Materials and Methods....79
5.2.1 Fibrin Microthread Manufacturing....79
5.2.1.1 Material Preparation....79
5.2.1.2 Coextrusion....79
5.2.2 Microthread Material Characterization....81
5.2.2.1 Scanning Electron Microscopy (SEM)....81
5.2.2.2 Thread Swelling....81
5.2.2.3 Mechanical Properties....81
5.2.3 Statistical Analyses....83
5.3 Results....83
5.3.1 Effect of Rate Ratio Variation....84
5.3.2 Effect of Bath pH and Temperature....84
5.3.3 Fibrin Microthread Morphology....85
5.4 Discussion....85
Chapter 6: Cellular Interactions on FGF-loaded Fibrin Microthreads:
Effect of coextruded fgf-fibrin threads on fibroblast alignment, proliferation, and migration....91
6.1 Introduction....91
6.2 Materials and Methods....93
6.2.1 Fibrin Microthread Manufacture....93
6.2.2 Cell Culture....94
6.2.3 Attachment and Proliferation....94
6.2.3.1 Thread Bundle Seeding and Culture....94
6.2.3.2 Cell Count Quantification....96
6.2.4 Cell Outgrowth....96
6.2.5 Fixing and Staining....97
6.2.6 Scanning Electron Microscopy (SEM)....97
6.2.7 Statistical Analyses....98
6.3 Results....99
6.3.1 Attachment....99
6.3.2 Proliferation....99
6.3.3 Cell Outgrowth....100
6.3.4 Cell and Cytoskeletal Alignment....101
6.4 Discussion....103
Chapter 7: Discussion and Future Work:
Biopolymer Microthreads....107
7.1 Overview....107
7.2 Biopolymer Threads for ACL Regeneration....108
7.3 Method of Characterization....109
7.4 Fibrin Biopolymer Microthreads....111
7.5 Future Work....112
7.5.1 Biomaterial Development....112
7.5.2 Cell-Matrix Interactions....113

7.5.3 Alternative Applications.....114
7.6 Conclusions.....115
Appendix A: Automated Extrusion Device a1
Appendix B: Micromechanical Testing Device.....b1

TABLE OF FIGURES

Drawing of the Right Knee....7
Ligament Forces During Gait....8
Normal Properties of Human ACL....9
Tendon Heirarchy....10
BPTB Autograft....12
Phases of Lig Wound Healing....15
Synthetic Graft Failure....16
Collagen Self-Assembly....18
Table of Collagen Thread Research....20
Table of Collagen Thread Research (cont.)....21
Matrix Signaling Schematic....23
Fibrin Assembly....26
FGF-2 Structure....27
Cell Migration Phases....30
Cell Speed vs Substratum Adhesiveness....31
Bioassay Schematic....44
Images of Bioassay....46
GFP vs Fura-2....48
Fura-2 Migration Images....49
Color Fura Thread Images....50
Migration Metric....51
Migration or Proliferation....52
Cellular Outgrowth Velocity - Self-assembled vs Insoluble....53
Culluar Outgrowth Velocity - Self-assembled vs Controls....54
Ceullar Outgrowth Velocity with Crosslinking....55
Collagen Thread Characteristic Stress Strain Curves....64
UTS With Crosslinking....65
Properties of Collagen Threads With Crosslinking Table....66
Mechanical Properties of Collagen Threads With Crosslinking Table....66
Modulus of Collagen Threads With Crosslinking....67
Strain To Failure of Collagen Threads With Crosslinking....68
Swelling Ratio of Collagen Threads With Crosslinking....69
Crosslink Density Correlates With UTS....70
Degradation of Collagen Threads With Crosslinking....71
Cellar Outgrowth Velocity with Crosslinking....72
Fibronectin Adsorption With Crosslinking....73
Tensile Strength Correlates With Cellular Outgrowth....74
Coextrusion Schematic for Fibrin Microthreads....80
Characteristic Stress Strain Curves of Fibrin Microthreads....82
Effect of Rate Ratio on UTS and Load at Failure for Fibrin Microthreads....83

Effect of Rate Ratio on Wet Diameter and SAF for Fibrin Microthreads.....84
Effects of pH and Temp on Fibrin Microthread UTS.....85
Collagen vs Fibrin Table.....86
SEM of Fibrin and Collagen Microthreads.....87
Proliferation Quantification.....95
Attachment to Fibrin Microthreads with Increasing FGF-2.....98
Proliferation on Fibrin Microthreads with FGF-2 and Time.....99
Proliferation with FGF-2, Total Cell Number (Day 5 and 7).....100
Fold Increase in Proliferation with Increasing FGF-2 and Time.....101
Effect of FGF-2 On Cell Outgrowth.....101
Alignment - Phalloidin.....102
Alignment - SEM.....103
Attachment Live/Dead.....104
Proliferation Live/Dead.....105

TABLE OF TABLES

Geometry and Mechanical Properties of Normal ACL.....9
Phases of Ligament Wound healing.....15
Collagen Thread Research.....20-21
Swelling, Molecular Weight Between Crosslinks, and Crosslink Density of Crosslinked Collagen Threads.....66
Mechanical Properties of Collagen Threads with Crosslinking.....66
Collagen Versus Fibrin Comparison Chart.....86

CHAPTER 1: OVERVIEW

Rupture of the anterior cruciate ligament (ACL) of the knee leads to chronic joint instability and reduced range of motion while the long term results are marred by a high prevalence of degenerative joint disease especially osteoarthritis.[1, 2] The ACL has limited intrinsic regenerative capacity necessitating surgical repair, typically utilizing autografts which are limited by the need for a secondary surgical/donor site and still lead to laxity or possible secondary revision surgery.[3, 4] Functional tissue engineering methods have been suggested as a means for achieving the ideal replacement of ACL, however, no tissue engineered ACL has reached clinical trials due to a need for a readily available cell source and adequate biomaterial scaffolds.[5] Furthermore, the research and development of implants is in need of quantitative *in vitro* and *in vivo* methods of characterization.[5] Therefore, our goal is to develop and characterize biomaterials for ligament regeneration.

PART I: COLLAGEN THREADS FOR LIGAMENT REGENERATION

Threads composed of type I collagen, the native structural protein of tendons and ligaments, have been widely investigated for ACL regeneration. Bundles of threads or fibers extruded from dispersions of acid-insoluble collagen demonstrated strengths similar to native tendon and ligament tissues with crosslinking[6-17] and induced neotendon and neoligament formation[15, 18-20] during *in vivo* implantation studies. However, functional regeneration of collagen-based ligament grafts was impeded by

insufficient tissue ingrowth from the wound margin to completely repopulate the graft, remodel, and regenerate the tissue.[9] Furthermore, the cellular infiltration into the grafts was inconsistent and difficult to control.[9] Self-assembled type I collagen threads were developed with an increased biomimetic substructure. These threads, self-assembled from solutions of acid soluble collagen, possess a fibrillar substructure marked by a D periodic banding pattern[21] and mechanical properties comparable to native ligament with crosslinking.[22] While these self assembled collagen biomaterials offer considerable promise as scaffolds for ligament regeneration, their strength and tissue ingrowth characteristics for ligament regeneration have yet to be determined.

Therefore, the first goal of this thesis was to develop an in vitro *method to quantitatively characterize tissue ingrowth, in order to assess the utility of thread scaffolds for ACL tissue regeneration.*

The development of a novel method for quantitatively characterizing tissue ingrowth on the surface of collagen thread scaffolds is discussed in Chapter 3. Threads were suspended across elevated platforms seeded with fibroblast-populated collagen lattices. Fibroblast populations were visualized and imaged on each discrete thread and the distance to the furthest cell was measured at time intervals. Evaluation of this metric, termed cellular outgrowth velocity, showed similar velocities between self-assembled collagen threads and native tendon controls. Furthermore, increased cellular outgrowth was seen on self-assembled type I collagen threads relative to the first generation of collagen threads derived from insoluble collagen. However, these rates were attenuated on threads crosslinked by a dehydrothermal treatment (DHT) commonly employed for increasing *in vivo* stability. This novel in vitro model system allows examination of tissue ingrowth from a wound margin onto biomaterials to determine the effects of various cell types, matrix materials, and surface biochemistries on cell-matrix interactions. Ultimately, this assay will allow us to identify design parameters that will be most effective for enhancing the rate of tissue ingrowth on fiber-based collagen scaffolds for soft tissue regeneration.

Chapter 4 describes the application of the quantitative method developed in Chapter 3 to crosslinking of collagen threads. Collagen threads are commonly crosslinked to increase the mechanical properties and decrease the otherwise rapid *in vivo* rate of degradation in a wound site. The initial studies in Chapter 3 determined that the cellular outgrowth velocity was attenuated after crosslinking with a technique selected because of its prevalence during prior *in vivo* studies. We hypothesized that implementation of

alternate crosslinking modalities that had yet to be tested on self-assembled collagen threads could increase thread stability without the concurrent decrease in tissue ingrowth seen with DHT crosslinking. The major limitations of collagen threads, including limited tissue ingrowth, could thereby be circumvented. The mechanical properties and cellular outgrowth rates were measured for self-assembled collagen threads utilizing the most promising crosslinking strategies. Although all the techniques investigated increased the strength and decreased the rate of degradation, they also subsequently decreased the *in vitro* rate of tissue ingrowth. These findings indicate that there remains a need to develop a scaffold material that both provides mechanical stability and promotes new tissue ingrowth. To meet these additional requirements, novel biopolymer microthreads were developed to promote rapid tissue ingrowth and tissue regeneration in conjunction with collagen threads.

Part II: Fibrin Threads For Ligament Regeneration

While self-assembled collagen threads structurally and biochemically mimic native tendon and ligament, our studies suggested that when crosslinked they may not elicit a response that best promotes the spatially and temporally complex process of tissue regeneration. A key initial step of tissue regeneration is the deposition of a fibrin provisional matrix that fills the wound space and promotes fibroblast infiltration from the wound margin. Fibrin matrix regulates cell migration, proliferation, and gene expression through integrin signaling[23-25] and through the localization of matrix bound signaling proteins resulting from fibrin's high binding affinity for growth factors, especially fibroblast growth factor-2 (FGF-2).[26, 27] We hypothesize that the development of a fibrin biomaterial with a thread-like structural morphology would promote the cellular alignment seen on fiber scaffolds[28] with sufficient mechanical stability to allow for integration with other thread scaffolds such as collagen. Furthermore, fibrin threads incorporating FGF will deliver growth factors and stimulate migration and proliferation to ultimately guide wound healing.

Therefore, the second goal of this thesis was to develop fibrin microthreads with a comparable morphology to collagen threads that can be combined with other matrices for ligament tissue regeneration. Ultimately these microthreads will guide wound healing spatially and temporally, through aligned regeneration, growth factor delivery, and variable matrix signaling.

The development of fibrin microthreads is described in Chapter 5, focusing on the optimization of production parameters for consistent structural morphology and maximum tensile strength. Fibrin microthreads were produced by co-extruding solutions of 70mg/ml fibrinogen and 6 U/ml thrombin through small diameter polyethylene tubing using an automated extrusion device. Fibrin microthreads averaged 55-65 μm in hydrated diameter and achieved ultimate tensile strengths approaching 4.5 MPa. In conjunction with surface structural analyses, these results demonstrate the development of fibrin microthreads with comparable morphological properties to the previously investigated collagen threads.

The potential of fibrin microthreads to regenerate tissues such as the ACL through aligned regeneration and growth factor delivery is investigated in Chapter 6. Fibroblast growth factor (FGF-2) was coextruded into fibrin microthreads and investigated for the ability to increase cell proliferation and cellular outgrowth. Fibroblasts cultured on bundles of fibrin microthreads with FGF-2 showed increased proliferation, while the rate of cellular outgrowth increased on discrete fibrin microthreads containing FGF-2. Furthermore, cells cultured on bundles and discrete fibrin threads demonstrated alignment along the long axis of the threads regardless of FGF incorporation. Thus, the increase in alignment over flat substrata was attributed to contact guidance and the cylindrical fiber morphology.

Conclusions

Collagen and fibrin biopolymer microthreads are promising technologies for the repair of torn ACLs. This thesis utilized mechanical testing and novel *in vitro* cellular techniques for the evaluation of various biopolymer threads for their potential application to the repair of torn ACL. Second generation, self-assembled collagen threads demonstrated improved properties over the first generation of insoluble collagen threads. These collagen threads attain strengths capable of withstanding the initial loading environment of the ACL with crosslinking and have demonstrated some success during *in vivo* implantation studies. However, the regenerative capabilities of these biomimetic threads are ultimately hampered by the current crosslinking techniques required.

The paradigm shift towards the development of fibrin biopolymer microthreads allows for the continued use of aligned biomimetic structures, with the simple incorporation of growth factors and the potential of early wound healing integrin signaling. Fibrin microthreads have morphologically cylindrical geometries comparable

to collagen threads with diameters in the 50-100 μm range and promote cell alignment. Furthermore these threads are orders of magnitude stronger than fibrin gels, and can be readily incorporated into other fiber or thread matrices. The growth factor FGF-2, commonly found matrix bound and shown to be a cofactor with fibrinogen, was incorporated into fibrin threads and lead to increased fibroblast proliferation and cellular outgrowth. Ultimately, these results suggest that composites of collagen and fibrin biopolymer microthreads could be used to control the spatially and temporally complex process of tissue regeneration to improve the repair of torn ACLs.

REFERENCES

[1] Hill CL, Seo GS, Gale D, Totterman S, Gale ME & Felson DT. Cruciate ligament integrity in osteoarthritis of the knee. *Arthritis Rheum* **52**: pp. 794-799. (2005).
[2] Mayr HO, Weig TG & Plitz W. Arthrofibrosis following acl reconstruction--reasons and outcome. *Arch Orthop Trauma Surg* **124**: pp. 518-522. (2004).
[3] Fu F & Musahl V. Review article: the future of knee ligament surgery. *Acta Clinica* **2**: pp. 101-107. (2002).
[4] Harner CD, Fu FH, Irrgang JJ & Vogrin TM. Anterior and posterior cruciate ligament reconstruction in the new millennium: a global perspective. *Knee Surg Sports Traumatol Arthrosc* **9**: pp. 330-336. (2001).
[5] Vunjak-Novakovic G, Altman G, Horan R & Kaplan DL. Tissue engineering of ligaments. *Annu Rev Biomed Eng* **6**: pp. 131-156. (2004).
[6] Bellincampi LD, Closkey RF, Prasad R, Zawadsky JP & Dunn MG. Viability of fibroblast-seeded ligament analogs after autogenous implantation. *J Orthop Res* **16**: pp. 414-420. (1998).
[7] Caruso AB & Dunn MG. Functional evaluation of collagen fiber scaffolds for acl reconstruction: cyclic loading in proteolytic enzyme solutions. *J Biomed Mater Res A* **69**: pp. 164-171. (2004).
[8] Dunn MG, Avasarala PN & Zawadsky JP. Optimization of extruded collagen fibers for acl reconstruction. *J Biomed Mater Res* **27**: pp. 1545-1552. (1993).
[9] Dunn MG, Liesch JB, Tiku ML & Zawadsky JP. Development of fibroblast-seeded ligament analogs for acl reconstruction. *J Biomed Mater Res* **29**: pp. 1363-1371. (1995).
[10] Gentleman E, Lay AN, Dickerson DA, Nauman EA, Livesay GA & Dee KC. Mechanical characterization of collagen fibers and scaffolds for tissue engineering. *Biomaterials* **24**: pp. 3805-3813. (2003).
[11] Kato YP, Christiansen DL, Hahn RA, Shieh SJ, Goldstein JD & Silver FH. Mechanical properties of collagen fibres: a comparison of reconstituted and rat tail tendon fibres. *Biomaterials* **10**: pp. 38-42. (1989).
[12] Koob TJ, Willis TA, Qiu YS & Hernandez DJ. Biocompatibility of ndga-polymerized collagen fibers. ii. attachment, proliferation, and migration of tendon fibroblasts in vitro. *J Biomed Mater Res* **56**: pp. 40-48. (2001).
[13] Koob TJ, Willis TA & Hernandez DJ. Biocompatibility of ndga-polymerized collagen fibers. i. evaluation of cytotoxicity with tendon fibroblasts in vitro. *J Biomed Mater Res* **56**: pp. 31-39. (2001).
[14] Law JK, Parsons JR, Silver FH & Weiss AB. An evaluation of purified reconstituted type 1 collagen fibers. *J Biomed Mater Res* **23**: pp. 961-977. (1989).
[15] Wasserman AJ, Kato YP, Christiansen D, Dunn MG & Silver FH. Achilles tendon replacement by a collagen fiber prosthesis: morphological evaluation of neotendon formation. *Scanning Microsc* **3**: p. 1183-97; discussion 1197-200. (1989).

[16] Weadock KS, Miller EJ, Bellincampi LD, Zawadsky JP & Dunn MG. Physical crosslinking of collagen fibers: comparison of ultraviolet irradiation and dehydrothermal treatment. *J Biomed Mater Res* **29**: pp. 1373-1379. (1995).
[17] Weadock KS, Miller EJ, Keuffel EL & Dunn MG. Effect of physical crosslinking methods on collagen-fiber durability in proteolytic solutions. *J Biomed Mater Res* **32**: pp. 221-226. (1996).
[18] Dunn MG, Tria AJ, Kato YP, Bechler JR, Ochner RS, Zawadsky JP & Silver FH. Anterior cruciate ligament reconstruction using a composite collagenous prosthesis. a biomechanical and histologic study in rabbits. *Am J Sports Med* **20**: pp. 507-515. (1992).
[19] Goldstein JD, Tria AJ, Zawadsky JP, Kato YP, Christiansen D & Silver FH. Development of a reconstituted collagen tendon prosthesis. a preliminary implantation study. *J Bone Joint Surg Am* **71**: pp. 1183-1191. (1989).
[20] Kato YP, Dunn MG, Zawadsky JP, Tria AJ & Silver FH. Regeneration of achilles tendon with a collagen tendon prosthesis. results of a one-year implantation study. *J Bone Joint Surg Am* **73**: pp. 561-574. (1991).
[21] Pins GD, Christiansen DL, Patel R & Silver FH. Self-assembly of collagen fibers. influence of fibrillar alignment and decorin on mechanical properties. *Biophys J* **73**: pp. 2164-2172. (1997).
[22] George D. Pins, Eric K. Huang, David L. Christiansen, Frederick H. Silver. Effects of static axial strain on the tensile properties and failure mechanisms of self-assembled collagen fibers. *J Appl Polym Sci* **63**: pp. 1429-1440. (1997).
[23] Feng X, Clark RA, Galanakis D & Tonnesen MG. Fibrin and collagen differentially regulate human dermal microvascular endothelial cell integrins: stabilization of alphav/beta3 mrna by fibrin1. *J Invest Dermatol* **113**: pp. 913-919. (1999).
[24] Gailit J, Clarke C, Newman D, Tonnesen MG, Mosesson MW & Clark RA. Human fibroblasts bind directly to fibrinogen at rgd sites through integrin alpha(v)beta3. *Exp Cell Res* **232**: pp. 118-126. (1997).
[25] Xu J & Clark RA. Extracellular matrix alters pdgf regulation of fibroblast integrins. *J Cell Biol* **132**: pp. 239-249. (1996).
[26] Sahni A, Odrljin T & Francis CW. Binding of basic fibroblast growth factor to fibrinogen and fibrin. *J Biol Chem* **273**: pp. 7554-7559. (1998).
[27] Sahni A, Sporn LA & Francis CW. Potentiation of endothelial cell proliferation by fibrin(ogen)-bound fibroblast growth factor-2. *J Biol Chem* **274**: pp. 14936-14941. (1999).
[28] Rovensky Y & Samoilov V. Morphogenetic response of cultured normal and transformed fibroblasts, and epitheliocytes, to a cylindrical substratum surface. possible role for the actin filament bundle pattern. *J Cell Sci* **107 (Pt 5)**: pp. 1255-1263. (1994).

CHAPTER 2: BACKGROUND

Ligaments in the human body are aligned bundles of dense connective tissue linking adjacent bones to stabilize and guide joint motion. In connecting long bones, ligaments often present as white and shiny bands, sheets, or bundles anchored directly through fibrocartilage insertions to bones. Of particular interest, due to their propensity for injury, are the four ligaments of the knee, especially the anterior cruciate ligament (ACL).

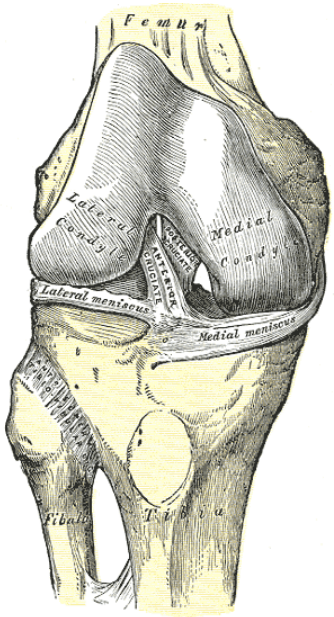

Figure 2.1: Ventral view of a right knee joint[1]

2.1 ANTERIOR CRUCIATE LIGAMENT (ACL)

2.1.1 Healthy ACL

The ACL is one of two decussating ligaments of the knee acting as a major joint stabilizer connecting the anterior side of the tibia at the intercondylar eminence to the medial surface of the lateral femoral condyle, well posterior to the longitudinal axis of the femoral shaft (Figure 2.1).[2] In general the ACL accounts for approximately 85% of the resistance to anterior displacement of the tibia when the knee is at 90 degrees flexion and neutral rotation.[2, 3] The general mechanical properties of

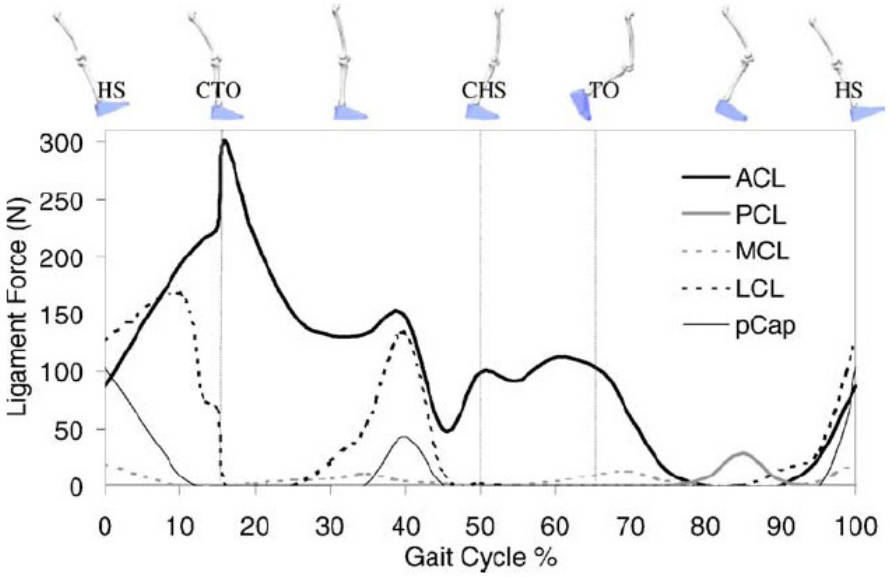

Figure 2.2: Forces transmitted to the cruciate ligaments, the collateral ligaments, and the posterior capsule of the knee over one cycle of normal level walking. The knee ligaments were more heavily loaded in stance than in swing. The ACL bore the largest overall force with a peak transmitted force of 1/2 body weight at 15% gait cycle.[5]

the ACL are summarized in Table 2.1, however, the biomechanical role of the ACL in the knee is more complex than a simple rope connecting the tibia and femur. The ACL consists of two bundle subunits which become differentially taut during full range of motion[4] leading to forces of about 300 N during walking alone (Figure 2.2).[5] The anteromedial subunit of the ACL is primarily tight throughout extension and tighter during flexion, while the posterolateral subunit becomes relaxed while the knee is flexed.[6]

The ACL is an intercapsular ligament covered by a thin layer of synovium.[7] Nutrients are supplied to the ACL from the middle genicular artery that gives rise to periligamentous vessels that ensheath the ACL within the synovial membrane.[8, 9] The central portion of the ACL is considerably less vascular than the proximal or distal portions while the osseous-ligament attachments are largely avascular.[8, 9] The poor vascularity of the tissue is linked in part to the demonstrably lower healing potential of the ACL in comparison to other tendons and ligaments (see 2.1.1.3, pg. 13).[10]

2.1.1.1 ACL Composition

Matrix

The ACL, like most ligaments, is composed predominantly of type I collagen, including upwards of 80% of the dry weight,[11, 12] arranged in a highly aligned hierarchical structure. Type I collagen, is a long rod-like protein comprised of three chains of the approximately 1000 amino acid repeat of glycine-X-Y where X and Y are often proline and hydroxyproline, respectively.[13] The abundance of glycine, a residue with an extremely small non-polar R-group, and the three amino acid repeat allows for the tight 100 nm pitch width coiling of the three chains into a left-handed triple helix stabilized by hydrogen bonds.[14] The soluble protein, assembled intracellularly and packaged into vesicles, initially termed procollagen, is only 1.5 nm in diameter, but 290 nm in length with short 10 and 15 nm non-coiled telopeptide ends. During matrix synthesis, cells secrete procollagen into the extracellular matrix, specific proteinases cleave the telopeptide ends, and the resulting collagen molecules self-assemble laterally into tightly packed arrays of collagen fibrils. [15] The molecules within the arrays are packed in a quarter staggered manner leading to the collagen fibril characteristic 67 nm striated banding pattern visible after heavy metal staining and electron microscopy.[15] Adjacent molecules in these arrays are crosslinked for strength and stability through lysyl

Table 2.1: Geometry and mechanical properties of normal ACL

Dimensions		**Reference**
Length	22-41 mm (32 mean)	Duthon et al., *Knee Surg Sprts Traum Arth* (2006)
Width	7-12 mm	Duthon et al., *Knee Surg Sprts Traum Arth* (2006)
Cross-sect. Area	34-42 mm^2	Duthon et al., *Knee Surg Sprts Traum Arth* (2006)
Mechanical Strength		
Failure Load	2160 N	Woo et al., *Am J Sports Med* (1991)
Tensile Strength	38 MPa	Silver, *ISBN 0412412608* (1994)
Stiffness (Modulus)	242 N/mm	Woo et al., *Am J Sports Med* (1991)
Elongation to Failure	33%	Woo et al., *Am J Sports Med* (1991)
Normal Cyclic Loading		
Walking	300 N	Shelburnea et al., *J Biomech* (2004)
Total # of Cycles	1-2 $x10^6$ cycles/year	Shelburnea et al., *J Biomech* (2004)
Jogging	630 N	Chen et al., *J Biomed Mater Res* (1980)
Strain	up to 4.4% squatting	Heijne et al., *Med Sci Sports Exerc* 2004

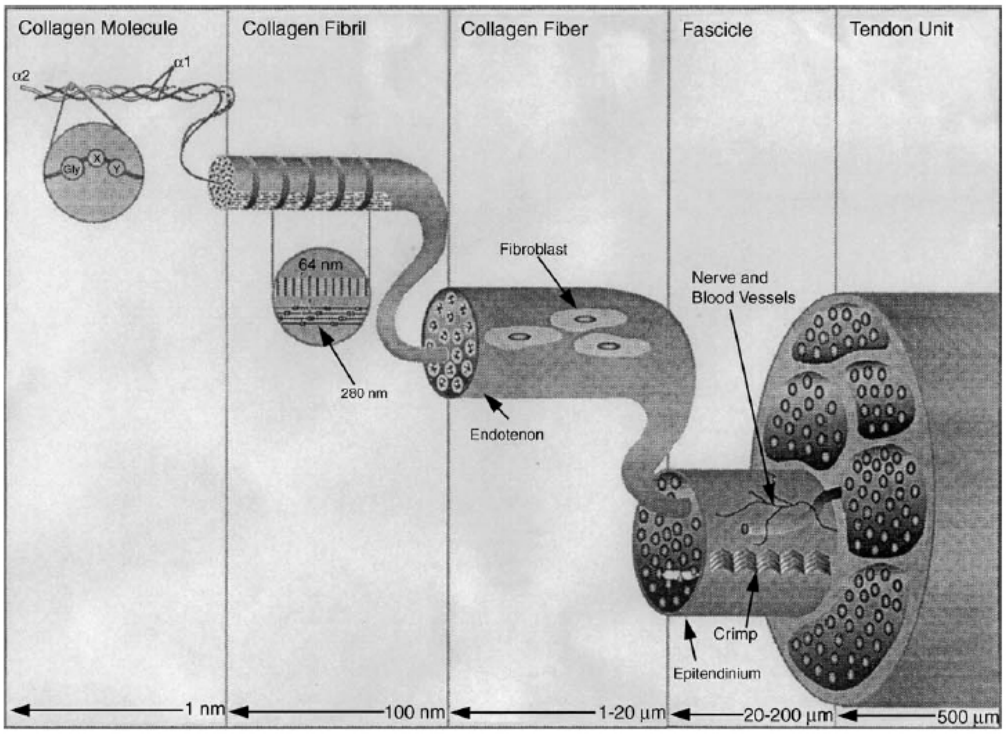

F.H. Silver et al. / Journal of Biomechanics 36 (2003) 1529–1553

Figure 2.3: A tendon or ligament is comprised of hierarchically aligned type I collagen molecules packed into larger scale fibrils, fibers and fascicles as well as a small percentage of fibroblasts.[15]

hydrosylysyl oxidation by the enzyme lysyl oxidase.[16] These fibrils are on the order of 10-300 nm in diameter but can be up to hundreds of microns long.[13, 15] The fibrils are further assembled into larger collagen fibers or fascicles (20-200 μm in diameter) that group to form the visible ligament structure. The ACL has an additional levels of structural complexity as the fascicles twist 180° from the femoral to tibial attachments.[8, 13]

While consisting of a large percentage of type I collagen, the matrix of the ACL is comprised other constituents including Type III collagen and glycosaminoglycans (GAGs). Type III collagen is a fibril forming collagen with three identical α chains connected by intramolecular disulfide crosslinks.[13] This particular collagen is typically localized to the loose connective tissue in the regions between type I collagen bundles.[8] While there is approximately 7.3 times more type I collagen than type III collagen,[12] it has been recently suggested that the type III collagen molecule is more flexible and therefore might alter the elastic modulus of collagen fibrils.[17] Ligaments contain two to four times as much GAG as tendons approaching 10 mg hexosamine/g dry tissue[11]

including chondroitin sulfate, hyaluronic acid, and dermatan sulfate.[18] Furthermore, the ACL has been found to contain more type III collagen and GAGs than the medial collateral ligament.[19, 20]

Cells

The ACL also contains a small percentage of ligament fibroblasts with morphological properties similar to fibroblasts from other tissues such as tendon or dermis, but with cellular characteristics that vary even within the ligament superfamily. Ligament fibroblasts are elongated spindle shaped connective tissue cells with small diameter processes attaching and extending between collagen fibrils while connecting in a vast three-dimensional network to each other through gap junctions.[7, 21, 22] Ligament fibroblasts are considered phenotypically different from tenocytes with increased metabolic activity, more plump cell nuclei,[11] and slower proliferation.[23] Similar decreases in proliferation and matrix synthesis were found when comparing ligament fibroblasts to dermal fibroblasts.[24] Furthermore, fibroblasts isolated from the ACL have decreased migration,[25] proliferation,[26] and collagen synthesis[27] compared to fibroblasts from the medial collateral ligament (MCL). These characteristics of ACL fibroblasts have been correlated to the poor intrinsic healing capacity of the ACL compared with tendons or the MCL. However, the intraarticular synovial environment of the ACL is linked to the decreased healing because the nutrient and metabolite exchange for ACL fibroblasts is increasingly dependent on diffusion[7] (See Blood Supply above and ACL: Injury and Healing below).

2.1.1.2 ACL Injury and Repair

Clinical Significance

In 2003, more than 9.5 million people visited orthopaedic surgeons with knee problems, including a high prevalence of ACL injury.[28] These ACL injuries occur most frequently as a result of a non-contact deceleration or landing situation that produces valgus twisting of the knee during athletic activities.[29-32] Complete tears of the ACL heal very poorly, are painful, and lead to joint instability, increased occurrences of meniscal tears and early osteoarthritis.[33-35] Surgical intervention by means of complete ACL reconstruction has reduced the frequency and severity of these complications. However, the long term results of the ACL injury are still marred by a high prevalence of degenerative joint disease (DJD), including reports of as many as 88% of patients demonstrating radiological signs of DJD[36] especially osteoarthritis[37] in both men[38] and women[39] regardless of the surgical repair technique. Patients with

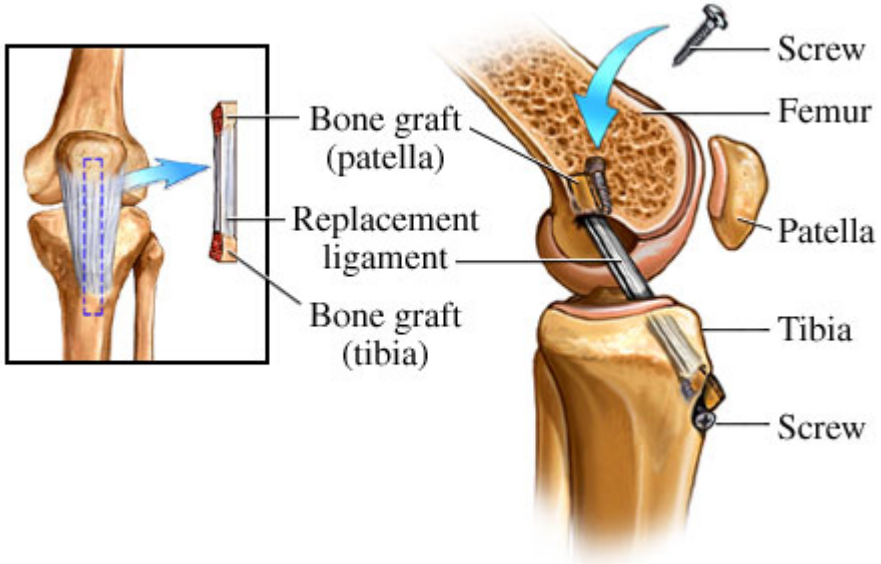

Figure 2.4: The current surgical repair strategy for a torn ACL included the the use of a bone-patellar tendon-bone (BPTB) autograft. The BPTB autograft is inserted through a drilled tibial tunnel, into the femoral tunnel, and secured with interference screws.(image courtesy of Nucleus Communications, 2002)

reconstructed ACLs also still have increased occurrences of meniscal damage,[40, 41] biomechanical alterations to their normal gait,[42, 43] as well as reduced range of motion[36] and chronic instability.[44] Surgical reconstructions of the ACL occur with increasing frequency, with recent estimates ranging from 100-200,000 occurring annually in the United States alone [2, 12, 45-48] that cost a reported five billion dollars.[12, 45, 48] While other orthopedic injuries in non-geriatric patients, such as ankle sprains and tibia fractures, have decreased more than 85% in the last 15 years, knee ligament injuries have increased 172%[49] with an incidence rate of about 1 in 3000 Americans.[50]

Surgical Repair

Patellar or hamstring tendon local autografts are currently considered the standard for ACL replacement because of their size, strength, and availability.[7, 46, 51] During surgical revision, the medial third of the patellar tendon including the tibial and patellar bony attachments is resected. This autograft is then most commonly inserted through drilled femoral and tibial tunnels and secured with interference screws (Figure 2.4). Despite relative success compared with non-surgical treatments, the long term success rates still do not exceed 85%[46] and studies have shown these autografts fail to reach strengths comparable to native ACLs with strength deficits measured at greater than 34% when compared to the contralateral limb after rehabilitation.[52] These procedures

require a secondary surgical and donor site to retrieve autograft tissue that is of limited quantity, and even after repair often lead to joint laxity as well as patellar tendon abnormalities.[46, 51, 53] Furthermore, due to complications from the first surgery or reinjury, between 10-15% of these procedures require secondary revision surgery with successful results occurring less than 60% of the time.[51] Although a feasible solution, allografts, mostly acquired from cadavers, could potentially transmit disease[54] or elicit an undesired immunologic response. It has also been suggested that these allografts cannot be sterilized without altering the mechanical properties of the tissue.[47]

2.1.1.3 ACL Healing

Wound healing of the ACL is considered to occur following principles similar to most other soft connective tissues (see Stages of Ligament Wound Healing 2.1.1.3, pg. 14), however the ACL specifically demonstrates limited healing capacity. This limited healing capacity is seen during investigations both in comparison to tendons as well as in contrast to other ligaments of the knee such as the MCL. The phenomenon has been attributed to wide variety of causes including intrinsic cell deficiencies, the intraarticular synovial environment, limited blood supply and complete separation of the torn ligament ends.

Variations in ACL ligament fibroblasts have been seen in comparison to tenocytes, dermal fibroblasts, mesenchymal stem cells and MCL fibroblasts. Van Eijk et al. investigated multiple cells sources for properties and parameters of importance to ligament tissue engineering. They found that both mesenchymal stem cells and dermal fibroblasts proliferated more rapidly and produced higher collagen content than ACL fibroblasts.[24] Bellincampi et al. found increased survival of dermal fibroblasts over ACL ligament fibroblasts during intraarticular implantation studies.[55] Those same researchers found ACL fibroblast to be more plump with decreased proliferation on collagen threads compared with patellar tenocytes.[23] Differences have also been seen with regard to response of ligament fibroblasts to growth factors[56, 57] and adhesive strength.[58-60] Furthermore, several studies have reported decreases in migration, proliferation, collagen synthesis, and response to growth factors of ACL fibroblasts compared to MCL fibroblasts.[25, 26, 61-63]

Other researchers have suggested that the environment may be the limiting factor in ligament regeneration rather than intrinsic cellular characteristics. Being an intraarticular ligament, the vascularity of the ACL is less than that of extraarticular ligaments such as the MCL or tendons, which are attached to highly perfused muscles.[8-10] Furthermore,

it has been suggested that the synovial environment of the ACL limits diffusional nutrient exchange, particularly important to the least vascularized central portion of the ligament.[7, 9] In a recent review, Patrigliano et al. suggested that disruption of the synovial sheath precludes the formation of a local hematoma that is the foundation for chemotactic cytokines and growth factors, leading to the paucity of healing.[64] Corroborating evidence for this hypothesis is supported from work in a ligament transection study that demonstrated partial healing of ligament where an intact synovial sheath facilitated the deposition of a fibrin mesh.[65]

Stages Of Ligament Wound Healing

The stages of ACL wound healing are considered similar to most other soft connect tissues and most information on ligament wound healing is garnered from work with the more consistently healing and easily accessible MCL.[66] Although the principles are the same, the number and delineations of these overlapping stages are arbitrary and vary by author, with one example in Table 2.2 and another described in stages as follows:

PHASE I: HEMORRAGE AND INFLAMMATION (0-72 HOURS)

After a ligament is torn, blood vessels rupture filling the discontinuity. Blood coagulation and platelet aggregation follow rapidly producing a blood clot to reestablish hemostasis. The trapped platelets release a battery of growth factors, most notably platelet-derived growth factor (PDGF), transforming growth factor β (TGF-β), and insulin-like growth factor (IGF-I and IGF-II) that promote inflammation.[67] The blood clot matrix, formed largely of fibrin and fibronectin (see 2.1.1.3, pg. 13), acts as a provisional scaffold, soaking up cytokines and growth factors while trapping leukocytes and lymphocytes within several hours.[68] By 24-48 hours, inflammation begins with the arrival of macrophages that phagocytose necrotic tissue and further secrete growth factors that promote granulation tissue formation.[30]

PHASE II: REPOPULATION AND PROLIFERATION(3-7 DAYS)

By approximately day three, fibroblasts are recruited into the fibrin provisional matrix, induced by a lack of cell-cell contacts, matrix signaling, and chemotactic attractants released during the inflammation stage.[68] The fibroblasts migrate from both the neighboring tissue as well as the systemic circulation and proliferate within the matrix, ultimately synthesizing new extracellular matrix including collagens and GAGs.[30] These cells then begin to produce large amounts of type III and type I collagen in response to the milieu of growth factors, particularly PDGF and TGF-β.[67]

Table 2.2: The phases of ligament wound healing.[67]

Time (days)	Phase	Process
0	Immediately post-injury	Clot formation around the wound
0–1	Inflammatory	First battery of growth factors and inflammatory molecules produced by cells within the blood clot
1–2	Inflammatory	Invasion by extrinsic cells, phagocytosis
2–4	Proliferation	Further invasion by extrinsic cells, followed by a second battery of growth factors that stimulate fibroblast proliferation
4–7	Reparative	Collagen deposition; granulation tissue formation; revascularisation
7–14	Reparative	Injury site becomes more organised; extracellular matrix is produced in large amounts
14–21	Remodelling	Decreases in cellular and vascular content; increases in collagen type I
21+	Remodelling	Collagen continues to become more organised and cross-linked with healthy matrix outside the injury area. Collagen ratios, water content and cellularity begin to approach normal levels

PHASE III: REMODELING AND REGENERATION(1-8 WEEKS)

The final phase of ligament wound healing is marked by the long term remodeling of the ECM and can last many months. The migrated fibroblasts in the wound gradually switch from migratory phenotype into a profibrotic myofibroblast phenotype, marked by the presence of a smooth muscle actin, that is responsible for contracting the wound.[69-71] With time, the fibrin provisional matrix is slowly degraded and replaced with increased type I collagen content and density, while the high cellularity decreases as many of these fibroblasts apoptose.[72] Eventually GAG content increases and the matrix becomes longitudinally oriented, although this scar tissue will never attain normal morphological characteristics and mechanical properties.[30]

2.1.1.4 ACL Regeneration

Due to the poor regenerative capacity of the ACL and the suboptimal results of the standard surgical repair techniques with autografts, many researchers have suggested investigating the regeneration of ACL tissue utilizing tissue engineering techniques.[6, 12, 30, 47, 64] In general, tissue engineering applies the use of a degradable scaffold, cells, and growth factors, in any combination to promote the complete regeneration of an injured or damaged tissue. Specifically for ligament regeneration, the ideal scaffold would be designed to demonstrate mechanical properties similar to native ACL and slowly degrade under natural pathways matching the rate of new tissue synthesis to ultimately regenerate the damaged tissue without further surgical revision. The scaffold's compositional, degradative, and mechanical properties are considered to dictate the mass transport and mechanotransduction at both a cell and tissue scale.[12] Furthermore, an ideal scaffold should cause minimal inflammatory response, be porous, and promote the formation of neoligament tissue.[47]

Currently, no tissue engineered ACLs have yet reached clinical trials due to various reasons. Most researchers agree that current scaffolds lack appropriate mechanical properties. The strength, stiffness, and viscoelasticity of engineered ligaments do not match those of the healthy ACL and cannot withstand the complex *in vivo* loading.[6, 12, 30, 47, 73] Others mention the a lack of a readily available cell source.[12, 24] Furthermore, the blood supply is disrupted after injury and many consider the regeneration to be too slow.[6, 73] Also of major importance is the development of appropriate scaffolds that regulate cell stimuli to facilitate cell adaptation. Ideally the system should provide temporal matrix and cytokine stimulation dictated by the phases of regeneration (see Stages of Ligament Healing 2.1.1.3, pg. 14).[12, 64] In general, the field of ligament tissue engineering also lacks quantitative *in vitro* and *in vivo* methods of characterization.[12] The implications of matrix mediated signaling on cell function in tissue engineered constructs has yet to be investigated.

2.2 Thread Scaffolds for ACL Repair

Fiber or thread-based scaffolds have significant advantages as scaffolds for ACL regeneration including a natural structural homology to native tissues (see 2.1.1.1 ACL Composition, pg 9) as well as an ability to be woven or braided into larger, stronger, controlled porosity structures.[47] Additionally, studies have shown that contact guidance on cylindrical substrata less than 100 μm facilitates the alignment and orientation of cells.[74] Therefore, fiber-based scaffolds dominate current research for ACL regeneration. However, the materials investigated are quite diverse. These materials fall into two categories: Synthetic polymers threads made from degradable plastics and biopolymer threads derived from native ECM structural proteins.

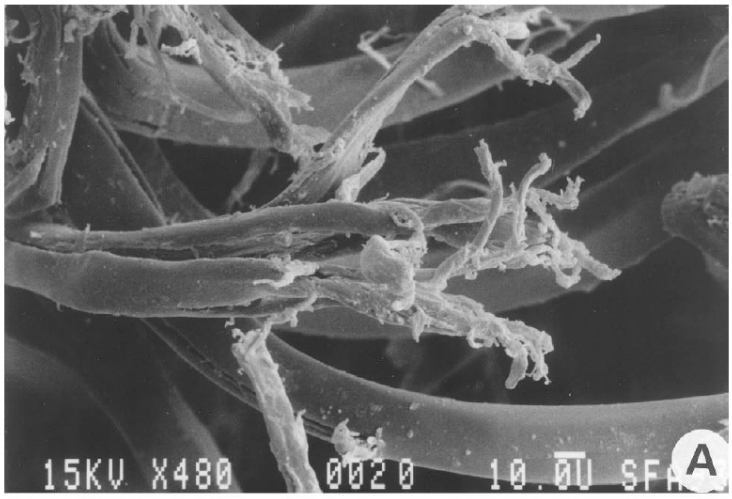

Figure 2.5: SEM of polyester fibers visualized after removal from an explanted ACL prosthesis demonstrating fracture and axial splitting.[75]

2.2.1 Synthetic Polymers

A wide range of polymer-based synthetic fiber grafts including polypropylene, polyethylene, polytetraflouroethylene (PTFE), and polyester were

manufactured and FDA approved for ACL replacement between the mid 1970's and the late 80's. These polymer grafts are no longer used because orthopedic surgeons reported high rates of failure due to flexural and torsional fatigue, leading to axial failure as well as structural changes and loss of integrity due to unpredictable tissue infiltration.[75] Recently, researchers have investigated a host of braided or woven degradable fibers including poly desaminotyrosyl-tyrosine ethyl carbonate (poly DTE carbonate),[76] polydioxanone (PDS),[77] and poly L-lactic acid (PLLA),[78] with the intention of developing a tissue engineered scaffold with controlled porosity and degradation to match tissue ingrowth and regeneration. Synthetic grafts, however, are limited by the formation of acidic bi-products during degradation with the possibility of long-term undesirable immunogenic response by the host tissue. Furthermore, these scaffolds have mechanical impediments including abrasive wear, stress shielding, and creeping.[75]

2.2.2 Biopolymer Threads

Biopolymer threads are materials reconstituted from basic ECM structural proteins found in nature, such as collagen and silk fibroin. These biomimetic materials not only provide the geometric advantages of fiber and thread matrices, but with the additional advantage of compositional homology. Biopolymer threads typically degrade under physiologically normal pathways that produce no acidic byproducts and are either reprocessed by the body or excreted. Furthermore, these proteins in certain cases provide biochemically relevant cell adhesion and signaling. Of this group of biopolymer threads, the most highly investigated are threads composed of type I collagen.

2.2.2.1 Collagen Threads

Threads composed of type I collagen, the native structural protein of soft connective tissues (), have been widely investigated for repair of torn tendons and ligaments. These collagen threads or fibers are typically produced by extrusion through small diameter tubing and bundled in large sets to form ligament prostheses. Research into the *in vitro* mechanical properties and degradation profiles of collagen threads has successfully demonstrated strengths comparable to native tendon and ligament tissues with crosslinking (Table 2.2). Studies of the cellular response on collagen threads *in vitro* have found that cells will attach and proliferate on thread bundles,[23, 55, 79] the threads did not lose strength during 20 days of culture with cells,[80, 81] and cells actually increased the strength of collagen thread bundles.[80, 81] *In vivo*, these scaffolds demonstrate promising results inducing neotendon and neoligament formation with varying degrees of success (Table 2.2). Overall, thread matrices that degraded too

slowly, typically in excess of one year, showed lower neo-ligament regeneration and advanced signs of long term immunogenicity.[82, 83] In general, the complete regeneration of collagen-based ligament grafts was impeded by insufficient tissue ingrowth from the wound margin to completely repopulate the graft, remodel, and regenerate the tissue while the cellular infiltration was inconsistent and difficult to control.[23]

Self-Assembly Of Type I Collagen Threads

The spontaneous self-assembly of collagen molecules *in vitro* can be exploited to develop novel collagen threads with improved properties. Collagen threads are most commonly produced from insoluble aggregates of collagen derived from blended, highly crosslinked tissues such as tendon and corium. However, it has been well established that solutions of soluble type I collagen self-assemble into fibrils possessing the characteristic 67 nm repeat through thermodynamically favorable interactions between collagen molecules that allow for increased water mobility by phase separation.[15, 84] This knowledge was leveraged to develop novel self-assembled collagen threads with improved properties over those extruded from insoluble collagen aggregates.[85] The ultimate tensile strength and elastic modulus of self-assembled threads were found to be comparable to native rat tail tendon fibers and greater than reconstituted insoluble

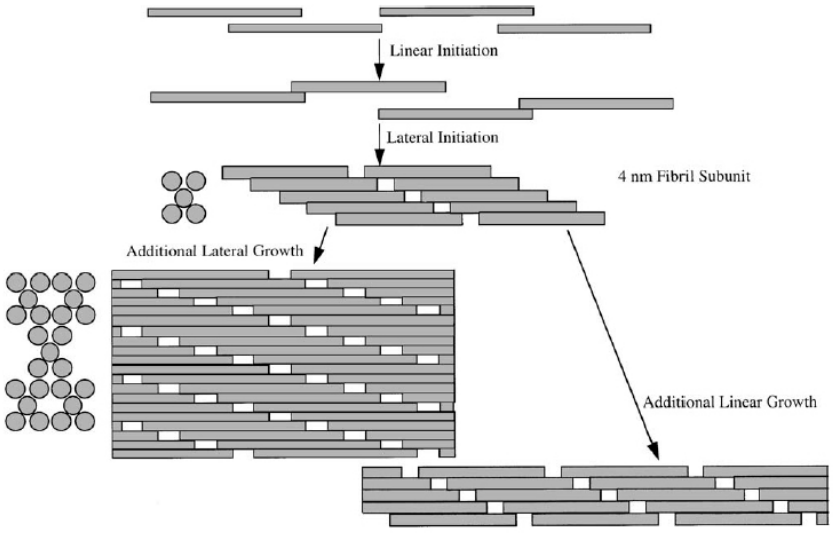

Figure 2.6: Schematic model of in vitro *collagen self-assembly. Collagen molecules initially assemble linearly and laterally resulting in the formation of staggered dimers. Once formed, these approximately 4 nm subunits fuse laterally and longitudinally[15]*

collagen threads.[86] Furthermore, these self-assembled threads posses a fibrillar substructure marked by the D periodic banding pattern seen with electron microscopy as well as fibril diameters comparable to those seen in the early stages of development.[85] The results of these studies suggest that these threads are a promising scaffold material for the development of a second generation ligament replacement.

Collagen Crosslinking

Numerous crosslinking strategies have been investigated for collagen thread matrices to improve the mechanical stability of these materials. While *in vivo* crosslinking between collagen molecules occurs via the enzyme lysyl oxidase, collagen threads produced *in vitro* must be crosslinked post-extrusion to increase the macromolecular protein stability. These various collagen crosslinking methodologies employ either chemical or physical techniques to alter the proteins stability by inserting addition intermolecular and intramolecular crosslinks between adjacent collagen molecules. The positive mechanical outcomes of these processes are materials that demonstrate a decreased proteolytic degradation rate, increased stiffness, and increased tensile strength.

Numerous techniques that have been employed to add crosslinks to collagen matrices through either physical or chemical means . Specifically, collagen threads have been chemically crosslinked using gluteraldehyde, cyanamide, 1-3 ethyldimethyaminopropyl carbodiimide (EDC), and Nordihydroguaiaretic acid (NDGA)(see Table 2.3). Physical crosslinking techniques including dehydrothermal treatment (DHT) and exposure to UV light (UV) have also been employed in order to achieved the desired mechanical properties without the addition of possibly cytotoxic reaction products to the matrices (see Table 2.3). While each of these techniques has advantages and disadvantages, the effect of these crosslinking techniques on self-assembled collagen threads and their effect on cell matrix interactions is still unclear.

Year	Authors	Study Type	Investigation	Crosslinking	Important Outcomes
1989	Law	*in vivo*	biocompatibility and mechanical properties, intramuscular rat	Gluteraldehyde, DHTC	► DHT/C better than gluteraldehyde ► Hydrated strength much lower than dry strength ► Aligned ingrowth
1989	Kato	*in vitro*	mechanical properties vs. rat tail tendon	Gluteraldehyde, DHTC	► Both crosslinking methods achieved tensile strength equivalent to rat tail tendon
1989	Garg	*in vitro*	proteoglycans on fibril formation	Gluteraldehyde	► Chondroitan sulfate influences late stage fibril formation leading to increased tensile strength
1989	Wasserman	*in vivo*	rabbit Achilles tendon prosthesis	DHTC	► By 10 weeks, scaffold was resorbed and replaced with neotendon
1991	Kato	*in vivo*	rabbit Achilles tendon prosthesis	Gluteraldehyde, DHT/EDC	► After 1 year, gluteraldehyde not resorbed and encapsulated ► EDC showed neotendon similar but not identical to normal tendon
1992	Dunn	*in vivo*	Rabbit ACL prosthesis	Gluteraldehyde, DHT/EDC	► Glut had chronic inflammatory response, remained at 20 weeks ► Glut lower strength than unimplanted controls ► DHT/EDC by 20 weeks completely degraded ► DHT/EDC stronger than unimplanted prosthesis
1993	Dunn	*in vitro*	strength and degradation	Gluteraldehyde, DHTC	► DHTC has greater tensile strength and faster degradation rate
1993	Chvapil	*in vivo*	decellularized tendon fibers - braided goat ACL prosthesis	HMDIC	► At 6 months, 40-60% scaffold was degraded and replaced with neoligament ► Lost mechanical strength quickly
1995	Weadock	*in vitro*	mechanical properties and degradation with physical crosslinking	UV (15, 30, 60, 120, 240 min), DHT (3, 5 days)	► UV and DHT caused partial fragmentation in collagen a chains ► UV and DHT increase strength and stiffness ► Maximum UV crosslinking by 30 minutes
1995	Kemp	*in vivo*	remodeling of scaffolds in rat abdomin and canine ACL	EDC	► Increased crosslinking leads to slower or less remodeling ► Intramolecular crosslinks increase persistance time because natural crosslinks are intermolecular ► Successful implantion in canine ACL at 12 weeks

Table 2.3 Collagen Thread Research Summary. *Summary of collagen thread research, highlighting crosslinking and key results (cont. on next page…)*

...continued from previous page

Year	Authors	Study Type	Investigation	Crosslinking	Important Outcomes
1995	Pins	*in vitro*	self-assembled vs. insoluble	DHT (5 days)	► Strength similar to rat tail tendon and greater than insoluble ► Greater fibril packing density, alignment, and molecular orientation than insoluble
1995	Dunn	*in vitro*	ACL and PT fibroblast interactions with bundles	DHT (3 days)	► Collagen synthesis greater on threads than tissue culture dish ► Patellar tendon (PT) fibroblasts proliferate more than ACL fibroblasts
1997	Pins	*in vitro*	self-assembled threads with stretch	DHT (5 days)	► Stretch increase strength and collagen fibril alignment
1997	Pins	*in vitro*	self-assembled with stretch and decorin	DHT (5 days)	► Stretch increases fibril alignment and tensile strength ► Decorin increased tensile strength
1997	Bellincampi	*in vitro*	mechanical properties, cell attachment and proliferation with crosslinking	Uncrosslinked, UV (30 min), DHT (3, 5 days), HMDIC	► Increased tensile strength and stiffness with all crosslinking types ► No difference in cell number between UV and DHT ► Cytotoxic effect of HMDIC
2001	Koob I & II	*in vitro*	biocompatibility	NDGA	► NDGA is cytotoxic but can be rinsed out ► Cells migrate from explants onto NDGA/Coll threads in similar quanties to control ► Cells attach to NDGA/Collagen coated plates similar to control
2002	Koob	*in vitro*	mechanical properties	NDGA	► Tensile strength greater than gluteraldehyde or EDC
2003	Gentleman	*in vitro*	structural and viscoelastic properties	EDC	► Thread diameter effects tensile strength ► Addition of cells increased strength of fiber imbedded gel scaffolds
2004	Dunn	*in vitro*	mechanical properties with cyclic loading in enzymatic solutions	UV (30 min), EDC	► Cyclic loading decrease tensile strength in enzymatic solutions greater for UV than EDC
2006	Gentleman	*in vitro*	tissue engineered ligament - cell seeded thread/gel	EDC	► Over 20 days in culture, scaffolds did not degrade or lose strength ► Scaffold with cells were stronger than unseeded ► Scaffolds showed ligament-like staining

2.2.2.2 Other Novel Biopolymer Threads

Although collagen threads have typically been the mostly highly investigated thread for ACL regeneration, researchers have recently begun investigating alternatives including silk and chitosan hybrid co-polymers. Research by Altman, Kaplan, and colleagues has investigated the use of spider silk for ACL repair because of the inherent mechanical strength of the material. Bundles of twisted silk threads have mechanical strengths large enough to withstand normal ACL loading,[87] and have been modified by coating in RGD sequences to improve attachment and proliferation on the matrices *in vitro*.[88] While these materials have demonstrated some success *in vitro*, silk based biomaterials necessitate the removal of sericin to avoid biocompatibility issues, can lead to encapsulation when proteolytic attack by macrophages and giant cells is aborted, and have possible sensitization or allergic responses in certain individuals.[89] Furthermore, these materials have markedly slow *in vivo* degradation profiles that may not be suitable to match the rate of neoligament synthesis for tissue regeneration applications.[89] Investigators have also begun to examine chitosan[90, 91] and chitosan/hyaluronan hybrids[92, 93] because of the advantageous cell adhesive properties of these matrices.[94] Chitosan, a cationic polysaccharide, was mixed with alginate, an anionic polysaccharide, to make polyion threads with tensile strengths reaching those necessary for applications in ligament regeneration.[90, 91] However, these ultimate tensile strengths were determined dry, while the hydrated strength has been estimated to decrease greater than 40%.[90] Furthermore the *in vivo* degradation profiles are unclear while the strength of the matrices are determined by calcium ions which are readily removed *in vivo* causing rapid degradation and loss of strength.[90]

2.3 Extracellular Matrix (ECM)

The ECM makes up the structural environment surrounding connective tissue cells, providing the bulk of the mechanical properties of connective tissue. ECM also asserts a strong influence on cell shape, growth, metabolism, migration, differentiation and ultimately in cell fate (Figure 2.7). Although collagens make up a significant portion of healthy connective tissue (see ACL Composition 2.1.1.1, pg. 9), the ECM contains numerous other families of molecules that play significant roles in cell signaling including proteoglycans, GAGs, and other matrix glycoproteins such as fibronectin and tenascin. Furthermore, during wound healing, a strikingly different ECM milieu surrounds a cell signaling it to slowly remodel and regenerate healthy tissue. This matrix signaling occurs largely through cell to matrix connections called integrins.

2.3.1 Integrins and Matrix Signaling

Integrins are heterodimeric transmembranous proteins that anchor a cell to the ECM and connect the matrix outside the cell to the cytoskeleton and ultimately regulate gene expression. Integrins consist of two subunits, α and β, noncovalently bound to each other, that in various combinations have different binding and signaling specificity.[95] Both subunits have long extracellular domains, a transmembrane portion, and often short cytoplasmic tails that attach to the cytoskeleton, enabling integrins to act as the link between the ECM and cytoskeleton.[95] As integrins bind to the ECM, they cluster and associate with signaling complexes that promote the assembly of cytoskeletal actin filaments.[96] In a positive feedback loop, this reorganization of actin filaments, in turn, increases integrin clustering leading to large aggregates called focal adhesions that can be

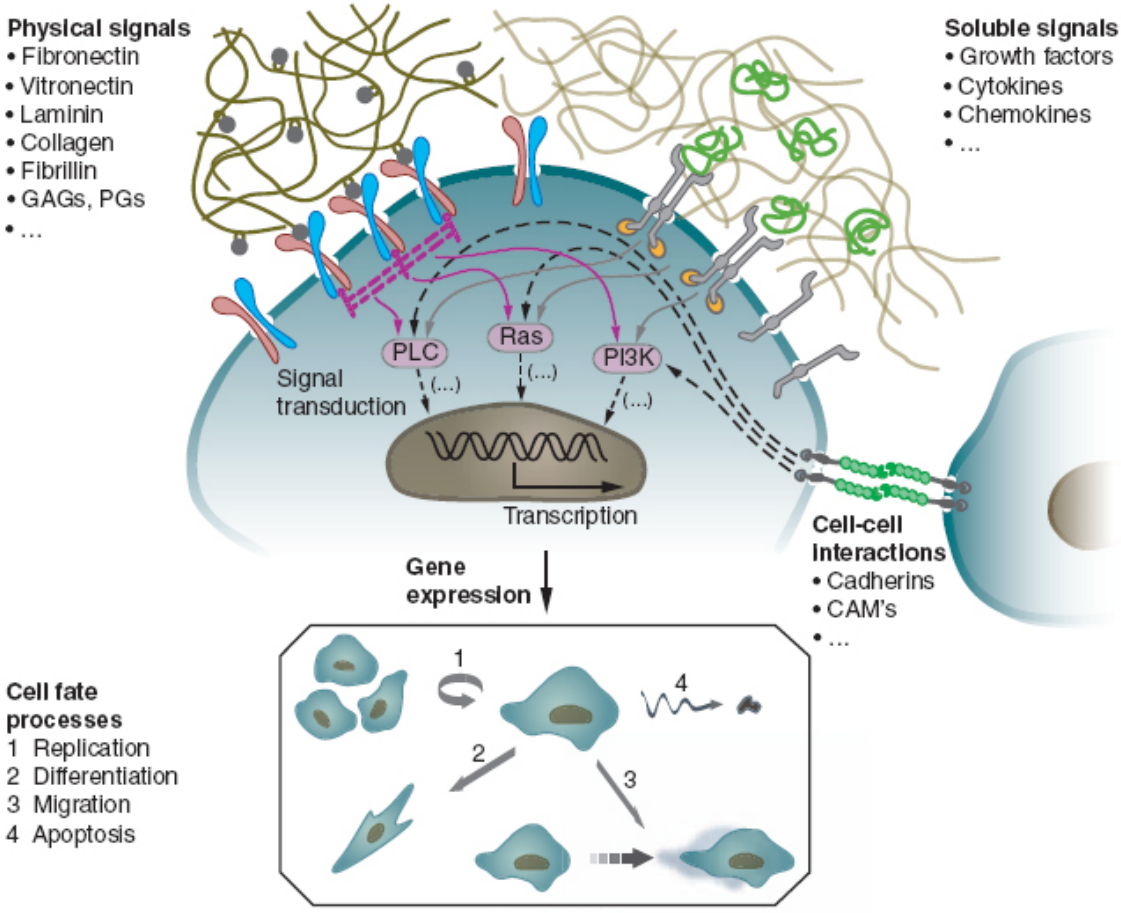

Figure 2.7: ECM control of cell signaling. The matrix, through transmembranous integrin receptors, sends signals to the nucleus that regulate transcription and gene expression. The changes in gene expression ultimately alter cell fate processes such as differentiation and migration.[96b]

visualized with immunofluorescence microscopy.[96] Consequently, the high local concentrations of integrins and associated signaling proteins facilitate the regulation of intracellular signaling pathways ultimately leading to changes in gene expression.[96]

In this manner, cells actively attach to the matrix, modify the matrix, and are regulated by the matrix simultaneously. The ability of a cell to make these anchorages dictate whether it will migrate, proliferate, differentiate, or synthesize matrix.[97] Furthermore, as a cell modifies the surrounding ECM, the surrounding ECM alters the cell signaling in a continually changing feedback loop termed dynamic reciprocity. Dynamic reciprocity plays a critical role in modulating fibroblast function in the spatially and temporally complex environment of a healing wound.

2.3.2 ECM in Wound Healing

During wound healing, the ECM acts not only as structural support, but helps actively direct and guide wound healing. A provisional matrix composed largely of fibrin, fibronectin, and a host of growth factors (see Fibrin Provisional Matrix 2.4.1, pg. 24) is initially formed in the wound and gradually replaced with new ECM components such as type I collagen and type III collagen. All of these components have been implicated in directing cell migration, proliferation, and differentiation through matrix signaling. Fibroblasts migrate into the wound attaching readily to fibronectin bound to fibrin[98-100] and likely fibrin itself.[68, 101] Once the fibroblasts have repopulated the wound, they switch from a migratory phenotype to a profibrotic phenotype marked by the drastic increase in collagen production[71] as well as TGF-β production,[102] which concurrently stimulates increased collagen production[103, 104] in a positive feedback loop.[68] However, as the fibrin matrix is degraded and replaced with the newly synthesized collagen, the fibroblasts cease collagen production despite the persistence of TGF-β expression.[102] Furthermore, collagen matrix has been demonstrated to suppress fibroblast proliferation[105] while fibrin matrices show no effect on the proliferative or matrix synthesizing potential of fibroblasts.[68, 102]

2.4 Fibrin, FGF-2, and the Provisional Matrix

2.4.1 Fibrin Provisional Matrix

The provisional matrix acts not only as hemostatic plug to prevent blood loss, but also promotes granulation tissue formation by providing a scaffold for the contact guided migration and proliferation of fibroblasts into the wound and a sponge for cytokines and

growth factors.[106] The basic structural protein of this matrix is fibrin, assembled from the plasma protein fibrinogen (see Fibrin Formation, pg. 25). Fibrin has a high binding affinity for cytokines, growth factors, proteases, and protease inhibitors. It therefore binds and localizes key ingredients from the plasma milieu to the matrix to promote key cell functions of wound healing. Fibrin directly binds matrix proteins that support cell migration including fibronectin,[107] vitronectin,[108] and hyaluronan[109] as well growth factors that promote proliferation and matrix synthesis including TGF-β,[110] FGF-2,[111] and PDGF.[110] Also, due to its ability to bind heparin and heparin sulfate,[112] fibrin indirectly alters other heparin-binding growth factors and can modulate those growth factor's functions.[113] Furthermore, through integrin signaling, fibrin itself has demonstrated some control over cell function and response to other factors through integrin signaling.[102, 114] When combined, the elements of the provisional matrix including fibrin, growth factors, and other biologically active molecules act synergistically to promote cellular infiltration and remodeling to ultimate regenerate injured tissues.

2.4.2 Fibrin

Fibrin is formed from the conversion of fibrinogen, a glycoprotein found circulating in blood plasma at a concentration of 3-7 mg/ml, into fibrin by the enzyme thrombin.[110, 111] Fibrinogen is an elongated protein, 45 nm in length, with two D domains on the outside, connected by chains to a central E domain. Upon exposure to thrombin, binding sites are exposed through cleavage on the top (E_A) and bottom (E_B) of the central E domain. These open binding sites then allow for association with outer D-domains of adjacent fibrinogen molecules, leading to the aligned, end-to-middle staggered overlap arrangement. As polymerization occurs, protofibrils are further assembled laterally and branch forming a complex intertwined network.(Figure 2.8).[106, 115] This network is naturally crosslinked by the formation of intermolecular isopeptide bonds between γ chains by factor XIIIa.[116, 117]

2.4.2.1 Fibrin Biomaterials

Because of the role fibrin plays in the provisional matrix for wound healing (see Fibrin Provisional Matrix 2.4.1, pg. 24) and as a model of fibroplasia,[118] fibrin biomaterials have been studied for diverse applications in the healing injured tissues. Currently, the use of fibrin for applications in ligament regeneration have not been investigated due to the limited initial mechanical strength of typical fibrin gel matrices. However, biomaterials produced *in vitro* of fibrin can have widely varying mechanical

and structural properties dependent on the initial concentration of fibrinogen.

For example, fibrin hydrogels are produced at low fibrinogen concentrations and have been widely studied for engineering applications ranging from cardiovascular grafts[119-122] to bioengineered cartilage.[123-125] However, like most gels, these materials lack sufficient mechanical strength necessary for the functional replacement of load bearing tissue structures. Higher fibrinogen concentrations are commercially available in adhesive sprays or glues used as sealants to control bleeding during surgery[126-129] and have recently been investigated for cell delivery.[130-132] To take advantage of the wound healing cell signaling capabilities of fibrin and compensate for its lack of mechanical strength, cells have been seeded in fibrin gels onto a polymer mesh[133] for cardiovascular[134] and orthopedic applications.[135, 136]

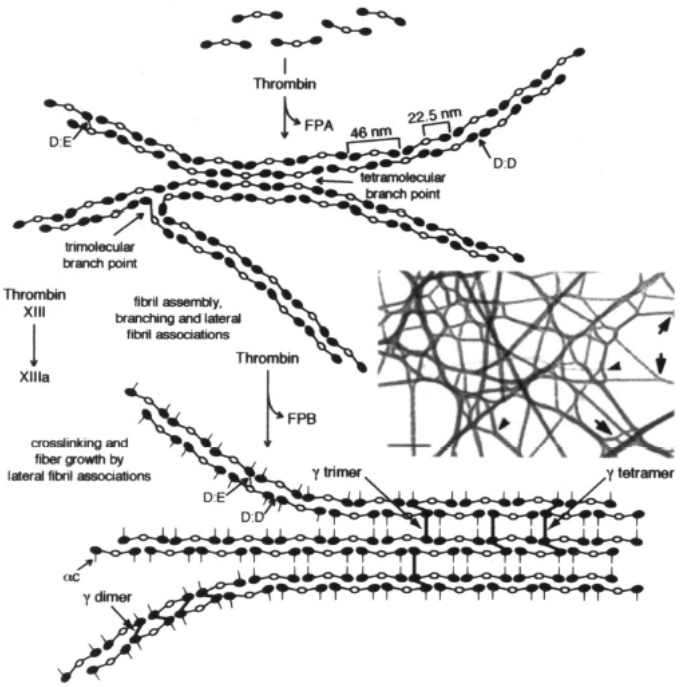

Figure 2.8: Schematic diagram of fibrin assembly. (Top) *Assembly of fibrin begins with non-covalent interactions (D:E) to form end-to-middle staggered overlapping double-stranded fibrils. Fibrils also branch and undergo lateral associations to form wider fibrils and fibers. [Inset: critical point dried thin fibril matrix containing branch junctions (arrows); bar, 100 nm].* (Bottom) *After cleavage of fibrinopeptide B (FPB) , αC domains become available for self-association with other αC domains, thereby promoting lateral fibril associations and fiber assembly. [115]*

2.4.3 FGF-2

Fibroblast growth factor-2, (basic FGF (bFGF); FGF-2), is one of a family of 22 fibroblast growth factors originally isolated and investigated for it's mitogenic effect on cells.[137] Typical FGF-2 is an 18 kD, single-chain polypeptide constructed from 146 amino acids in a trigonal pyramid shape formed by 12 antiparallel β strands including a 100 amino core region largely conserved across the FGF family of growth factors.[137-139] FGFs activate a small subset of 4 specific single pass transmembrane receptors

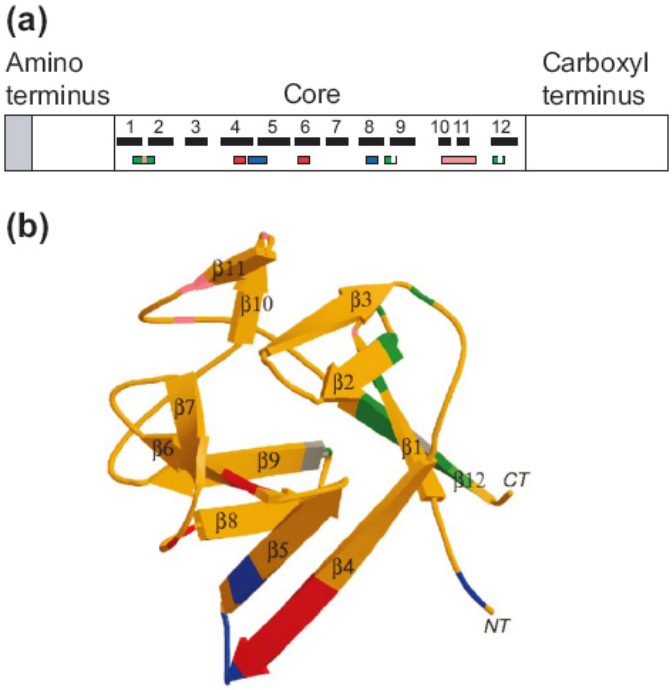

Figure 2.9: FGF-2 Structure. (a) Diagram of conserved core regions (black), heparin-binding domains (pink) and FGFR binding domains (green) on FGF-2. (b) 3-D diagram of FGF-2 color coded as above.[137]

(FGFR1-4) with tyrosine kinase activity.[137, 138] Ligand binding to the extracellular domain of the FGFR initiates receptor dimerization[113] leading to signal transduction that ultimately regulates gene expression.

FGF-2 plays a role during both development and wound healing in a vast array of tissue types including bone, nerve, and lung as well as soft connective tissue including skin, tendon, and ligament.[140] While generally considered a mitogen to most cell types, FGF-2 causes cell type dependent effects on migration, proliferation, differentiation, and apoptosis.[138] For example, while FGF-2 promotes proliferation in keratinocytes[141] and endothelial cells,[142] it arrests the cell cycle in chondrocytes[143] and promotes differentiation of neuronal stem cells.[144] How any particular cell is affected is dependent on not only cell type, but maturation stage as well as other concurrent signaling events.[138] One notable confounding factor is matrix binding, especially to heparin and fibrin, which can significantly modulate FGF-2 activity.

2.4.3.1 ECM and FGF-2 Combinatorial Signaling

The ultimate response to FGF-2 is not dictated independently by the growth factor, but rather the effects are mediated by extracellular matrix interactions in concert with growth factor receptor binding. Traditionally, FGF signaling involves heparin or heparin sulfate binding, likely forming a ternary complex between FGF and FGFR.[113] Dimerization of receptors required for activation are promoted by heparin,[145] increasing receptor-FGF-2 affinity 10 fold.[146] However, the 3-D structure determined by x-ray crystallography has shown the receptor binding site and heparin binding site are separated by approximately 25 angstroms and are on different faces of the protein, suggesting that these functions could interact independently.[139] Heparin has been

found to bind fibrin and considered present in the provisional matrix[112] where importantly, FGF-2 binding to heparin helps to prevent thermal, proteolytic, or pH dependent degradation.[113]

Although not investigated as abundantly as heparin and heparin sulfate, fibrin has also been implicated in the regulation of FGF-2 signaling. FGF-2 binds specifically and saturably to both fibrinogen and polymerized fibrin with a low Kd values ranging from 1.3 nM for high affinity sites to 260 nM for low affinity binding sites.[111] Therefore in normal plasma concentrations (approximately 7 μM for fibrinogen and 6 pM or less for FGF-2) all FGF-2 should be bound to fibrinogen[111] and *in vivo,* FGF is likely stored in a bound state, becoming functionally available upon release[147]. Similar to heparin and heparin sulfate, FGF-2 binding to fibrin prevents proteolytic degradation. [148] Furthermore the binding of FGF-2 to fibrin also has the potential to facilitate the aggregation of growth factor and integrin receptors to promote signal integration.[149] Integrin $\alpha_v\beta_3$ and FGFR1 colocalize when both fibrinogen and FGF-2 are present [150] within the focal adhesion complex.[151] Together fibrin and FGF-2 potentiate cell proliferation[142] in a manner not seen with FGF-1[149] and requires the integrin $\alpha_v\beta_3$.[150, 152] Additionally, fibrin acts as a cofactor with FGF-2 in regulating gene expression of proteins involved in pericellular matrix degradation.[153] Combined, this data suggests that the matrix aids in the spatial regulation of growth factor receptors, integrins, and signaling molecules.

2.4.3.2 FGF-2 In Tendon/Ligament

Specifically, the effects of FGF-2 have been investigated on tendon and ligament during both *in vitro* and *in vivo* experiments and most typically demonstrating increased wound healing characteristics.[154] *In vitro*, FGF-2 increases proliferation[155, 156] as well as migration of tendon fibroblasts in a wound closure model[156] while upregulating the expression of integrins $\alpha_v\beta_3$ and $\alpha_5\beta_1$, which are important for angiogenesis and tendon healing.[152] *In vivo*, after injection into healing tendons, FGF-2 increased type III collagen content as well as tenocyte proliferation.[157] Using an *in vivo* canine ligament model, addition of FGF-2 increased the healing response marked by enhanced neovascularization.[158] Similarly, early wound healing was enhanced with the addition of FGF-2 in a fibrin gel to a defect MCL model.[159]

Like many growth factors, the effects of FGF-2 are considered both dose-dependent and time-dependent. FGF-2 stimulated proliferation as well as type I and type III collagen production in rotator cuff tenocytes at low doses, but at higher values suppressed

collagen production in a dose-dependent manner.[155] During injury and surgical reconstruction studies, researchers have seen time dependent effects. Chang et al. found expression of FGF-2 post injury remained elevated from the first postoperative day and remained elevated through the 56 day length of experimentation.[160] Similarly, Kuroda et al. measured growth factors including FGF-2 during ACL reconstruction surgery. They found high levels of FGF-2 at early post-operative times with levels increasing up to 3 weeks, followed by a precipitous decline.[161] The authors suggest that these temporal effects mimic the pattern of extrinsic cell infiltration and revascularization and could therefore be partially attributed to those phenomena.[161]

2.5 Migration in Wound Healing

Cell migration plays a fundamental role in the healing of tissues including the ACL. In order to repair torn tissues such as the ACL, cells, typically fibroblasts, must migrate from the wound margin to repopulate and ultimately regenerate the damaged tissue. This migration can be induced by stimuli ranging from a lack of cell-cell contacts to chemotactic gradients, while the rate of migration is modulated by numerous chemical and physical signals. Furthermore, in vivo studies of collagen thread prostheses have implicated a lack of fibroblast tissue ingrowth as a crucial impediment to complete regeneration of torn ligaments.[23] The following sections describe current *in vitro* models of cell migration and the stimuli that have shown to modulate migration in these systems.

2.5.1 Mechanics of Cell Migration

Cell migration occurs through the coordination of dynamic matrix adhesion and propulsion by cytoskeletal contraction. Although occurring simultaneously, the mechanics of cell migration can be conceptually divided into steps. The process begins by the protrusion of lamellipodia at the leading edge of the cell, extended outwards through actin filament polymerization. The cell then actively adheres to the matrix via integrins which cluster into focal adhesions. Contraction by myosin motor interaction with actin filaments translocates the cytoplasm and organelles forward. Finally, adhesions in the rear of the cell must detach to release the cell while integrins are recycled to the leading edge to form new adhesions.[163, 164] Although the direction of locomotion is generally considered random in the absence of variable stimuli, cells are polarized in the direction of movement and persistent, oriented migration commonly occurs *in vivo* and *in vitro* through various stimuli.[164]

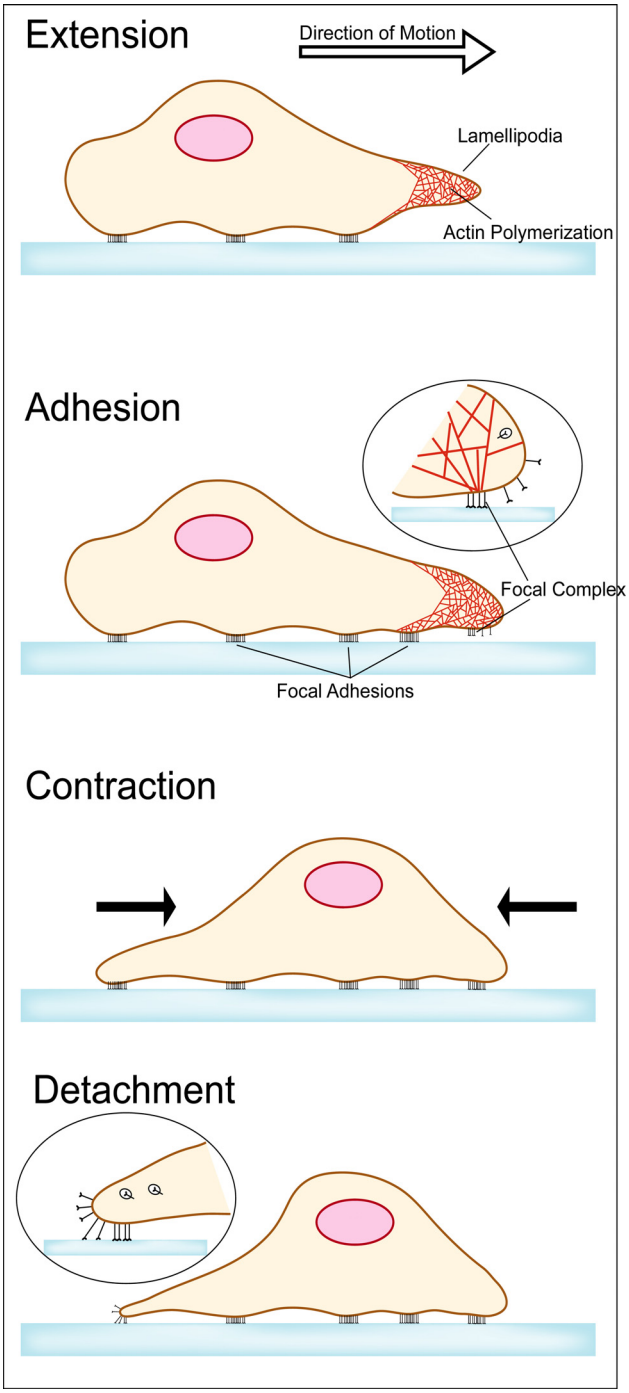

Figure 2.10: Cell migration occurs in several simultaneous steps. Lamellipodia extend by actin polymerization and create new attacments to the matrix through focal adhesions. The cytoskeleton contracts to pull the cell forward and old focal adhesions at the rear of the cell are detached. [162, 163]

2.5.2 Stimuli of Cell Migration

Numerous pathophysiological conditions such as a lack of cell-cell contact after injury induce the directed migration of fibroblasts into the provisional matrix. Both the speed (rate) and velocity (vector) of cell migration can be altered through several stimuli including chemotaxis, haptotaxis, durotaxis and contact guidance.[165, 166] Chemotaxis is the directed migration of cells in response to soluble factors, in this case in the wound milieu. During wound healing, chemoattractants diffuse from a source to an area of lower concentration, while cells including leukocytes and fibroblast migrate up the gradient. With haptotaxis, cell migration is promoted directionally by the substratum rather than soluble factors. Protruding lamellopodia compete for finite attachments and will preferentially extend in the direction of increasing attachments sites. Although still related to the substratum like haptotaxis, contact guidance is simply the tendency of cells to align along discontinuities in the substrata and preferentially migrate in this oriented direction.[165] The stiffness or rigidity of the matrix upon which or within which a cell exists also has been shown to alter the rate and

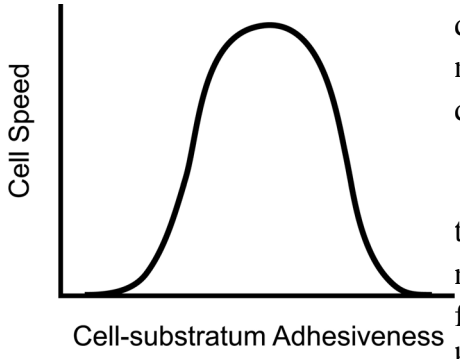

Figure 2.11: The rate at which a cell migrates on a particular substratum is a function of how well it attaches to the surface. Too many or two few attachments will reduce cell speed.[166]

directionality of cell migration with preferential migration towards stiffer substrates,[167] termed durotaxis.

During wound healing, the migration of cells into the provisional matrix is strongly influence by the matrix itself. The fibrin-fibronectin matrix stimulates fibroblast migration through a combination of haptotaxis and fibrin fibril mediated contact guidance.[165] Furthermore, the ability of a cell to both make and break adhesions with the matrix influence the rate of motility (Figure 2.11).[166, 168] Attachments in granulation tissue are facilitated by fibronectin while hyaluronan has been implicated in the low impedance to cell motility or disadhesion from the matrix.[165]

2.5.3 *In Vitro* Models of Cell Migration

Cell migration studies *in vitro* typically employ Boyden chambers or visualize migration on flat surface-coated two-dimensional substrates, however these studies do not accurately reflect the complex three-dimensional environment of wound healing. To improve on these systems, wound healing research has investigated alternative migration models utilizing reconstituted fibrin gels. Fibroblast migration has been modeled by placing explants of tendons in a fibrin gel and measuring the migration and proliferation of fibroblast from the explants into the matrix.[169] Other researchers have placed fibrin gels over cultured fibroblasts[170] or placed fibroblasts on plasma clots[171, 172] and measured the migration on and into the clots. Greiling and Clark developed the most sophisticated of these systems by placing cells in a collagen gel and surrounding the cell-seeded gel with a fibrin matrix.[173, 174] In this manner, they were able to visualize cells migrating from the collagen gel, generally considered an *in vitro* model of dermis or wound margin tissue, and into a fibrin matrix that acts as a 3-D ECM structural model of granulation tissue.

While no *in vitro* model of ligament wound healing or ligament scaffold regeneration currently exists, some relevant assays have been developed specifically for tendon and ligament. For example, ACL and MCL fibroblasts were investigated in a wounded tissue culture monolayer. After reaching confluence, half of a monolayer culture of ACL or MCL fibroblasts were scraped from a culture dish allowing the remaining fibroblasts to

migrate into the newly empty area and imaged.[62] Ricci et al. measured tendon cell growth rates on synthetic fibers by placing tendon explants perpendicularly across carbon fibers elevated above tissue culture plates and measuring the migration of cells out of the explants onto the fibers.[175, 176] Other researchers have measured the outgrowth of ACL and MCL fibroblasts from explants placed onto culture dishes[177] and onto collagen/GAG sponges.[178, 179] Finally, during studies of the biocompatibility of collagen threads crosslinked with a novel NDGA crosslinker, Koob and researchers placed threads into a tendon explant and measured the quantity of cells grown onto the threads at various time points.[180]

REFERENCES

[1] Gray H, "" in *Anatomy of the human body*, Lewis W (Ed.), Bartleby, 2000. .

[2] Miller R, "Knee Injuries" in *Campbell's operative orthopaedics*, Canale S (Ed.), Mosby, 2003. pp. 2165-2337.

[3] Butler D, Noyes F & Grood E. Ligamentous restraints to anterior-posterior drawer in the human knee. a biomechanical study. *J Bone Joint Surg Am* **62**: pp. 259-270. (1980).

[4] Butler D. Anterior cruciate ligament: its normal response and replacement. *J Orthop Res* **7**: pp. 910-921. (1989).

[5] Shelburne KB, Pandy MG, Anderson FC & Torry MR. Pattern of anterior cruciate ligament force in normal walking. *J Biomech* **37**: pp. 797-805. (2004).

[6] Ge Z, Yang F, Goh JCH, Ramakrishna S & Lee EH. Biomaterials and scaffolds for ligament tissue engineering. *J Biomed Mater Res A* **77**: pp. 639-652. (2006).

[7] Buckwalter J & Woo S, "Ligaments" in *Orthopaedic sports medicine*, DeLee J & Drez D (Eds.), Saunders, 2003. pp. 39-50.

[8] Duthon VB, Barea C, Abrassart S, Fasel JH, Fritschy D & Menetrey J. Anatomy of the anterior cruciate ligament. *Knee Surg Sports Traumatol Arthrosc* **14**: pp. 204-213. (2006).

[9] Toy B, Yeasting R, Morse D & McCann P. Arterial supply to the human anterior cruciate ligament. *J Athl Train* **30**: pp. 149-152. (1995).

[10] Bray RC, Leonard CA & Salo PT. Correlation of healing capacity with vascular response in the anterior cruciate and medial collateral ligaments of the rabbit. *J Orthop Res* **21**: pp. 1118-1123. (2003).

[11] Amiel D, Frank C, Harwood F, Fronek J & Akeson W. Tendons and ligaments: a morphological and biochemical comparison. *J Orthop Res* **1**: pp. 257-265. (1984).

[12] Vunjak-Novakovic G, Altman G, Horan R & Kaplan DL. Tissue engineering of ligaments. *Annu Rev Biomed Eng* **6**: pp. 131-156. (2004).

[13] Linsenmayer T, "Collagen" in *Cell biology of extracellular matrix*, Hay E (Ed.), Plenum Press, 1991. pp. 7-44.

[14] Yannas I, "Natural Materials" in *Biomaterials science*, Ratner B, Hoffman A, Schoen F & Lemons J (Eds.), Elsevier Academic Press, 2004. pp. 127-137.

[15] Silver FH, Freeman JW & Seehra GP. Collagen self-assembly and the development of tendon mechanical properties. *J Biomech* **36**: pp. 1529-1553. (2003).

[16] Schoen F & Mitchell R, "Tissues, The Extracellular Matrix, and Cell-Biomaterial Interactions" in *Biomaterials science*, Ratner B, Hoffman A, Schoen F & Lemons J (Eds.), Elsevier Academic Press, 2004. pp. 260-281.

[17] Silver FH, Horvath I & Foran DJ. Mechanical implications of the domain structure of fiber-forming collagens: comparison of the molecular and fibrillar flexibilities of the alpha1-chains found in types i-iii collagen. *J Theor Biol* **216**: pp. 243-254. (2002).

[18] Watanabe M, Nojima M, Shibata T & Hamada M. Maturation-related biochemical changes in swine anterior cruciate ligament and tibialis posterior tendon. *J Orthop Res* **12**: pp. 672-682. (1994).
[19] Hart RA, Woo SL & Newton PO. Ultrastructural morphometry of anterior cruciate and medial collateral ligaments: an experimental study in rabbits. *J Orthop Res* **10**: pp. 96-103. (1992).
[20] Lyon RM, Akeson WH, Amiel D, Kitabayashi LR & Woo SL. Ultrastructural differences between the cells of the medical collateral and the anterior cruciate ligaments. *Clin Orthop Relat Res* : pp. 279-286. (1991).
[21] Benjamin M & Ralphs JR. Tendons and ligaments--an overview. *Histol Histopathol* **12**: pp. 1135-1144. (1997).
[22] McNeilly CM, Banes AJ, Benjamin M & Ralphs JR. Tendon cells in vivo form a three dimensional network of cell processes linked by gap junctions. *J Anat* **189 (Pt 3)**: pp. 593-600. (1996).
[23] Dunn MG, Liesch JB, Tiku ML & Zawadsky JP. Development of fibroblast-seeded ligament analogs for acl reconstruction. *J Biomed Mater Res* **29**: pp. 1363-1371. (1995).
[24] Van Eijk F, Saris DBF, Riesle J, Willems WJ, Van Blitterswijk CA, Verbout AJ & Dhert WJA. Tissue engineering of ligaments: a comparison of bone marrow stromal cells, anterior cruciate ligament, and skin fibroblasts as cell source. *Tissue Eng* **10**: pp. 893-903. (2004).
[25] Geiger MH, Green MH, Monosov A, Akeson WH & Amiel D. An in vitro assay of anterior cruciate ligament (acl) and medial collateral ligament (mcl) cell migration. *Connect Tissue Res* **30**: pp. 215-224. (1994).
[26] Nagineni CN, Amiel D, Green MH, Berchuck M & Akeson WH. Characterization of the intrinsic properties of the anterior cruciate and medial collateral ligament cells: an in vitro cell culture study. *J Orthop Res* **10**: pp. 465-475. (1992).
[27] Wiig ME, Amiel D, Ivarsson M, Nagineni CN, Wallace CD & Arfors KE. Type i procollagen gene expression in normal and early healing of the medial collateral and anterior cruciate ligaments in rabbits: an in situ hybridization study. *J Orthop Res* **9**: pp. 374-382. (1991).
[28] National Center for Health Statistics & Centers for Disease Control and Prevention. National ambulatory medical care survey. : . (2003).
[29] Woo SL, Livesay GA & Engle C. Biomechanics of the human anterior cruciate ligament. acl structure and role in knee motion. *Orthop Rev* **21**: pp. 835-842. (1992).
[30] Woo SL, Hildebrand K, Watanabe N, Fenwick JA, Papageorgiou CD & Wang JH. Tissue engineering of ligament and tendon healing. *Clin Orthop Relat Res* : p. S312-23. (1999).
[31] Gillquist J, "Knee stability: Its effect on articular cartilage" in *Articular cartilage and knee joint function: basic science and arthroscopy*, Ewing DD (Ed.), Raven Press, 1990. .
[32] Mow VC, Setton LA & Ratcliff A, " Structure-function relationship of articular cartilage and the effects of joint instability and trauma on cartilage" in *Cartilage changes in osteoarthritis*, Brandt KD (Ed.), Indiana University School of Medicine, 1990. .
[33] Barrack RL, Bruckner JD, Kneisl J, Inman WS & Alexander AH. The outcome of nonoperatively treated complete tears of the anterior cruciate ligament in active young adults. *Clin Orthop Relat Res* : pp. 192-199. (1990).
[34] Caborn DN & Johnson BM. The natural history of the anterior cruciate ligament-deficient knee. a review. *Clin Sports Med* **12**: pp. 625-636. (1993).
[35] Irvine GB & Glasgow MM. The natural history of the meniscus in anterior cruciate insufficiency. arthroscopic analysis. *J Bone Joint Surg Br* **74**: pp. 403-405. (1992).
[36] Mayr HO, Weig TG & Plitz W. Arthrofibrosis following acl reconstruction--reasons and outcome. *Arch Orthop Trauma Surg* **124**: pp. 518-522. (2004).
[37] Hill CL, Seo GS, Gale D, Totterman S, Gale ME & Felson DT. Cruciate ligament integrity in osteoarthritis of the knee. *Arthritis Rheum* **52**: pp. 794-799. (2005).
[38] von Porat A, Roos EM & Roos H. High prevalence of osteoarthritis 14 years after an anterior cruciate ligament tear in male soccer players: a study of radiographic and patient relevant outcomes. *Ann Rheum Dis* **63**: pp. 269-273. (2004).

[39] Lohmander LS, Ostenberg A, Englund M & Roos H. High prevalence of knee osteoarthritis, pain, and functional limitations in female soccer players twelve years after anterior cruciate ligament injury. *Arthritis Rheum* **50**: pp. 3145-3152. (2004).
[40] Bray RC & Dandy DJ. Meniscal lesions and chronic anterior cruciate ligament deficiency. meniscal tears occurring before and after reconstruction. *J Bone Joint Surg Br* **71**: pp. 128-130. (1989).
[41] Keene GC, Bickerstaff D, Rae PJ & Paterson RS. The natural history of meniscal tears in anterior cruciate ligament insufficiency. *Am J Sports Med* **21**: pp. 672-679. (1993).
[42] Ferber R, Osternig LR, Woollacott MH, Wasielewski NJ & Lee J. Gait mechanics in chronic acl deficiency and subsequent repair. *Clin Biomech (Bristol, Avon)* **17**: pp. 274-285. (2002).
[43] Osternig LR, Ferber R, Mercer J & Davis H. Human hip and knee torque accommodations to anterior cruciate ligament dysfunction. *Eur J Appl Physiol* **83**: pp. 71-76. (2000).
[44] Bray RC, Flanagan JP & Dandy DJ. Reconstruction for chronic anterior cruciate instability. a comparison of two methods after six years. *J Bone Joint Surg Br* **70**: pp. 100-105. (1988).
[45] Albright J, Carpenter J, Graf B, Richmond JC, *Knee and leg: soft tissue trauma. orthopaedic knowledge update 6*, , American Academy of Orthopaedic Surgeons, 1999.
[46] Fu F & Musahl V. Review article: the future of knee ligament surgery. *Acta Clinica* **2**: pp. 101-107. (2002).
[47] Laurencin CT & Freeman JW. Ligament tissue engineering: an evolutionary materials science approach. *Biomaterials* **26**: pp. 7530-7536. (2005).
[48] Pennisi E. Tending tender tendons. *Science* **295**: p. 1011. (2002).
[49] Stone K, "Anterior Cruciate Ligament Repair" in *The knee joint: injury and repair*, , The Stone Foundation, (2005).
[50] Fu FH, Bennett CH, Lattermann C & Ma CB. Current trends in anterior cruciate ligament reconstruction. part 1: biology and biomechanics of reconstruction. *Am J Sports Med* **27**: pp. 821-830. (1999).
[51] Harner CD, Fu FH, Irrgang JJ & Vogrin TM. Anterior and posterior cruciate ligament reconstruction in the new millennium: a global perspective. *Knee Surg Sports Traumatol Arthrosc* **9**: pp. 330-336. (2001).
[52] Hiemstra LA, Webber S, MacDonald PB & Kriellaars DJ. Knee strength deficits after hamstring tendon and patellar tendon anterior cruciate ligament reconstruction. *Med Sci Sports Exerc* **32**: pp. 1472-1479. (2000).
[53] Cook JL, Feller JA, Bonar SF & Khan KM. Abnormal tenocyte morphology is more prevalent than collagen disruption in asymptomatic athletes' patellar tendons. *J Orthop Res* **22**: pp. 334-338. (2004).
[54] Lutz B, Ratard R, Dodson D, Malecki JM, Morse AC, Wiersma S, Perrotta D. Septic arthritis following anterior cruciate ligament reconstruction using tendon allografts --- florida and louisiana, 2000. *Morbidity and Mortality Weekly Report* **50**: pp. 1081-1083. (2001).
[55] Bellincampi LD, Closkey RF, Prasad R, Zawadsky JP & Dunn MG. Viability of fibroblast-seeded ligament analogs after autogenous implantation. *J Orthop Res* **16**: pp. 414-420. (1998).
[56] Marui T, Niyibizi C, Georgescu HI, Cao M, Kavalkovich KW, Levine RE & Woo SL. Effect of growth factors on matrix synthesis by ligament fibroblasts. *J Orthop Res* **15**: pp. 18-23. (1997).
[57] Spindler KP, Imro AK, Mayes CE & Davidson JM. Patellar tendon and anterior cruciate ligament have different mitogenic responses to platelet-derived growth factor and transforming growth factor beta. *J Orthop Res* **14**: pp. 542-546. (1996).
[58] Sung KL, Kwan MK, Maldonado F & Akeson WH. Adhesion strength of human ligament fibroblasts. *J Biomech Eng* **116**: pp. 237-242. (1994).
[59] Sung KL, Yang L, Whittemore DE, Shi Y, Jin G, Hsieh AH, Akeson WH, et al.. The differential adhesion forces of anterior cruciate and medial collateral ligament fibroblasts: effects of tropomodulin, talin, vinculin, and alpha-actinin. *Proc Natl Acad Sci U S A* **93**: pp. 9182-9187. (1996).
[60] Yang L, Tsai CM, Hsieh AH, Lin VS, Akeson WH & Sung KL. Adhesion strength differential of human ligament fibroblasts to collagen types i and iii. *J Orthop Res* **17**: pp. 755-762. (1999).

[61] Amiel D, Nagineni CN, Choi SH & Lee J. Intrinsic properties of acl and mcl cells and their responses to growth factors. *Med Sci Sports Exerc* **27**: pp. 844-851. (1995).
[62] Kobayashi K, Healey RM, Sah RL, Clark JJ, Tu BP, Goomer RS, Akeson WH, et al.. Novel method for the quantitative assessment of cell migration: a study on the motility of rabbit anterior cruciate (acl) and medial collateral ligament (mcl) cells. *Tissue Eng* **6**: pp. 29-38. (2000).
[63] Lee J, Green MH & Amiel D. Synergistic effect of growth factors on cell outgrowth from explants of rabbit anterior cruciate and medial collateral ligaments. *J Orthop Res* **13**: pp. 435-441. (1995).
[64] Petrigliano FA, McAllister DR & Wu BM. Tissue engineering for anterior cruciate ligament reconstruction: a review of current strategies. *Arthroscopy* **22**: pp. 441-451. (2006).
[65] Hefti FL, Kress A, Fasel J & Morscher EW. Healing of the transected anterior cruciate ligament in the rabbit. *J Bone Joint Surg Am* **73**: pp. 373-383. (1991).
[66] Frank CB, Hart DA & Shrive NG. Molecular biology and biomechanics of normal and healing ligaments--a review. *Osteoarthritis Cartilage* **7**: pp. 130-140. (1999).
[67] Molloy T, Wang Y & Murrell G. The roles of growth factors in tendon and ligament healing. *Sports Med* **33**: pp. 381-394. (2003).
[68] Clark R, "Wound Repair: Overview and General Considerations" in *The molecular and cellular biology of wound repair*, Clark R (Ed.), Plenum, 1996. .
[69] Desmouliere A & Gabbiani G, "The Role of the Myofibroblast in Wound Healing and Fibrocontractive Disease" in *The molecular and cellular biology of wound repair*, Clark R (Ed.), Plenum, 1996. .
[70] Gabbiani G, Schmid E, Winter S, Chaponnier C, de Ckhastonay C, Vandekerckhove J, Weber K, et al.. Vascular smooth muscle cells differ from other smooth muscle cells: predominance of vimentin filaments and a specific alpha-type actin. *Proc Natl Acad Sci U S A* **78**: pp. 298-302. (1981).
[71] Welch MP, Odland GF & Clark RA. Temporal relationships of f-actin bundle formation, collagen and fibronectin matrix assembly, and fibronectin receptor expression to wound contraction. *J Cell Biol* **110**: pp. 133-145. (1990).
[72] Desmouliere A, Redard M, Darby I & Gabbiani G. Apoptosis mediates the decrease in cellularity during the transition between granulation tissue and scar. *Am J Pathol* **146**: pp. 56-66. (1995).
[73] Goh JC, Ouyang H, Teoh S, Chan CKC & Lee E. Tissue-engineering approach to the repair and regeneration of tendons and ligaments. *Tissue Eng* **9 Suppl 1**: p. S31-44. (2003).
[74] Rovensky Y & Samoilov V. Morphogenetic response of cultured normal and transformed fibroblasts, and epitheliocytes, to a cylindrical substratum surface. possible role for the actin filament bundle pattern. *J Cell Sci* **107 (Pt 5)**: pp. 1255-1263. (1994).
[75] Guidoin MF, Marois Y, Bejui J, Poddevin N, King MW & Guidoin R. Analysis of retrieved polymer fiber based replacements for the acl. *Biomaterials* **21**: pp. 2461-2474. (2000).
[76] Bourke SL, Kohn J & Dunn MG. Preliminary development of a novel resorbable synthetic polymer fiber scaffold for anterior cruciate ligament reconstruction. *Tissue Eng* **10**: pp. 43-52. (2004).
[77] Buma P, Kok HJ, Blankevoort L, Kuijpers W, Huiskes R & Van Kampen A. Augmentation in anterior cruciate ligament reconstruction-a histological and biomechanical study on goats. *Int Orthop* **28**: pp. 91-96. (2004).
[78] Lu HH, Cooper JAJ, Manuel S, Freeman JW, Attawia MA, Ko FK & Laurencin CT. Anterior cruciate ligament regeneration using braided biodegradable scaffolds: in vitro optimization studies. *Biomaterials* **26**: pp. 4805-4816. (2005).
[79] Koob TJ, Willis TA & Hernandez DJ. Biocompatibility of ndga-polymerized collagen fibers. i. evaluation of cytotoxicity with tendon fibroblasts in vitro. *J Biomed Mater Res* **56**: pp. 31-39. (2001).
[80] Gentleman E, Lay AN, Dickerson DA, Nauman EA, Livesay GA & Dee KC. Mechanical characterization of collagen fibers and scaffolds for tissue engineering. *Biomaterials* **24**: pp. 3805-3813. (2003).
[81] Gentleman E, Livesay G, Dee K & Nauman E. Development of ligament-like structural organization and properties in cell-seeded collagen scaffolds in vitro. *Ann Biomed Eng* : pp. 1-11. (2006).

[82] Kato YP, Dunn MG, Zawadsky JP, Tria AJ & Silver FH. Regeneration of achilles tendon with a collagen tendon prosthesis. results of a one-year implantation study. *J Bone Joint Surg Am* **73**: pp. 561-574. (1991).
[83] Kemp P, Cavallaro J & Hastings D. Effects of carbodiimide crosslinking and load environment on the remodeling of collagen scaffolds. *Tissue Engineering* **1**: pp. 71-79. (1995).
[84] Cooper A. Thermodynamic studies of the assembly in vitro of native collagen fibrils. *Biochem J* **118**: pp. 355-365. (1970).
[85] Pins GD, Christiansen DL, Patel R & Silver FH. Self-assembly of collagen fibers. influence of fibrillar alignment and decorin on mechanical properties. *Biophys J* **73**: pp. 2164-2172. (1997).
[86] Pins G & Silver F. A self-assembled collagen scaffold suitable for use in soft and hard tissue replacement. *Materials Science and Engineering:C* **3**: pp. 101-107. (1995).
[87] Altman GH, Horan RL, Lu HH, Moreau J, Martin I, Richmond JC & Kaplan DL. Silk matrix for tissue engineered anterior cruciate ligaments. *Biomaterials* **23**: pp. 4131-4141. (2002).
[88] Chen J, Altman GH, Karageorgiou V, Horan R, Collette A, Volloch V, Colabro T, et al.. Human bone marrow stromal cell and ligament fibroblast responses on rgd-modified silk fibers. *J Biomed Mater Res A* **67**: pp. 559-570. (2003).
[89] Altman GH, Diaz F, Jakuba C, Calabro T, Horan RL, Chen J, Lu H, et al.. Silk-based biomaterials. *Biomaterials* **24**: pp. 401-416. (2003).
[90] Majima T, Funakosi T, Iwasaki N, Yamane S, Harada K, Nonaka S, Minami A, et al.. Alginate and chitosan polyion complex hybrid fibers for scaffolds in ligament and tendon tissue engineering. *J Orthop Sci* **10**: pp. 302-307. (2005).
[91] Wan ACA, Yim EKF, Liao I, Le Visage C & Leong KW. Encapsulation of biologics in self-assembled fibers as biostructural units for tissue engineering. *J Biomed Mater Res A* **71**: pp. 586-595. (2004).
[92] Funakoshi T, Majima T, Iwasaki N, Yamane S, Masuko T, Minami A, Harada K, et al.. Novel chitosan-based hyaluronan hybrid polymer fibers as a scaffold in ligament tissue engineering. *J Biomed Mater Res A* **74**: pp. 338-346. (2005).
[93] Funakoshi T, Majima T, Iwasaki N, Suenaga N, Sawaguchi N, Shimode K, Minami A, et al.. Application of tissue engineering techniques for rotator cuff regeneration using a chitosan-based hyaluronan hybrid fiber scaffold. *Am J Sports Med* **33**: pp. 1193-1201. (2005).
[94] Howling GI, Dettmar PW, Goddard PA, Hampson FC, Dornish M & Wood EJ. The effect of chitin and chitosan on the proliferation of human skin fibroblasts and keratinocytes in vitro. *Biomaterials* **22**: pp. 2959-2966. (2001).
[95] Ruoslahti E, "Integrins as Receptors for Extracellular Matrix" in *Cell biology of extracellular matrix*, Hay E (Ed.), Plenum Press, 1991. pp. 343-363.
[96] Giancotti FG & Ruoslahti E. Integrin signaling. *Science* **285**: pp. 1028-1032. (1999).
[96b] Lutolf MP & Hubbell JA. Synthetic biomaterials as instructive extracellular microenvironments for morphogenesis in tissue engineering. *Nat Biotechnol* **23**: pp. 47-55. (2005).
[97] Juliano RL & Haskill S. Signal transduction from the extracellular matrix. *J Cell Biol* **120**: pp. 577-585. (1993).
[98] Garcia-Pardo A, Pearlstein E & Frangione B. Primary structure of human plasma fibronectin. characterization of a 31,000-dalton fragment from the cooh-terminal region containing a free sulfhydryl group and a fibrin-binding site. *J Biol Chem* **260**: pp. 10320-10325. (1985).
[99] Lark MW, Laterra J & Culp LA. Close and focal contact adhesions of fibroblasts to a fibronectin-containing matrix. *Fed Proc* **44**: pp. 394-403. (1985).
[100] Mosher DF & Johnson RB. Specificity of fibronectin--fibrin cross-linking. *Ann N Y Acad Sci* **408**: pp. 583-594. (1983).
[101] Dejana E, Vergara-Dauden M, Balconi G, Pietra A, Cherel G, Donati MB, Larrieu MJ, et al.. Specific binding of human fibrinogen to cultured human fibroblasts. evidence for the involvement of the e domain. *Eur J Biochem* **139**: pp. 657-662. (1984).

[102] Clark RA, Nielsen LD, Welch MP & McPherson JM. Collagen matrices attenuate the collagen-synthetic response of cultured fibroblasts to tgf-beta. *J Cell Sci* **108 (Pt 3)**: pp. 1251-1261. (1995).
[103] Ignotz RA & Massague J. Transforming growth factor-beta stimulates the expression of fibronectin and collagen and their incorporation into the extracellular matrix. *J Biol Chem* **261**: pp. 4337-4345. (1986).
[104] Roberts AB, Sporn MB, Assoian RK, Smith JM, Roche NS, Wakefield LM, Heine UI, et al.. Transforming growth factor type beta: rapid induction of fibrosis and angiogenesis in vivo and stimulation of collagen formation in vitro. *Proc Natl Acad Sci U S A* **83**: pp. 4167-4171. (1986).
[105] Grinnell F. Fibroblasts, myofibroblasts, and wound contraction. *J Cell Biol* **124**: pp. 401-404. (1994).
[106] Clark RA. Fibrin and wound healing. *Ann N Y Acad Sci* **936**: pp. 355-367. (2001).
[107] Makogonenko E, Tsurupa G, Ingham K & Medved L. Interaction of fibrin(ogen) with fibronectin: further characterization and localization of the fibronectin-binding site.. *Biochemistry* **41**: pp. 7907-7913. (2002).
[108] Preissner KT & Jenne D. Vitronectin: a new molecular connection in haemostasis.. *Thromb Haemost* **66**: pp. 189-194. (1991).
[109] Weigel PH, Frost SJ, LeBoeuf RD & McGary CT. The specific interaction between fibrin(ogen) and hyaluronan: possible consequences in haemostasis, inflammation and wound healing.. *Ciba Found Symp* **143**: p. 248-61; discussion 261-4, 281-5. (1989).
[110] Clark RAF. Fibrin is a many splendored thing. *J Invest Dermatol* **121**: p. xxi-xxii. (2003).
[111] Sahni A, Odrljin T & Francis CW. Binding of basic fibroblast growth factor to fibrinogen and fibrin. *J Biol Chem* **273**: pp. 7554-7559. (1998).
[112] Odrljin TM, Shainoff JR, Lawrence SO & Simpson-Haidaris PJ. Thrombin cleavage enhances exposure of a heparin binding domain in the n-terminus of the fibrin beta chain. *Blood* **88**: pp. 2050-2061. (1996).
[113] Mohammadi M, Olsen SK & Ibrahimi OA. Structural basis for fibroblast growth factor receptor activation. *Cytokine Growth Factor Rev* **16**: pp. 107-137. (2005).
[114] Schwartz MA, Schaller MD & Ginsberg MH. Integrins: emerging paradigms of signal transduction.. *Annu Rev Cell Dev Biol* **11**: pp. 549-599. (1995).
[115] Mosesson MW, Siebenlist KR & Meh DA. The structure and biological features of fibrinogen and fibrin. *Ann N Y Acad Sci* **936**: pp. 11-30. (2001).
[116] Greenberg CS, Birckbichler PJ & Rice RH. Transglutaminases: multifunctional cross-linking enzymes that stabilize tissues.. *FASEB J* **5**: pp. 3071-3077. (1991).
[117] Lorand L. Factor xiii: structure, activation, and interactions with fibrinogen and fibrin.. *Ann N Y Acad Sci* **936**: pp. 291-311. (2001).
[118] Tuan TL, Song A, Chang S, Younai S & Nimni ME. In vitro fibroplasia: matrix contraction, cell growth, and collagen production of fibroblasts cultured in fibrin gels. *Exp Cell Res* **223**: pp. 127-134. (1996).
[119] Jockenhoevel S, Zund G, Hoerstrup SP, Chalabi K, Sachweh JS, Demircan L, Messmer BJ, et al.. Fibrin gel -- advantages of a new scaffold in cardiovascular tissue engineering. *Eur J Cardiothorac Surg* **19**: pp. 424-430. (2001).
[120] Long JL & Tranquillo RT. Elastic fiber production in cardiovascular tissue-equivalents. *Matrix Biol* **22**: pp. 339-350. (2003).
[121] Ross JJ & Tranquillo RT. Ecm gene expression correlates with in vitro tissue growth and development in fibrin gel remodeled by neonatal smooth muscle cells. *Matrix Biol* **22**: pp. 477-490. (2003).
[122] Swartz DD, Russell JA & Andreadis ST. Engineering of fibrin-based functional and implantable small-diameter blood vessels. *Am J Physiol Heart Circ Physiol* **288**: p. H1451-60. (2005).
[123] Fussenegger M, Meinhart J, Hobling W, Kullich W, Funk S & Bernatzky G. Stabilized autologous fibrin-chondrocyte constructs for cartilage repair in vivo. *Ann Plast Surg* **51**: pp. 493-498. (2003).
[124] Hunter CJ, Mouw JK & Levenston ME. Dynamic compression of chondrocyte-seeded fibrin gels: effects on matrix accumulation and mechanical stiffness. *Osteoarthritis Cartilage* **12**: pp. 117-130. (2004).

[125] Sims CD, Butler PE, Cao YL, Casanova R, Randolph MA, Black A, Vacanti CA, et al.. Tissue engineered neocartilage using plasma derived polymer substrates and chondrocytes. *Plast Reconstr Surg* **101**: pp. 1580-1585. (1998).
[126] Clark RA. Fibrin sealant in wound repair: a systematic survey of the literature. *Expert Opin Investig Drugs* **9**: pp. 2371-2392. (2000).
[127] Silver FH, Wang MC & Pins GD. Preparation and use of fibrin glue in surgery. *Biomaterials* **16**: pp. 891-903. (1995).
[128] Spotnitz WD & Prabhu R. Fibrin sealant tissue adhesive--review and update. *J Long Term Eff Med Implants* **15**: pp. 245-270. (2005).
[129] Amrani DL, Diorio JP & Delmotte Y. Wound healing. role of commercial fibrin sealants.. *Ann N Y Acad Sci* **936**: pp. 566-579. (2001).
[130] Gorodetsky R, Clark RA, An J, Gailit J, Levdansky L, Vexler A, Berman E, et al.. Fibrin microbeads (fmb) as biodegradable carriers for culturing cells and for accelerating wound healing. *J Invest Dermatol* **112**: pp. 866-872. (1999).
[131] Wechselberger G, Russell RC, Neumeister MW, Schoeller T, Piza-Katzer H & Rainer C. Successful transplantation of three tissue-engineered cell types using capsule induction technique and fibrin glue as a delivery vehicle. *Plast Reconstr Surg* **110**: pp. 123-129. (2002).
[132] van Griensven M, Zeichen J, Tschernig T, Seekamp A & Pape H. A modified method to culture human osteoblasts from bone tissue specimens using fibrin glue. *Exp Toxicol Pathol* **54**: pp. 25-29. (2002).
[133] Hokugo A, Takamoto T & Tabata Y. Preparation of hybrid scaffold from fibrin and biodegradable polymer fiber. *Biomaterials* **27**: pp. 61-67. (2006).
[134] Mol A, van Lieshout MI, Dam-de Veen CG, Neuenschwander S, Hoerstrup SP, Baaijens FPT & Bouten CVC. Fibrin as a cell carrier in cardiovascular tissue engineering applications. *Biomaterials* **26**: pp. 3113-3121. (2005).
[135] Ameer GA, Mahmood TA & Langer R. A biodegradable composite scaffold for cell transplantation. *J Orthop Res* **20**: pp. 16-19. (2002).
[136] Lee CR, Grad S, Gorna K, Gogolewski S, Goessl A & Alini M. Fibrin-polyurethane composites for articular cartilage tissue engineering: a preliminary analysis. *Tissue Eng* **11**: pp. 1562-1573. (2005).
[137] Ornitz DM & Itoh N. Fibroblast growth factors. *Genome Biol* **2**: p. REVIEWS3005. (2001).
[138] Dailey L, Ambrosetti D, Mansukhani A & Basilico C. Mechanisms underlying differential responses to fgf signaling. *Cytokine Growth Factor Rev* **16**: pp. 233-247. (2005).
[139] Eriksson AE, Cousens LS, Weaver LH & Matthews BW. Three-dimensional structure of human basic fibroblast growth factor. *Proc Natl Acad Sci U S A* **88**: pp. 3441-3445. (1991).
[140] Bikfalvi A, Klein S, Pintucci G & Rifkin DB. Biological roles of fibroblast growth factor-2. *Endocr Rev* **18**: pp. 26-45. (1997).
[141] Gospodarowicz D, Plouet J & Malerstein B. Comparison of the ability of basic and acidic fibroblast growth factor to stimulate the proliferation of an established keratinocyte cell line: modulation of their biological effects by heparin, transforming growth factor beta (tgf beta), and epidermal growth factor (egf). *J Cell Physiol* **142**: pp. 325-333. (1990).
[142] Sahni A, Sporn LA & Francis CW. Potentiation of endothelial cell proliferation by fibrin(ogen)-bound fibroblast growth factor-2. *J Biol Chem* **274**: pp. 14936-14941. (1999).
[143] Sahni M, Ambrosetti DC, Mansukhani A, Gertner R, Levy D & Basilico C. Fgf signaling inhibits chondrocyte proliferation and regulates bone development through the stat-1 pathway. *Genes Dev* **13**: pp. 1361-1366. (1999).
[144] Itoh T, Satou T, Dote K, Hashimoto S & Ito H. Effect of basic fibroblast growth factor on cultured rat neural stem cell in three-dimensional collagen gel. *Neurol Res* **27**: pp. 429-432. (2005).
[145] Springer BA, Pantoliano MW, Barbera FA, Gunyuzlu PL, Thompson LD, Herblin WF, Rosenfeld SA, et al.. Identification and concerted function of two receptor binding surfaces on basic fibroblast growth factor required for mitogenesis. *J Biol Chem* **269**: pp. 26879-26884. (1994).
[146] Pantoliano MW, Horlick RA, Springer BA, Van Dyk DE, Tobery T, Wetmore DR, Lear JD, et al.. Multivalent ligand-receptor binding interactions in the fibroblast growth factor system produce a

cooperative growth factor and heparin mechanism for receptor dimerization. *Biochemistry* **33**: pp. 10229-10248. (1994).
[147] Sahni A & Francis CW. Plasmic degradation modulates activity of fibrinogen-bound fibroblast growth factor-2. *J Thromb Haemost* **1**: pp. 1271-1277. (2003).
[148] Sahni A, Baker CA, Sporn LA & Francis CW. Fibrinogen and fibrin protect fibroblast growth factor-2 from proteolytic degradation. *Thromb Haemost* **83**: pp. 736-741. (2000).
[149] Sahni A, Altland OD & Francis CW. Fgf-2 but not fgf-1 binds fibrin and supports prolonged endothelial cell growth. *J Thromb Haemost* **1**: pp. 1304-1310. (2003).
[150] Sahni A & Francis CW. Stimulation of endothelial cell proliferation by fgf-2 in the presence of fibrinogen requires alphavbeta3. *Blood* **104**: pp. 3635-3641. (2004).
[151] Plopper GE, McNamee HP, Dike LE, Bojanowski K & Ingber DE. Convergence of integrin and growth factor receptor signaling pathways within the focal adhesion complex. *Mol Biol Cell* **6**: pp. 1349-1365. (1995).
[152] Harwood FL, Goomer RS, Gelberman RH, Silva MJ & Amiel D. Regulation of alpha(v)beta3 and alpha5beta1 integrin receptors by basic fibroblast growth factor and platelet-derived growth factor-bb in intrasynovial flexor tendon cells.. *Wound Repair Regen* **7**: pp. 381-388. (1999).
[153] Sahni A, Sahni SK, Simpson-Haidaris PJ & Francis CW. Fibrinogen binding potentiates fgf-2 but not vegf induced expression of u-pa, u-par, and pai-1 in endothelial cells. *J Thromb Haemost* **2**: pp. 1629-1636. (2004).
[154] Hsu C & Chang J. Clinical implications of growth factors in flexor tendon wound healing. *J Hand Surg [Am]* **29**: pp. 551-563. (2004).
[155] Takahashi S, Nakajima M, Kobayashi M, Wakabayashi I, Miyakoshi N, Minagawa H & Itoi E. Effect of recombinant basic fibroblast growth factor (bfgf) on fibroblast-like cells from human rotator cuff tendon.. *Tohoku J Exp Med* **198**: pp. 207-214. (2002).
[156] Chan BP, Chan KM, Maffulli N, Webb S & Lee KK. Effect of basic fibroblast growth factor. an in vitro study of tendon healing.. *Clin Orthop Relat Res* : pp. 239-247. (1997).
[157] Chan BP, Fu S, Qin L, Lee K, Rolf CG & Chan K. Effects of basic fibroblast growth factor (bfgf) on early stages of tendon healing: a rat patellar tendon model.. *Acta Orthop Scand* **71**: pp. 513-518. (2000).
[158] Kobayashi D, Kurosaka M, Yoshiya S & Mizuno K. Effect of basic fibroblast growth factor on the healing of defects in the canine anterior cruciate ligament.. *Knee Surg Sports Traumatol Arthrosc* **5**: pp. 189-194. (1997).
[159] Fukui N, Katsuragawa Y, Sakai H, Oda H & Nakamura K. Effect of local application of basic fibroblast growth factor on ligament healing in rabbits.. *Rev Rhum Engl Ed* **65**: pp. 406-414. (1998).
[160] Chang J, Most D, Thunder R, Mehrara B, Longaker MT & Lineaweaver WC. Molecular studies in flexor tendon wound healing: the role of basic fibroblast growth factor gene expression.. *J Hand Surg [Am]* **23**: pp. 1052-1058. (1998).
[161] Kuroda R, Kurosaka M, Yoshiya S & Mizuno K. Localization of growth factors in the reconstructed anterior cruciate ligament: immunohistological study in dogs.. *Knee Surg Sports Traumatol Arthrosc* **8**: pp. 120-126. (2000).
[162] Palsson B & Bhatia S, "" in *Tissue engineering*, , Prentice Hall, 2004. .
[163] Sheetz MP, Felsenfeld D, Galbraith CG & Choquet D. Cell migration as a five-step cycle. *Biochem Soc Symp* **65**: pp. 233-243. (1999).
[164] Lauffenburger DA & Horwitz AF. Cell migration: a physically integrated molecular process. *Cell* **84**: pp. 359-369. (1996).
[165] McCarthy J, Iida J & Furcht L, "Mechanisms of Parenchymal Cell Migration into Wounds" in *The molecular and cellular biology of wound repair*, Clark R (Ed.), Plenum, 1996. .
[166] Lauffenburger D & Linderman J, "" in *Receptors: models for binding, trafficking, and signaling*, , Oxford University Press, 1993. .
[167] Lo CM, Wang HB, Dembo M & Wang YL. Cell movement is guided by the rigidity of the substrate. *Biophys J* **79**: pp. 144-152. (2000).

[168] DiMilla PA, Barbee K & Lauffenburger DA. Mathematical model for the effects of adhesion and mechanics on cell migration speed. *Biophys J* **60**: pp. 15-37. (1991).
[169] Graham MF, Diegelmann RF & Cohen IK. An in vitro model of fibroplasia: simultaneous quantification of fibroblast proliferation, migration, and collagen synthesis. *Proc Soc Exp Biol Med* **176**: pp. 302-308. (1984).
[170] Brown LF, Lanir N, McDonagh J, Tognazzi K, Dvorak AM & Dvorak HF. Fibroblast migration in fibrin gel matrices. *Am J Pathol* **142**: pp. 273-283. (1993).
[171] Knox P, Crooks S & Rimmer CS. Role of fibronectin in the migration of fibroblasts into plasma clots. *J Cell Biol* **102**: pp. 2318-2323. (1986).
[172] Knox P, Crooks S, Scaife MC & Patel S. Role of plasminogen, plasmin, and plasminogen activators in the migration of fibroblasts into plasma clots. *J Cell Physiol* **132**: pp. 501-508. (1987).
[173] Clark RAF, Lin F, Greiling D, An J & Couchman JR. Fibroblast invasive migration into fibronectin/fibrin gels requires a previously uncharacterized dermatan sulfate-cd44 proteoglycan. *J Invest Dermatol* **122**: pp. 266-277. (2004).
[174] Greiling D & Clark RA. Fibronectin provides a conduit for fibroblast transmigration from collagenous stroma into fibrin clot provisional matrix. *J Cell Sci* **110 (Pt 7)**: pp. 861-870. (1997).
[175] Ricci JL & Alexander H. In-vitro tendon cell growth on synthetic fiber implant materials: biological implications. *Bull Hosp Jt Dis Orthop Inst* **50**: pp. 126-138. (1990).
[176] Ricci JL, Gona AG & Alexander H. In vitro tendon cell growth rates on a synthetic fiber scaffold material and on standard culture plates. *J Biomed Mater Res* **25**: pp. 651-666. (1991).
[177] Murray MM, Bennett R, Zhang X & Spector M. Cell outgrowth from the human acl in vitro: regional variation and response to tgf-beta1. *J Orthop Res* **20**: pp. 875-880. (2002).
[178] Murray MM, Martin SD & Spector M. Migration of cells from human anterior cruciate ligament explants into collagen-glycosaminoglycan scaffolds. *J Orthop Res* **18**: pp. 557-564. (2000).
[179] Murray MM & Spector M. The migration of cells from the ruptured human anterior cruciate ligament into collagen-glycosaminoglycan regeneration templates in vitro. *Biomaterials* **22**: pp. 2393-2402. (2001).
[180] Koob TJ, Willis TA, Qiu YS & Hernandez DJ. Biocompatibility of ndga-polymerized collagen fibers. ii. attachment, proliferation, and migration of tendon fibroblasts in vitro. *J Biomed Mater Res* **56**: pp. 40-48. (2001).

CHAPTER 3: CELL OUTGROWTH BIOASSAY:
DEVELOPMENT OF AN *IN VITRO* METHOD OF CHARACTERIZING TISSUE INGROWTH ON DISCRETE THREADS.

3.1 INTRODUCTION

Research and development of biomaterials for ACL regeneration requires quantitative *in vitro* and *in vivo* methods of characterizing interactions between scaffold materials and cells.[1] In particular, *in vitro* tools allow for the evaluation of the efficacy of ligament specific biomaterials or biomaterial modifications in a controlled environment, without the use of costly and time-consuming implantation studies. Furthermore, improvements on these assays could allow for the high-throughput screening of many conditions with limited extra resources.

A vast subset of biomaterial scaffolds of specific interest to ligament regeneration investigated with these tools are fiber or thread-based scaffolds (Chapter 2.2). Thread scaffolds have been extensively investigated for the repair of highly aligned tissues due to both the structural homology and the ability to promote aligned regeneration (Chapter 2.2). In particular, collagen threads have been investigated because of their biochemical and morphological similarities to native ligament, as well as for their ability to degrade under natural pathways to replace soft tissues. However, the results of implantation studies (Chapter 2, Table 3) indicated that the scaffolds required improvements in tissue

ingrowth and cellular infiltration to repopulate and regenerate the replaced ligament tissue.[2] We have developed a second generation of collagen threads, self-assembled from solutions of acid soluble type I collagen, that demonstrated an increased biomimetic, fibrillar substructure marked by a D periodic banding pattern[3] and mechanical properties comparable to native ligament with crosslinking.[4] While these self assembled collagen biomaterials offer considerable promise as scaffolds for ligament regeneration, their strength and tissue ingrowth characteristics for ligament regeneration have yet to be characterized in a wound healing model.

To predict the rate of new tissue ingrowth onto these aligned fibrous scaffolds for soft tissue regeneration, several studies have focused on developing *in vitro* assays to measure contact-guided cell migration (for more see Chapter 2.5.4). Koob et al. measured cell migration from tendon explants onto NDGA crosslinked collagen threads to determine material biocompatibility.[5] Ricci et al. developed a method for measuring cell colony growth rates on carbon fibers from tendon explants, but could not determine any variation in growth rates on different fiber types, except in the case where carbon fibers were compared with collagen-coated carbon fibers.[6, 7] Murray and Spector measured non-oriented cell migration and proliferation from anterior cruciate ligament (ACL) explants into collagen-glycosaminoglycan (GAG) matrices in multiple dimensions.[8, 9] While each of these techniques provides some measure of tissue responses to implantable threads, there is presently no quantitative and definitive *in vitro* method for characterizing cellular functions on the surfaces of biopolymer threads with varied surface biochemistries and extracellular matrix compositions.

Therefore the objective of the work described in this chapter is to develop a quantitative bioassay for investigating tissue ingrowth on biopolymer threads in order to assess the utility of thread scaffolds for ACL regeneration.

This chapter will focus on the development of a novel method for quantitatively characterizing tissue ingrowth on the surface of collagen thread scaffolds. Threads were suspended across elevated platforms seeded with fibroblast populated collagen lattices. Fibroblast populations were visualized and imaged on each discrete thread and the distance to the furthest cell was measured at time intervals. Evaluation of this metric showed similar outgrowth velocities between self-assembled collagen threads and native tendon controls. Furthermore, increased cellular outgrowth was seen on self-assembled type I collagen threads relative to the first generation of collagen threads derived from insoluble collagen. This novel in vitro model system allows examination of tissue

ingrowth from a wound margin onto biomaterials to determine the effects of various cell types, matrix materials, and surface biochemistries on cell-matrix interactions. Ultimately, this assay will allow us to identify design parameters that will be most effective for enhancing the rate of tissue ingrowth on fiber-based collagen scaffolds for soft tissue regeneration.

3.2 Materials and Methods

3.2.1 Preparation of Collagen Solutions

Acid soluble type I collagen was obtained from rat tails as previously described.[10] Briefly, tendon fibers were dissected from Sprague-Dawley rats, rinsed in PBS and stirred in 1000 mL of 3% (vol/vol) acetic acid overnight at 4°C. The supernatant was separated from the stock solution by centrifugation at 12,800g at 4°C for 2 hours. The supernatant was precipitated with 200 ml of 30% NaCl (wt/vol) solution, and the pellet was collected by centrifugation at 4420g at 4°C for 30 minutes. The pellet was dissolved in 200 mL of 0.6% (vol/vol) acetic acid and dialyzed five times against 1.0 L of 1 mM HCl. The resulting collagen solution was lyophilized and stored at 4°C. The purity of the starting material was verified by sodium dodecyl sulfate polyacrylamide gel electrophoresis (SDS-PAGE). For collagen thread extrusion, a small quantity of type I collagen was dissolved in 5 mM HCl solution at a final concentration of 10 mg/ml and stored in syringes at 4°C.

Insoluble type I collagen from bovine Achilles tendon (Sigma, St. Louis, MO) was prepared as previously described.[11] For collagen thread extrusion, a 1% (wt/vol, 10 mg/mL) dispersion of insoluble type I collagen was prepared by blending 1.0 gram of collagen material in 100 mL of 5 mM HCl for 10 minutes. The dispersion was degassed by centrifugation at 4420g at 4°C for 30 minutes and was stored in syringes at 4°C.

3.2.2 Collagen Thread Extrusion

Collagen threads were extruded from solutions of either soluble or insoluble type I collagen following a procedure similar to that described previously.[3] Briefly, collagen solutions were extruded through 0.38 mm inner diameter polyethylene tubing (Becton Dickinson, Inc., Franklin, NJ) using a syringe pump (KD Scientific, New Hope, PA) set at a flow rate of 0.7 mL/min. Threads were extruded into a bath of fiber formation buffer (pH 7.42, 135mM NaCl, 30mM TrizmaBase (Tris) and 5mM $NaPO_4$ dibasic, Sigma, St. Louis, MO) maintained at 37°C overnight. The buffer was then replaced with a fiber

incubation buffer (pH 7.42, 135mM NaCl, 10mM Tris, and 30mM sodium phosphate dibasic, Sigma, St. Louis, MO) that was maintained at 37°C for 24 hours. The incubation buffer was then replaced with distilled water, and the threads were incubated at 37°C overnight. Finally, the threads were removed from the water bath, air dried, and stored at room temperature in a desiccator.

Half of the threads extruded from both soluble and insoluble collagen solutions were subsequently crosslinked by thermal dehydration (DHT) in which they were heated to 105°C under 100 mTorr vacuum for 24 hours.[4] These crosslinked threads were also stored at room temperature in a desiccator.

Native collagen thread controls were obtained by dissecting collagen fibers from rat tail tendons of Sprague-Dawley rats. Tendon fibers were split repeatedly along their axes under a microscope until the fibers were approximately 75 μm in diameter. These fibers were washed in distilled water, air dried while hanging, and stored in a desiccator.

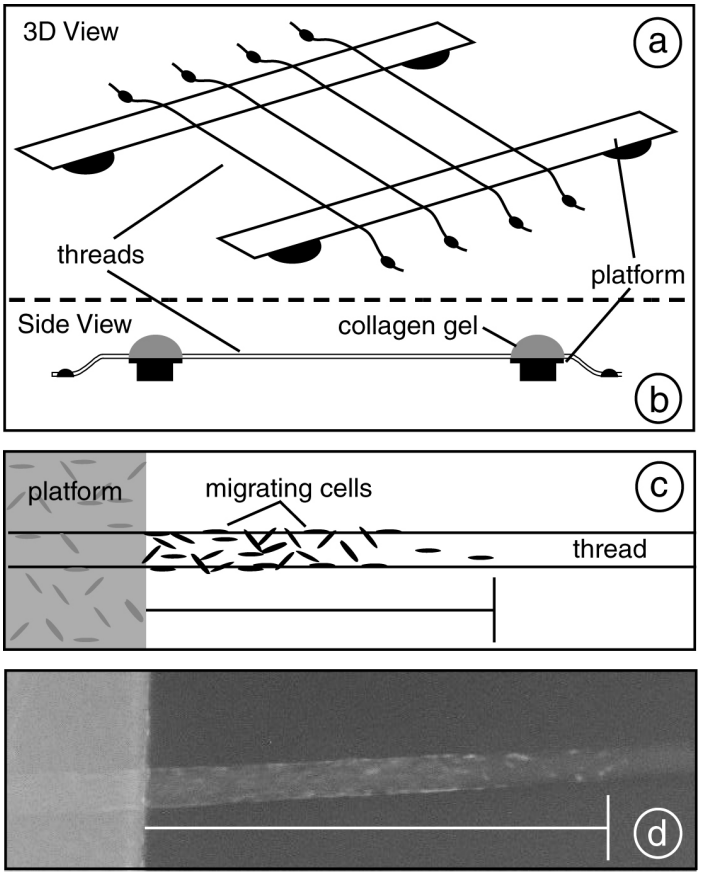

Figure 3.1: Bioassay schematic. A schematic illustration showing the bioassay in both a 3-D view (a) and a side view (b). A schematic illustration (c) and a digital image at day 4 (d) of cells fluorescently labeled with Fura-2 migrating from the platform onto a self-assembled collagen thread (SCT) as visualized under an inverted microscope. The measured distance to the furthest cell is illustrated by the horizontal bar in figures (c) and (d).

3.2.3 Fibroblast Culture

For the cell migration bioassays, primary human dermal fibroblasts were isolated from neonatal foreskins and cultured in Dulbecco's Modified Eagles Medium (DMEM; Gibco BRL, Gaithersburg, MD) supplemented with 10% fetal bovine serum (FBS; Atlanta Biologicals, Lawrenceville, GA) and penicillin/streptomycin (100 U/ 100 μg per mL) (Gibco BRL,

Gaithersburg, MD)). Briefly, sections of dermis from human neonatal foreskins were cut and placed onto scored areas of standard tissue culture dishes. The sections were allowed to dry for 30 minutes, and then were incubated in DMEM with 10% FBS and penicillin/streptomycin (100 U/ 100 μg per mL) at 37°C and 10% CO_2 until the culture dishes were confluent with fibroblasts. The fibroblasts were then removed by trypsin and expanded in culture. Passages 5-9 were used for all migration experiments.

3.2.4 Genetically Modified Fibroblasts

3.2.4.1 Retrovirus production and cell culture

For the cell migration experiments, normal human dermal fibroblasts were genetically modified to express green fluorescent protein (GFP). GFP-encoding amphotropic retrovirus producing cells (originally provided by Dr. Steven J. Greenberg, Roswell Park Cancer Institute, Buffalo, NY)[12] were produced by transfection of murine fibroblast derived PA317 packaging cells with the LXCGN retroviral vector.[13, 14] Retrovirus was harvested from producer cells as described previously. [15] Briefly, fresh medium (32mL in 182-cm^2 tissue culture flasks (Marsh Biomedical, Rochester, NY)) was added to confluent cultures of virus producer cells. After 24 hr the virus-containing medium was harvested, filtered through 0.45 μm pore sized bottle top filters (Corning Costar, Corning, NY), aliquoted and stored at -75^{o}C until use. The virus titer (~1x10^7cfu/mL) was measured by quantifying the neomycin resistant colonies as described previously.[16]

3.2.4.2 Retroviral Transduction

Primary human fibroblasts were transduced on recombinant fibronectin as described previously.[17] Briefly 2 mL of 10 μg/mL recombinant fibronectin (rFN; Takara Mirus Bio Corporation, Madison, WI) was loaded onto non-tissue culture treated 6-well plates overnight at 4°C. On the next day, GFP-encoding retrovirus (2 mL/well) was loaded onto FN-coated surfaces for 7.5 hr at 10% CO_2 and 37°C. After removal of unbound virus, primary human fibroblasts were plated at 15,000 cells/$cm^2$and transduction was allowed to occur overnight at 37°C. The next day, cells were exposed to a fresh stock of retrovirus (2 mL/well) in the absence of polybrene. After 2 hr incubation, retrovirus was removed from the wells and replaced with fresh culture medium containing 1 mg/mL Geneticin (GibcoBRL). After 4 weeks of selection, cells were cryopreserved until they were used for experiments.

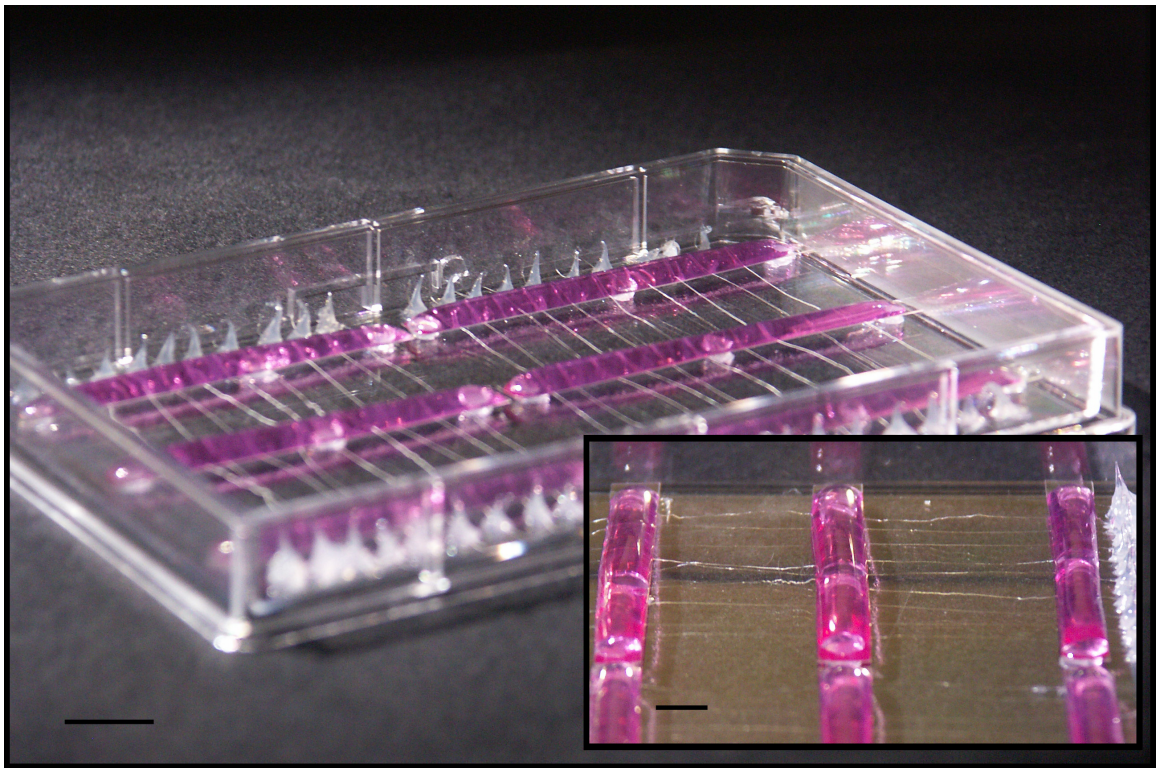

Figure 3.2: Bioassay consisting of threads elevated across platforms seeded with a fibroblast populated collagen lattice. Images were taken before the addition of cell culture media. Scale bar = 1.5 cm (inset = 6 mm)

3.2.5 Cell Outgrowth Bioassay

3.2.5.1 Construction

Tissue culture systems for measuring the migration of cells onto threads were modeled on methods described previously.[6] Raised platforms of Thermanox® tissue culture plastic (5.5 mm X 15 mm) (Nalge Nunc, Rochester, NY) were elevated 1.5 mm above the surface of tissue culture dishes using molded silicone plugs of polydimethylsiloxane (PDMS, Sylgard 184, Dow Corning, Midland, MI) (Figure 3.1a, b, Pg. 44). Threads were laid across the raised platforms, and the ends were attached to the tissue culture plates with Silastic® medical adhesive made from silicone type A (Dow Corning, Midland, MI) (Figure 3.1, pg. 44). Each experimental system contained 6 different thread types, including crosslinked (-X) and uncrosslinked collagen threads (self-assembled from acid-soluble type I collagen (SCT) or reconstituted from insoluble type I collagen (ICT)), native tendon threads from rat tails (NTT) for positive controls

and Prolene® polypropylene suture (PPT) for negative controls (Ethicon, Somerville, NJ).

Migration tissue culture systems including all thread types were sterilized 48 hours prior to migration experiments. The systems were rehydrated in distilled water for 60 minutes, and then soaked in 70% isopropyl alcohol overnight. The alcohol was removed with 3 rinses of sterile distilled water for at least 60 minutes. The systems were then air dried in a laminar flow hood.

3.2.5.2 Cell Seeding

To seed cell migration assays, 0.5 mL aliquots of fibroblast-populated collagen lattice were placed onto each platform (Figure 3.2, pg. 46). These lattices were produced by mixing 3.0 mL of $5x10^5$ cells/mL subconfluent human dermal fibroblasts (passages 5-9) with 2.4 mL of acid soluble type I collagen (2.5 mg/mL) and 0.6 mL 5x DMEM. After the gels were allowed to set at room temperature for 2 hours, the migration plates were filled with 15 mL of DMEM supplemented with 10% FBS to a height just above the platforms and threads (Figure 3.1 a, b, pg. 44 And Figure 3.2, pg. 46).

3.2.5.3 Measurement

To measure cell migration on the collagen threads, fibroblasts were stained with a fluorescent intracellular Ca^{2+} probe, Fura-2 AM (Molecular Probes, Eugene, OR), every 24 hours. 100 μL of 50mM Fura-2 in DMSO was added to the cell culture media of the system and incubated for 30 minutes. The media was then replaced with 15mL of fresh culture medium before the plates were viewed on a Nikon Eclipse TS100 inverted epifluorescent microscope coupled with a SpotRT CCD Camera (Diagnostic Instruments, Sterling Heights, MI) (Figure 3.1c, d, pg.44). At each time point, measurements of distances migrated were made from the edge of the platform to the furthest fluorescently labeled cell using a calibrated reticle in the eye piece of the microscope.

In isolated cases, the threads detached from the plate and floated above the collagen gel on the platforms. These cases were considered to be invalid data points and therefore excluded from our analyses.

3.2.6 Inhibition of Proliferation

For experiments investigating the mechanism of cell front translation, subsets of fibroblasts were chemically pretreated to inhibit proliferation. Two hours prior to

seeding on platforms, the media was removed for subconfluent monolayer fibroblast cultures and replaced with DMEM (10% FBS, 1% penicillin streptomycin) containing 10 μg/ml mitomycin C. After 2 hours of incubation, the cultures were rinsed three times with sterile DMEM, chemically detached from tissue cultures plates with trypsin, and seeded into collagen lattices as previously described. In these assays, the thread type was held constant using only self-assembled collagen threads.

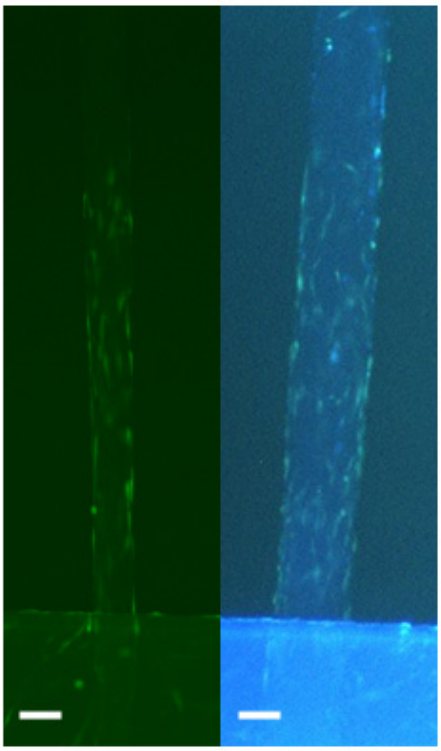

Figure 3.3: Fibroblasts genetically modified to over-express green fluorescent protein (GFP) improved visualization of fibroblasts and increased the bioassay consistency by removing the need for daily staining. Scale bars represent 50 μm.

3.2.7 Statistical Analyses

All migration data was analyzed using SPSS for Windows (SPSS Inc., Chicago, IL). Data points of migration versus time were fit with a standard linear regression ($r \geq 0.95$) to determine how well the outgrowth velocities represented the data. The data points of outgrowth velocity were then tested with a one-way ANOVA to determine a significant difference between the means. Post hoc comparisons between two sample groups were made with Tukey's honest significant difference (HSD) test with $p < 0.05$ indicating significant difference between groups.

3.3 Results

3.3.1 Imaging

One of the challenges associated with the development of this assay system was the visualization of cells on threads. Initial studies used a daily staining regiment of Fura-2 (see Measurement 3.2.5.3). To improve the imaging consistency and reliability, fibroblasts modified to express green fluorescent protein were used. This increased the ease of fibroblast visualization by working in a spectrum with less collagen autofluorescence as well as by removing certain stain uptake inconsistencies involved with daily application of intracellular calcium indicators. Fibroblasts were significantly easier to distinguish on the threads when expressing GFP than when stained with Fura-2 (Figure 3.3)

3.3.2 Metric Development

Fluorescent microscopy was used to measure cell migration distances from the edges of the cell-seeded platforms to the farthest fibroblast on various threads in order to quantitatively evaluate the capability of cells to interact with aligned scaffolding materials indicative of tissue ingrowth. Observationally, no fluorescently labeled cells were visualized on any threads for the first 48 hours (Figure 3.4a, d; pg. 49 And Figure 3.5, pg. 50). However, 72 hours after seeding the platforms with fibroblasts, cells began to migrate onto the threads (Figure 3.4b, e; pg 49 and Figure 3.5, pg. 50). Consequently, day 3 was considered the first time point for outgrowth velocity analyses. By day 4, while only a small number of cells were observed on the PPT threads, a large number of cells were observed on the SCT threads (Figure 3.4c, f; pg. 49).

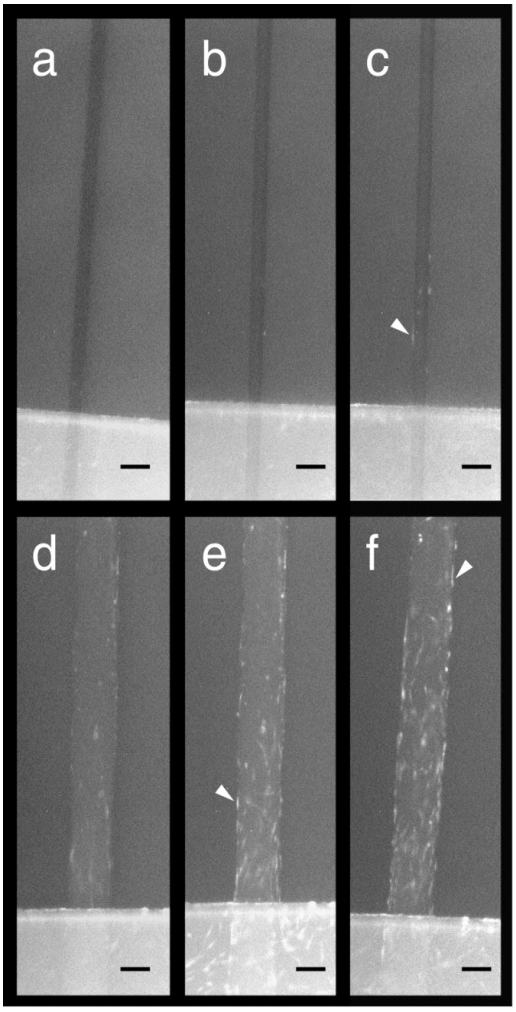

Figure 3.4: Fluorescent microscopy images of fibroblast cell outgrowth. Inverted fluorescent microscopy images of Fura-2 labeled cells migrating onto a polypropylene thread (a-c) and a self-assembled collagen thread (SCT) (d-f) at day 2 (a,d), day 3 (b,e), and day 4 (c,f). Cells cannot be seen at day 2 on either thread. By day 4 a few initial cells can be seen leaving the platform onto the polypropylene thread (PPT)while many cells have migrated onto the self-assembled collagen thread (SCT). Examples of labeled cells are indicated with white arrowheads. Scale bars represent 100μm.

To quantify these observations, the total cell migration distance traveled each day was averaged for each type of thread and plotted as a function of time. These plots for each thread type were accurately modeled by standard linear regression ($R>0.95$), including both positive and negative controls (Figure 3.6, pg 51). Since the rate of migration is linear as a function of time, we averaged the distance traveled by the cells on days 3 through 8 to determine our metric, an outgrowth velocity, along each thread (outgrowth velocity/thread). These 5-day average values were each represented as single data point for a particular thread extending from a particular platform. From all of these data points, averages and

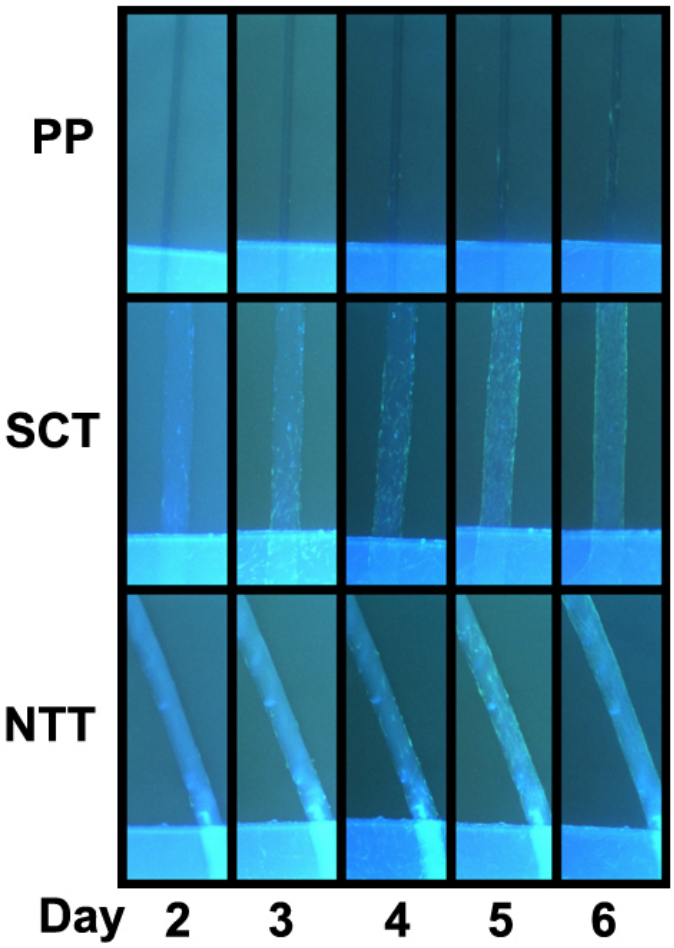

Figure 3.5: Images of fibroblast cell outgrowth with time. Fibroblasts stained with Fura-2 were imaged every 24 hours. No cells can be seen at day 2 on any thread type. Therefore measurements began at day 3 of incubation. By day 6, fibroblasts fill the image area on self-assembled collagen threads (SCT) and the positive control native tendon threads (NTT) while very few cells are seen on the negative control polypropylene threads (PPT). Variance in population density can also be seen.

standard deviations were calculated, and statistical comparisons between thread types were made using analysis of variance (ANOVA).

3.3.3 Additional Model Considerations

The cell density of migrating cells varied widely on different thread types; some threads (SCT, NTT) maintained a relatively high cell density and a front of migrating cells while other threads (ICT-X, PPT) were found to have limited cell density with no definitive front of migrating cells. Quantification of this phenomenon was estimated (data not shown), but distinct differences between thread groups were equivocal.

To determine whether the extension of the fibroblast population front were migrating or proliferating, measurements were obtained for cells with and without inhibition of proliferation. In the same test apparatus, half the platforms were seeded with standard fibroblast populated collagen lattices, while the second half were seeded with mitomycin C pretreated fibroblasts in collagen lattices to inhibit proliferation. The inhibition of proliferation was verified simultaneously through continued culture under standard conditions on tissue culture plastic. The migration rate significantly decreased when cells chemically treated to inhibit proliferation, however, the values were non-zero (Figure 3.3, pg. 48) Furthermore, the visualized cell density was also decreased, but not quantified.

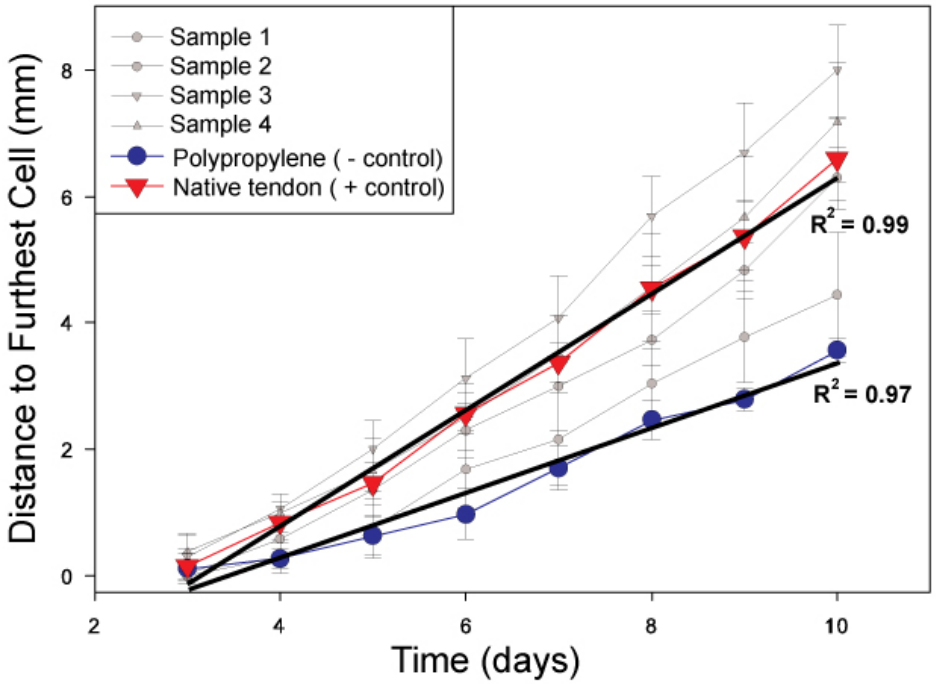

Figure 3.6: outgrowth velocities Represent Accurate Metrics. Graph of migration distance versus time highlighting control native tendon threads (NTT) and polypropylene threads (PPT). The strong fit with standard linear regression analysis demonstrates that outgrowth velocities were accurate metrics of data obtained as a function of time.

These findings suggest a combination of proliferation and migration of fibroblasts to extend the front.

3.3.4 Effect of Collagen Source and Crosslinking

We compared the effects of the two different collagen sources, as well as the effect of crosslinking, on the outgrowth velocity of fibroblasts on the surfaces of collagen threads. In these studies the cell migration rates ranged from 0.75 to 1.25 mm/day. All of the collagen threads and the native tendon fibers were found to facilitate significantly greater outgrowth velocities than the PPT negative control threads. SCT threads were found to promote a significantly greater migration rate than ICT threads under comparable crosslinking conditions (Figure 3.8, pg 53). Additionally, fibroblast migration rates on SCT threads were found to be comparable to the cell migration rates on NTT positive control threads (Figure 3.9, pg 53). When cell migration rates on uncrosslinked threads were compared with DHT crosslinked threads, it was found that DHT crosslinking significantly decreased the rate of fibroblast migration on both self-

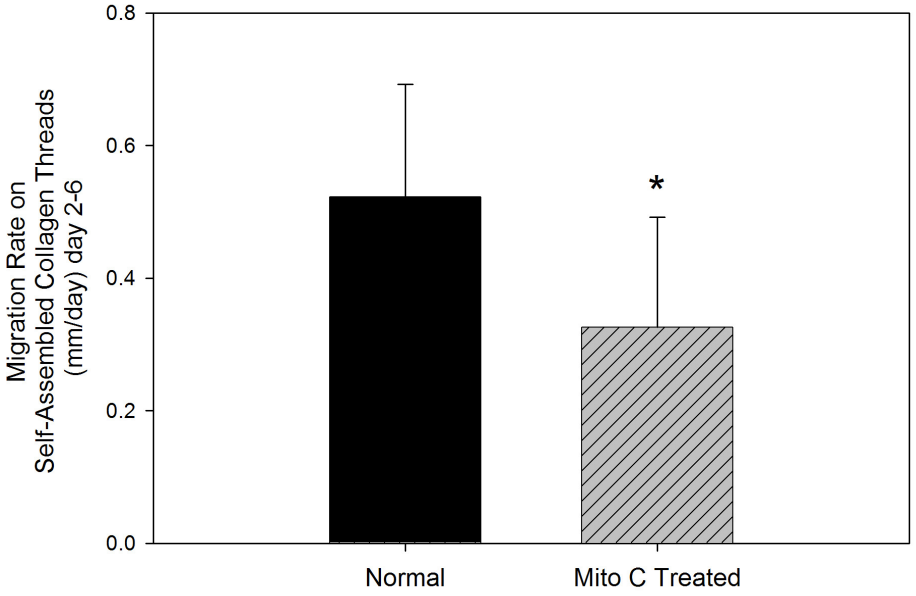

Figure 3.7: Migration With Proliferation Inhibited. The migration rate significantly decreased but was non-zero when fibroblasts were pretreated with Mitomycin C, a potent inhibitor of proliferation. Therefore the cell outgrowth metric is a combination of migration and proliferation.

assembled collagen threads and collagen threads reconstituted from insoluble collagen (Figure 3.10, pg. 55).

3.4 DISCUSSION

In this study, we describe a novel *in vitro* model system for quantitatively measuring tissue ingrowth onto discrete biopolymer thread matrices that closely mimics ACL tissue regeneration with acellular matrices. Cells suspended in fibroblast-populated collagen lattices migrated out of the 3-D matrix and onto threads that were suspended like bridges across platforms submersed in culture medium. Fibroblasts cultured in 3-D collagen lattices are commonly employed as an *in vitro* model of wound healing because the 3-D collagen matrix closely mimics the contextual cues of the native environment.[18] This environment provides the biochemistry of the ECM as well as the spatial regulation of the three-dimensional cellular environment.[18] In our model system we combine this widely accepted model of wound healing with high density collagen thread matrices developed for the regeneration of torn tendons and ligaments (Chapter 2.2.2.1). In this system we maintain a structurally and biochemically relevant 3-D contextual environment, but in a system that closely mimics the mechanisms of cellular repopulation

that occurs during ACL replacement surgery. During non-autograft ACL revision surgeries, the torn ligament is typically replaced with an acellular thread composite graft that triggers fibroblasts from the wound margin and surrounding tissue to migrate into the graft, repopulate and regenerate the tissue. In a similar manner, fibroblasts in our *in vitro* model, migrate and proliferate from the collagen gel wound margin onto collagen thread scaffolds. The combined mechanism of migration and proliferation observed in our model is supported by evidence suggesting that migration occurs in the absence of proliferation, but at reduced values and with reduced population density (Figure 3.3, pg. 48).

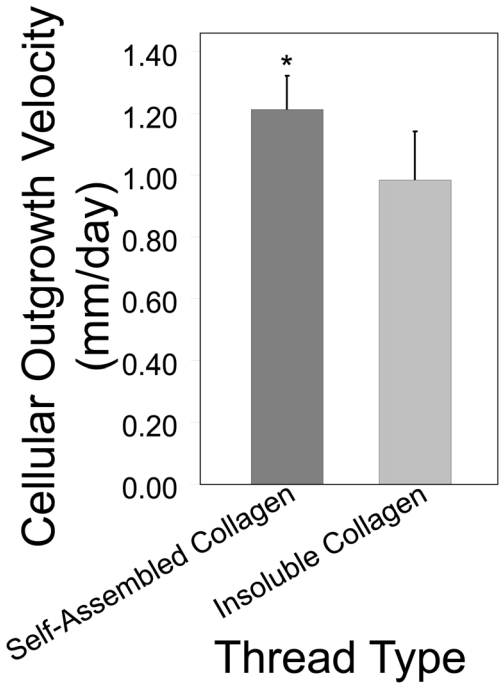

Figure 3.8: The outgrowth velocity is significantly greater on self-assembled collagen threads than on insoluble collagen threads

Within this model system, we have developed a metric quantitatively characterizing tissue ingrowth that enables us to differentiate variable cell matrix interactions and new tissue ingrowth in an accurate, repeatable manner. The distances traveled per day were approximately constant for any one particular thread type, as clearly demonstrated from the strong linear regression fit of the distance traveled with time data (Figure 3.6, pg. 51). Given that the measurements are uni-directional along the long axis of the threads, the best fit linear regression, or slope of the tangent on a position versus time graph, is by definition the *velocity* of outgrowth. Once determined, this outgrowth velocity provided a representative metric, for comparison between experimental conditions. The outgrowth velocity of fibroblasts on collagen threads were measured to be between 0.75 and 1.25 mm/day. These data are similar to published data which determined the rate of tendon cell colony growth from explants onto collagen coated Dacron fibers to be 1.53 ± 0.96 mm/day.[6]

The cell outgrowth velocity was variable and non-zero under all conditions tested. Because all of the threads, including common polypropylene suture threads, used in this experiment are generally considered biocompatible, it is unsurprising that none

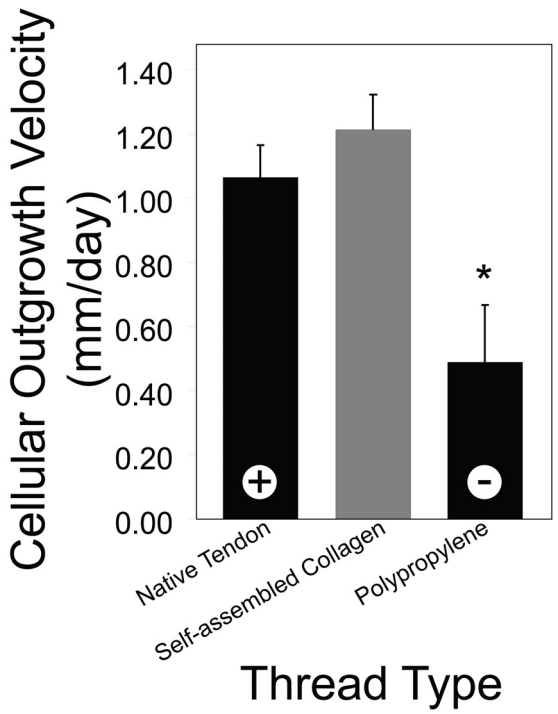

*Figure 3.9: Self-Assembled Similar to Native. The outgrowth velocity on self-assembled collagen threads was almost 3 times greater than on negative controls and no statistically different than positive controls (native tendon threads). *significant difference*

completely inhibited cell migration. However, all threads composed of collagen showed a significantly greater outgrowth velocity than synthetic threads. Since collagen is a ubiquitous structural element in soft connective tissues (Chapter 2.1.1.1), as well as a fundamental component of wound healing processes, these findings are consistent with our initial hypothesis that the biochemical cues on the surfaces of the threads enhance the rate of cell migration onto biopolymer scaffolds. These finding are also consistent with previous studies that showed tendon cell colonies grow faster on collagen-coated Dacron threads than on non-coated fibers.[6]

While both the first generation, insoluble collagen threads (ICT), and the second generation self-assembled collagen threads (SCT) are both composed of type I collagen, the results of this study indicate quite different outgrowth velocities. Threads self-assembled from solutions of soluble collagen molecules have previously been shown to possess improved mechanical properties with a higher density of aligned fibrils than threads extruded from insoluble collagen.[19] This increase in aligned fibril density in SCT threads more closely resembles the structure of native tendon threads. In this study, the SCT promoted higher outgrowth velocity than ICT threads (Figure 3.8, pg. 53) and have a velocity that was not significantly different than those seen on native NTT threads (Figure 3.9, pg. 54). This increase may be a result of the increased alignment of collagen fibrils in the SCT which may promote increased directional migration through contacted guidance; however, this increase is more likely a result of differences in serum protein interactions with the surfaces of the threads. In particular, differences in the binding of proteins such as fibronectin, a key mediator of cell adhesions, have been widely shown to dramatically alter migration.[20-22] Improved protein binding on the surface of self-assembled

collagen threads over ICT may account for the outgrowth velocity variation.

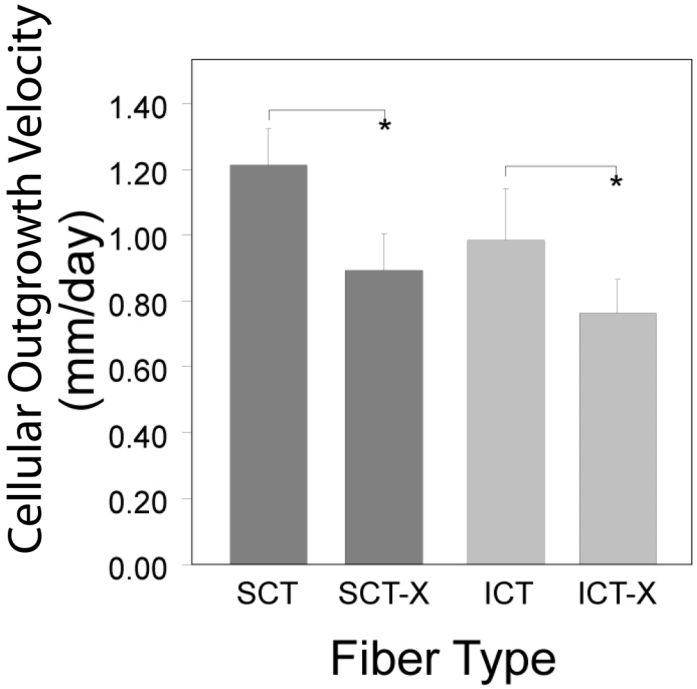

Figure 3.10: Crosslinking Decreases outgrowth velocity.. outgrowth velocities for self-assembled soluble collagen threads (SCT) and insoluble collagen threads (ICT). Crosslinked threads (-X) were found to have significantly ($p < 0.05$) slower outgrowth velocities than non-crosslinked threads of the same material.*

The results of this study suggest that DHT crosslinking may adversely effect cell-matrix interactions and the rate of tissue regeneration (Figure 3.10, pg. 55). Crosslinking of collagen using various techniques has been shown to increase the strength of collagen threads and decrease the rate of degradation. Crosslinking by severe dehydration, or DHT crosslinking, is a commonly used technique for physically crosslinking collagen and collagen threads (Chapter 2.2.2.1 - Crosslinking) without the addition of toxic chemicals that could be leached into the host tissue. While this technique has been shown to reduce collagen solubility, antigenicity, and degradation rate to stabilize the scaffolds upon implantation,[23, 24] it may also mask integrin binding sites or surface receptors that mediate cell attachment and migration as well decrease binding to adhesion mediating serum proteins. The preliminary results of this study suggest that crosslinking decreases the average cell outgrowth velocity on collagen threads, regardless of the source of the material. This finding supports our hypothesis that DHT crosslinking inhibits cell-matrix interactions. The duration of DHT crosslinking (between 1-5 days) increases the quantity of crosslinks, which correlates with both an increase in the mechanical strength and a decrease the solubility or rate of degradation.[25] Future tests should examine the effects of DHT crosslinking time on cell outgrowth velocity to definitively determine whether an increase in crosslink density results in a decrease in cell migration.

The rate and velocity of migration is a function of any number and combination of stimuli including chemotaxis, haptotaxis, durotaxis, and contact guidance (Chapter 1.5.2).

In this system, the exact mechanism regulating the velocity of ingrowth remains unclear; however, we hypothesize that haptotactic or chemotactic effects caused by varied serum protein binding to the surface of threads may be the dominant factor. In the absence of serum and serum proteins, no ingrowth occurred through 10 days of culture (data not shown), further supporting this hypothesis. Future studies should more clearly elucidate this mechanism. For example by using defined media and measuring outgrowth velocity with cells modified to lack receptors for particular ECM proteins, the haptoctic response of cells to particular surfaces could be probed. Another example would investigate the effect of durotaxis on outgrowth velocity by using threads increasingly crosslinked by a single agent to increase the stiffness of the material.

Although successful, the method for characterizing tissue ingrowth has various limitations. Current methods for quantifying population density were suboptimal due to poor image contrast, cell delineation detail, and limited imaging field of view. Improvements were clearly seen when daily staining protocols were replaced by the use of a GFP expressing fibroblast cell line; however, using fibroblasts modified to express GFP sequestered to the nucleus only, rather than the cytoplasm, could allow for simple quantification of cell number using image analysis software. Furthermore, the entire system could be improved by tracking cells in real time with an automated stage to reduce the day to day variations and experimental error.

The bioassay developed here may be useful in the future as an *in vitro* test of parameters that affect the regeneration of soft connective tissues including tendon and ligament tissue. The assay contains experimental parameters that can be altered for determination of differential characteristics including cell types, crosslinking methods, collagen substructure, or the microtopography on the surface of the threads. Ligaments have been found to have less healing capacity than tendons, resulting in the use of a patellar tendon as a common autograft for the repair of the anterior cruciate ligament in the knee.[26] One experiment might compare ligament fibroblasts with tendon fibroblasts to evaluate their relative abilities to migrate and proliferate on aligned collagen threads, and therefore their ability to interact with the extracellular matrix during wound healing. The addition of wound healing cytokines may help elucidate the different intrinsic ability of cell types to regenerate in an *in vitro* wound healing model. Fibroblasts that are responsible for the wound healing capability of tendons are thought to originate in the epitenon, or the fascia surrounding native tendon.[5] Separate cultures of epitenon fibroblasts and internal tendon fibroblasts may help answer the question of the origin of the fibroblasts responsible for the increased wound healing capability seen in

tendon. By keeping the cell type constant, crosslinking techniques, including both chemical and physical, may be evaluated for their suitability for engineering collagen thread constructs to optimize the rate of new tissue ingrowth.

Researchers have found that cells will migrate and proliferate on collagen threads under various crosslinking conditions *in vivo,*[5, 27] but currently there is no quantitative deterministic methodology to characterize how cells migrate or the cellular interactions with these threads. Thus, up until now no *in vitro* comparison between crosslinking methods, collagen sources, surface biochemistries, or microtopographies has been available. In this study we developed a sensitive technique to measure fibroblast migration on aligned fibrous scaffolds to elucidate the differences in cell matrix interactions and to predict the rate of tissue regeneration of grafts for soft tissue regeneration. Unlike previous studies which could not determine significant differences in migration rates on various synthetic fiber types,[6, 7] our method can accurately detect the fine variations between the measured migration rate on biological materials, which may be indicative of how well the scaffold will facilitate tissue ingrowth upon implantation. Using this technique, we found that self-assembled collagen threads increase fibroblast migration rates while DHT crosslinking decreases fibroblast migration rate. The system also establishes a wound healing model of fibroblast migration from a wound margin. In the future, this *in vitro* bioassay will enable us to identify parameters to optimize the rate of tissue ingrowth for the development of constructs for soft tissue regeneration, as well as to determine fine variations in the cell-matrix interactions as a function of matrix materials and surface biochemistries.

REFERENCES

[1] Vunjak-Novakovic G, Altman G, Horan R & Kaplan DL. Tissue engineering of ligaments. *Annu Rev Biomed Eng* **6**: pp. 131-156. (2004).

[2] Dunn MG, Liesch JB, Tiku ML & Zawadsky JP. Development of fibroblast-seeded ligament analogs for acl reconstruction. *J Biomed Mater Res* **29**: pp. 1363-1371. (1995).

[3] Pins GD, Christiansen DL, Patel R & Silver FH. Self-assembly of collagen fibers. influence of fibrillar alignment and decorin on mechanical properties. *Biophys J* **73**: pp. 2164-2172. (1997).

[4] George D. Pins, Eric K. Huang, David L. Christiansen, Frederick H. Silver. Effects of static axial strain on the tensile properties and failure mechanisms of self-assembled collagen fibers. *J Appl Polym Sci* **63**: pp. 1429-1440. (1997).

[5] Koob TJ, Willis TA, Qiu YS & Hernandez DJ. Biocompatibility of ndga-polymerized collagen fibers. ii. attachment, proliferation, and migration of tendon fibroblasts in vitro. *J Biomed Mater Res* **56**: pp. 40-48. (2001).

[6] Ricci JL & Alexander H. In-vitro tendon cell growth on synthetic fiber implant materials: biological implications. *Bull Hosp Jt Dis Orthop Inst* **50**: pp. 126-138. (1990).
[7] Ricci JL, Gona AG & Alexander H. In vitro tendon cell growth rates on a synthetic fiber scaffold material and on standard culture plates. *J Biomed Mater Res* **25**: pp. 651-666. (1991).
[8] Murray MM, Martin SD & Spector M. Migration of cells from human anterior cruciate ligament explants into collagen-glycosaminoglycan scaffolds. *J Orthop Res* **18**: pp. 557-564. (2000).
[9] Murray MM & Spector M. The migration of cells from the ruptured human anterior cruciate ligament into collagen-glycosaminoglycan regeneration templates in vitro. *Biomaterials* **22**: pp. 2393-2402. (2001).
[10] Elsdale T & Bard J. Collagen substrata for studies on cell behavior. *J Cell Biol* **54**: pp. 626-637. (1972).
[11] Gentleman E, Lay AN, Dickerson DA, Nauman EA, Livesay GA & Dee KC. Mechanical characterization of collagen fibers and scaffolds for tissue engineering. *Biomaterials* **24**: pp. 3805-3813. (2003).
[12] Selkirk SM, Greenberg SJ, Plunkett RJ, Barone TA, Lis A & Spence PO. Syngeneic central nervous system transplantation of genetically transduced mature, adult astrocytes. *Gene Ther* **9**: pp. 432-443. (2002).
[13] Miller AD & Buttimore C. Redesign of retrovirus packaging cell lines to avoid recombination leading to helper virus production. *Mol Cell Biol* **6**: pp. 2895-2902. (1986).
[14] Miller AD & Rosman GJ. Improved retroviral vectors for gene transfer and expression. *Biotechniques* **7**: p. 980-2, 984-6, 989-90. (1989).
[15] Lei P, Bajaj B & Andreadis ST. Retrovirus-associated heparan sulfate mediates immobilization and gene transfer on recombinant fibronectin. *J Virol* **76**: pp. 8722-8728. (2002).
[16] Danos O & Mulligan RC. Safe and efficient generation of recombinant retroviruses with amphotropic and ecotropic host ranges. *Proc Natl Acad Sci U S A* **85**: pp. 6460-6464. (1988).
[17] Bajaj BG, Lei P & Andreadis ST. Efficient gene transfer to human epidermal keratinocytes on fibronectin: in vitro evidence for transduction of epidermal stem cells. *Mol Ther* **11**: pp. 969-979. (2005).
[18] Grinnell F. Fibroblast biology in three-dimensional collagen matrices. *Trends Cell Biol* **13**: pp. 264-269. (2003).
[19] Pins G & Silver F. A self-assembled collagen scaffold suitable for use in soft and hard tissue replacement. *Materials Science and Engineering:C* **3**: pp. 101-107. (1995).
[20] Briggs SL. The role of fibronectin in fibroblast migration during tissue repair.. *J Wound Care* **14**: pp. 284-287. (2005).
[21] Clark RA. Potential roles of fibronectin in cutaneous wound repair.. *Arch Dermatol* **124**: pp. 201-206. (1988).
[22] Grinnell F. Fibronectin and wound healing.. *J Cell Biochem* **26**: pp. 107-116. (1984).
[23] Khor E. Methods for the treatment of collagenous tissues for bioprostheses. *Biomaterials* **18**: pp. 95-105. (1997).
[24] Weadock K, Olson RM & Silver FH. Evaluation of collagen crosslinking techniques. *Biomater Med Devices Artif Organs* **11**: pp. 293-318. (1983-84).
[25] Wang MC, Pins GD & Silver FH. Collagen fibres with improved strength for the repair of soft tissue injuries. *Biomaterials* **15**: pp. 507-512. (1994).
[26] Woo SL, Hildebrand K, Watanabe N, Fenwick JA, Papageorgiou CD & Wang JH. Tissue engineering of ligament and tendon healing. *Clin Orthop Relat Res* : p. S312-23. (1999).
[27] Bellincampi LD, Closkey RF, Prasad R, Zawadsky JP & Dunn MG. Viability of fibroblast-seeded ligament analogs after autogenous implantation. *J Orthop Res* **16**: pp. 414-420. (1998).

CHAPTER 4: OPTIMIZED SELF-ASSEMBLED COLLAGEN MICROTHREADS:

EFFECT OF CROSSLINKING ON COLLAGEN MICROTHREAD STRENGTH AND CELL OUTGROWTH.

4.1 INTRODUCTION

Design of biomaterials scaffolds that promote anterior cruciate ligament regeneration requires structures that replicate the mechanical properties of the native tissue, facilitate cell infiltration and biodegrade at a rate that matches the rate of tissue formation.[1] Fibrous biopolymer materials, especially collagen (see Chapter 2.2.2.1), have been studied as scaffolds to promote the repair and regeneration of torn tendons and ligaments due to their structural and biochemical homology to native ligament (see Chapter 2.1.1). However, their success has been limited both by insufficient tissue ingrowth from the wound margin[2] as well as insufficient initial mechanical stability without effective crosslinking strategies.

Numerous crosslinking strategies have been employed to improve the mechanical properties of collagen thread scaffolds (see Chapter 2.2.2.1 - Crosslinking). These techniques insert inter- and intramolecular crosslinks using either chemical of physical methodologies to ultimately decrease the rate of proteolytic degradation, increase the

material stiffness, and increase material tensile strength. However, our previous investigations utilizing a novel bioassay for the evaluation of *in vitro* tissue ingrowth (see Chapter 3) indicate that dehydrothermal (DHT) crosslinking, a commonly employed strategy for crosslinking collagen thread scaffolds, subsequently led to decreases in the *in vitro* rate of tissue ingrowth (see Chapter 3). During these previous studies, a decrease in cell outgrowth with crosslinking was evident on both insoluble collagen threads as well as our second generation collagen threads self-assembled from solutions of acid soluble collagen.

Self-assembled collagen threads represent a promising solution for ligament regeneration. They possess ultimate tensile strengths, stiffnesses, and structural properties comparable to native tendon fibers and significantly greater strengths than threads extruded from insoluble, type I collagen dispersions.[3-5] However, self-assembled collagen threads still require crosslinking to attain mechanical properties to match the ACL. The ultimate effects of the various available crosslinking techniques on the tensile strength and cellular outgrowth of self-assembled collagen threads has yet to be characterized.

Therefore the objective is to optimize the mechanical properties and cell outgrowth of self-assembled collagen threads for ACL regeneration utilizing current crosslinking techniques.

The focus of this chapter is to describe the application of the quantitative method of determining cellular ingrowth developed in Chapter 3 to crosslinking of collagen threads. Collagen threads are commonly crosslinked to increase the mechanical properties and decrease the otherwise rapid *in vivo* rate of degradation in a wound site. The initial studies in Chapter 3 determined that the cell outgrowth rate was attenuated after crosslinking with a technique selected because of it's prevalence during prior *in vivo* studies. We hypothesized that implementation of alternate crosslinking modalities that had yet to be tested on self-assembled collagen threads could increase thread stability without the concurrent decrease in cell outgrowth seen with DHT crosslinking. The major limitations of collagen threads, including limited tissue ingrowth, could thereby be circumvented. The mechanical properties and cell outgrowth rates were measured for self-assembled collagen threads utilizing the most promising crosslinking strategies. Although all the techniques investigated increased the strength and decreased the rate of degradation, they also subsequently decreased the *in vitro* rate of tissue ingrowth. These

findings indicate that there remains a need to develop a scaffold material that both provides mechanical stability and promotes new tissue ingrowth.

4.2 Materials and Methods

4.2.1 Production of Self-Assembled Collagen Threads

4.2.1.1 Preparation of acid soluble collagen

Acid soluble type I collagen was extracted from rat tails as previously described.[6] Briefly, tendon fibers were dissected from Sprague-Dawley rats with hemostats, rinsed twice in phosphate buffered saline, and dissolved in 1600 mL of 3% (vol/vol) acetic acid solution overnight at 4°C. The solution was refrigerated, centrifuged at 4°C for 2 hours at 8,000g, and the supernatant retained. A volume of 320 ml of 30% NaCl (wt/vol) solution was slowly dripped into the solution to precipitate the collagen. The entire solution and precipitate were centrifuged at 4°C for 30 minutes and the supernatant discarded. The pellets were resuspended in 400 ml of 0.6% (vol/vol) acetic acid solution and stirred at 4°C overnight or until completely dissolved. The solution was dialyzed five times against 4 L of 1mN HCl, each for at least 4 h. The resulting collagen solution was lyophilized and stored at 4°C until use. Prior to extruding threads, lyophilized collagen was dissolved in a rotating vessel overnight at 4°C in 5mM HCl, at a final concentration of 10mg/ml. The collagen solution was degassed by centrifugation before extrusion to remove trapped air bubbles.

4.2.1.2 Collagen thread extrusion

Collagen threads were extruded using a protocol described previously.[3] Briefly, the collagen solution was extruded through 0.86 mm inner diameter polyethylene tubing (Becton Dickinson, Inc., Franklin, NJ) using a syringe pump (KD Scientific, New Hope, PA) set at a flow rate of 0.7 mL/min. The threads were extruded into a bath of fiber formation buffer (pH 7.42, 135 m*M* NaCl, 30 m*M* TrizmaBase (Tris), and 5 m*M* $NaPO_4$ dibasic; Sigma, St. Louis, MO) maintained at 37°C. After 24 h, the buffer was replaced with a fiber incubation buffer (pH 7.42, 135 m*M* NaCl, 10 m*M* Tris, and 30 m*M* sodium phosphate dibasic, Sigma) that was maintained at 37°C. After 24 h, the incubation buffer was replaced with distilled water, and the threads were incubated at 37°C for an additional 24h. Finally, the threads were removed from the water bath, air dried, and stored at room temperature in a desiccator.

4.2.1.3 Collagen Thread Crosslinking

The self-assembled threads were separated into six groups, representing 5 crosslinking methods and an uncrosslinked control group. Two groups of threads were crosslinked by ultraviolet light in a UVP CL-1000 crosslinker as previously described.[7] Threads were centered on a reflective surface 4.5 inches from a bank of 5-8 watt UV tubes emitting at a primary wavelength of 254nm. The threads were exposed to UV light for either 15 minutes (UV-15) or 30 minutes (UV-30). Two groups of threads were crosslinked by severe dehydration as previously described.[4] This dehydrothermal crosslinking was achieved by placing the threads in a vacuum oven maintained at 50-100 mTorr at 110°C for either 1 day (DHT-1) or 3 days (DHT-3). The final group of threads was chemically crosslinked by soaking the scaffolds in a 1% (w/v) solution of N-(3-Dimethylaminopropyl)-N-ethylcarbodiimide hydrochloride (Sigma, St. Louis, MO) in distilled water for 24 hours at 4°C, then rinsed in distilled water 24 hours at 4°C and finally air dried (EDC).[8] For this study, collagen threads were only exposed to one level of EDC crosslinking (24 hours). Previous studies in our laboratory indicate that the maximum tensile strength of EDC crosslinked collagen threads reaches a plateau value when threads are treated with EDC for as little as 4 hours (unpublished data). All threads were stored at room temperature in a desiccator until use.

4.2.2 Swelling Ratio and Crosslink Density Calculations

Average molecular weight between crosslinks ($\bar{M}_c$) was calculated based on simplified version of the Flory-Rehner equation for equilibrium swelling in crosslinked polymeric networks[9-11]:

$$Q_v^{5/3} \simeq \left(\frac{\bar{v}\bar{M}_c}{V_1} \right) \left(\frac{1}{2} - \chi \right)$$

where Q_v is the volumetric swelling ratio, $\bar{v}$ is the specific volume of the dry polymer, V_1 is the molar volume of the solvent (18 mol/cm^3 for water), and χ is the Flory-Huggins polymer-solvent interaction parameter. A value of 0.49 ± 0.05 was used Flory-Huggins interaction parameter based on values determined in collagen gels.[12] The volumetric swelling ratio (Q_v) was calculated as the ratio of the wet cross-sectional area to the dry cross-sectional area assuming no swelling occurs along the long axis of the thread (less than 5% of volume change occurs along this axis, data not shown). The approximate cross-sectional areas were calculated from thread diameter measurements

using a Nikon Eclipse E400 microscope with a calibrated reticule and by assuming cylindrical thread geometry. The diameters were measured by mounting individual threads with adhesive (Silastic Silicone Type A, Dow Corning) on vellum frames containing precut analysis windows. Thread diameters were measured before (dry) and after (wet) rehydrating the materials for at least 30 minutes in phosphate buffered saline (PBS). Each thread diameter was calculated as the average of 4 measurements along the length of a thread.

The effective crosslink density (ν_e) was calculated from[9, 13]:

$$\nu_e = \frac{\rho_p}{\bar{M}_c}$$

where ρ_p is the density of the dry polymer, assumed to be the density of proteins ($1.35 g/cm^3$).[14]

4.2.3 Mechanical Testing of Collagen Threads

Threads from each crosslinking group were hydrated and mechanically loaded in uniaxial tension to obtain stress-strain curves. Individual threads were mounted vertically with adhesive (Silastic Silicone Type A, Dow Corning) on vellum frames with precut windows that defined the region of loading. For tensile testing, the samples in the vellum frames were clamped into a custom designed micromechanical testing unit (See Appendix B) consisting of a horizontal linearly actuated crosshead and a fixed 150g load cell. An initial gauge length of 20 mm was defined as the distance between adhesive spots at the edges of the precut window in the vellum frame. Test unit operations and data acquisition were controlled with LabView software (National Instruments, Austin, TX). Immediately prior to testing, the edges of the frames were cut leaving the threads intact; then the threads were loaded to failure at a 50% strain rate (10 mm/min). Curves of the 1st Piola Kirchhoff stress versus Green's Strain were calculated from the load displacement data assuming a cylindrical cross-sectional area of each thread and calculating cross-sectional area based on thread diameter measurements made as previously described for swelling ratio. Ultimate tensile strength (UTS), strain at failure (SAF), and modulus (E) were calculated from the stress-strain curves. Post-processing of the mechanical data considered a strain of zero to be when a thread was minimally loaded

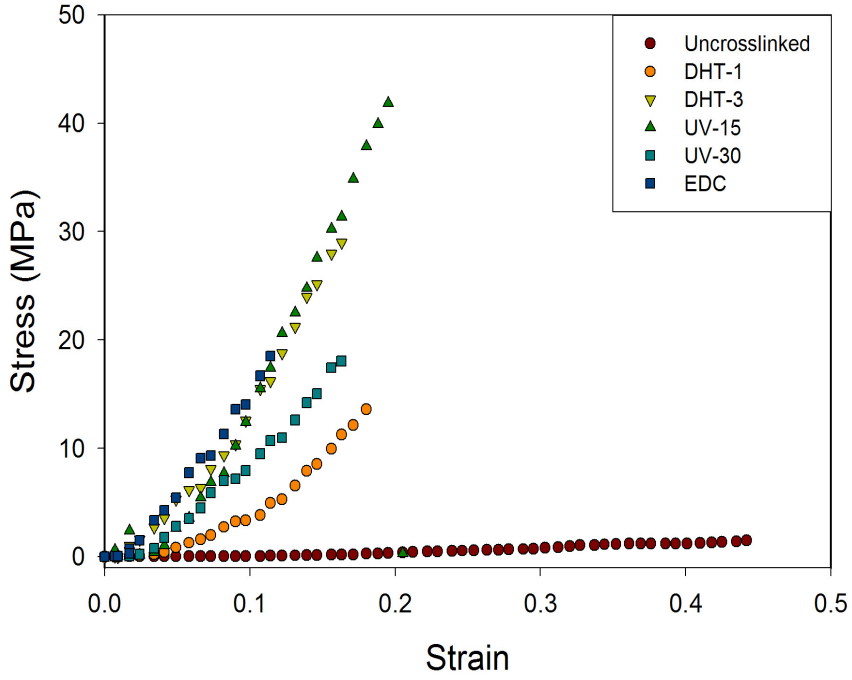

Figure 4.1: Characteristic stress-strain relationships for self-assembled collagen threads. Representative stress-strain curves for uncrosslinked and crosslinked collagen threads demonstrate a linear trend with failure occurring instantaneously. Threads were crosslinked by dehydrothermal treatment for 1 day (DHT-1) or 3 days (DHT-3), by exposure to ultraviolet light for 15 minutes (UV-15) or 30 minutes (UV-30) or by exposure to carbodiimide (EDC).

to a nominal threshold of 0.01 grams, or less than 1% of the ultimate load for the weakest uncrosslinked thread.

4.2.4 Enzymatic Degradation of Crosslinked Collagen Threads

Collagen thread degradation in collagenase was assayed for total protein content by ninhydrin reactivity.[15] Two-inch segments of each type of crosslinked threads including uncrosslinked control threads were cut into 8 pieces and placed in a microcentrifuge tube. The samples were incubated at 37°C in 200 µL of 0.1M Tris-base, 0.25M $CaCl_2$ solution (pH 7.4) containing 125 U/mL bacterial collagenase (Clostridium histolyticium, Calbiochem, Inc.) for either 4 or 24 hours. After incubation, the samples were centrifuged at 15,000 RCF for 10 minutes and the supernatant was reacted with 2% ninhydrin reagent (Sigma, St. Louis, MO) in boiling water for 10 minutes. The optical density was then measured at 570 nm in a spectrophotometer (SpectraMax, Molecular Devices, Sunnyvale, CA), and the relative optical density was calculated by subtracting

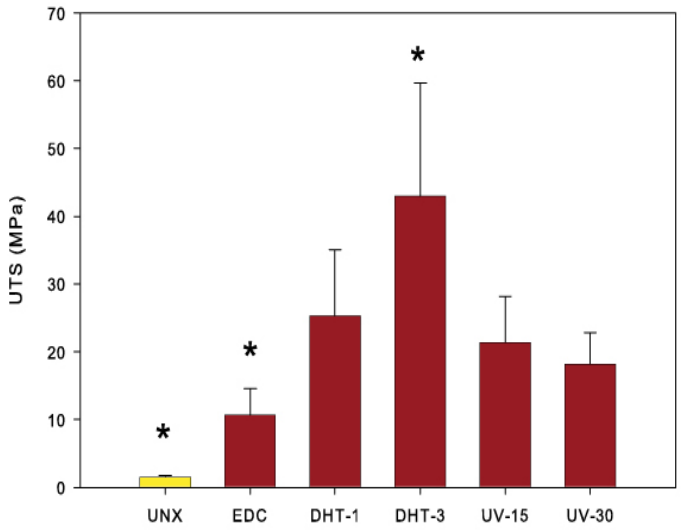

*Figure 4.2: Ultimate tensile strength of self-assembled collagen threads with crosslinking. * denotes statistical difference from all other conditions by one-way ANOVA*

the value of the background (collagenase only control) from the acquired optical density. The enzymatic degradation of each thread type was assayed in triplicate.

4.2.5 Cell Outgrowth Bioassay

Cell outgrowth bioassay systems were constructed using methods modified from those described in Chapter 3.2.5. Raised rectangular platforms (0.5 cm X 5 cm) of Thermanox® tissue culture plastic were elevated 1.5 mm above the surface of rectangular one-well plates (Nalge Nunc International, Rochester, NY). Threads were suspended across the raised platforms spaced 2.5 cm apart, and the thread ends attached to the tissue culture plates with Silastic® medical adhesive (Dow Corning, Midland, MI). The systems were sterilized with 70% isopropanol overnight and rinsed 3 times in sterile distilled water. The systems were air dried in a laminar flow hood prior to seeding.

To seed cell outgrowth bioassays, 0.5-mL aliquots of fibroblast-populated collagen lattice were placed onto each platform. These lattices were produced by mixing 3.0 mL of 5×10^5 cells/mL subconfluent GFP transduced fibroblasts with 2.4 mL of type I collagen (2.5 mg/mL) and 0.6 mL 5 × DMEM. After the gels were allowed to set at room temperature for 1 hr, the one-well plates were filled with 15 mL of DMEM supplemented with 10% FBS to a height just above the platforms and threads. Every 24 hours, the threads were visualized with a Nikon Eclipse TS100 inverted epifluorescent microscope coupled with a SpotRT CCD Camera (Diagnostic Instruments, Sterling Heights, MI). Measurements of the distance to the furthest cell on the thread from the edge of the platform as the cells migrated out of the gel onto the threads were taken using a calibrated reticule in the eyepiece of the microscope. The average velocities reported are averages of values measured daily between days 3-10. The system contained 3 samples of each

Table 4.1: Summary of Swelling Data and Effective Crosslink Density Calculations

	Sample Size	Dry Area (μm^2)	Hydrated Area (μm^2)	Swelling Ratio	M_c (g/mol) (x 10^3)	ν_e (mol/cm^3) (x 10^{-6})
UNX	20	2220 ± 770	25900 ± 5790	12.47 ± 3.6	170.2 ± 81.5	9.9 ± 4.8
DHT-1	20	2080 ± 560	6450 ± 1590	3.32 ± 1.3	19.9 ± 15.3	91.5 ± 43.0
DHT-3	20	2350 ± 560	5390 ± 1440	2.37 ± 0.7	10.3 ± 4.6	164.4 ± 89.5
UV-15	20	2600 ± 1180	5360 ± 1500	2.54 ± 2.1	18.6 ± 35.6	164.9 ± 86.7
UV-30	20	1970 ± 500	5170 ± 1250	2.70 ± 0.6	13.5 ± 5.9	115.1 ± 41.1
EDC	20	2620 ± 820	12100 ± 2630	4.78 ± 0.9	33.5 ± 10.3	43.8 ± 12.9

thread type with 4 sample readings possible per thread, yielding a sample size of 12 per crosslinking method. Individual threads were randomly placed in the system, and the experimenter was blinded to the identities until measurements were complete.

4.2.6 Fibronectin Adsorption on Collagen Threads

To visualize variations in protein adsorption with crosslinking on the surface of collagen threads, fluorescently labeled fibronectin was adsorbed to the surface of collagen threads. Collagen threads were placed in 100 μg/mL solutions of fibronectin (BD Biosciences, Bedford, MA) conjugated with Alexafluor 594 (Molecular Probes, Eugene, OR) for 24 hours to facilitate for protein adsorption to the surface. Threads were rinsed three times in phosphate buffered saline and viewed hydrated using a Texas Red filter on a Nikon Eclipse E400 microscope.

4.2.7 Statistical Analyses

Statistical differences between means of the data were conducted by one-way ANOVA with pairwise multiple comparisons (Holm-Sidak method) using SigmaStat

Table 4.2: Mechanical Properties Summary Table for Self-Assembled Collagen Threads

	Sample Size	UTS (MPa)	Strain at Failure	Modulus (MPa)
UNX	20	1.5 ± 0.2	0.42 ± 0.12	4.0 ± 1.2
DHT-1	18	25 ± 10	0.17 ± 0.08	166 ± 74
DHT-3	16	43 ± 17	0.18 ± 0.05	249 ± 95
UV-15	16	21 ± 7	0.13 ± 0.08	192 ± 65
UV-30	18	18 ± 5	0.10 ± 0.03	188 ± 62
EDC	17	11 ± 4	0.17 ± 0.04	68 ± 31

(Systat Software Inc., Point Richmond, CA). For mechanical testing and swelling ratio measurements, 20 samples of each type of crosslinked collagen thread were tested. A $p < 0.05$ indicated a significant difference between experimental groups.

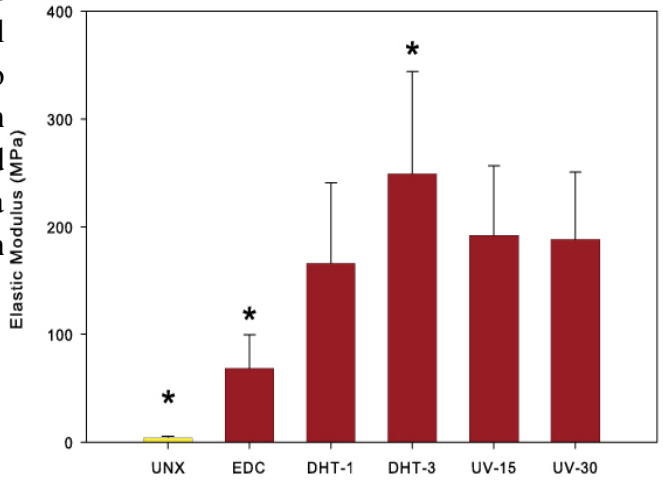

*Figure 4.3: Elastic modulus of self-assembled collagen threads with crosslinking. *denotes signicant difference from all other conditions by one-way ANOVA.*

4.3 Results

4.3.1 The Mechanical Properties of Self-Assembled Collagen Threads are Enhanced by Crosslinking

To characterize the mechanical properties of self-assembled collagen threads, discrete threads were loaded under uniaxial tension until failure. The results of this analysis are summarized in Table 4.1. Representative stress-strain curves for the threads, both uncrosslinked and crosslinked, were roughly linear in shape with failure generally occurring instantaneously (Figure 4.1, pg. 64). Due to the linearity of the loading profiles, the bulk elastic modulus of each sample was calculated using Hooke's Law ($\sigma=E\varepsilon$). Relative to the uncrosslinked threads, the ultimate tensile strengths (Figure 4.2, pg 65) and elastic moduli (Figure 4.3, pg. 67) of self-assembled collagen threads were significantly increased by each of the crosslinking methods that were examined. Similarly, the total elongation before tensile failure (strain at failure) for each crosslinked thread decreased significantly relative to uncrosslinked collagen threads (Figure 4.4, pg. 68).

Different crosslinking techniques, however, had different effects on the overall mechanical properties of self-assembled collagen threads (Figure 4.2 and Figure 4.3, pg. 65 and 67). The ultimate tensile strength and bulk elastic modulus of threads DHT crosslinked for 3 days (DHT-3) were significantly higher then all other crosslinking techniques. By 15 minutes of exposure, UV crosslinked threads achieved ultimate tensile strengths comparable to DHT crosslinking of 24 hours (UV-15 vs. DHT-1). Doubling the UV exposure time (UV-15 vs. UV-30) did not significantly increase the ultimate tensile strength or elastic modulus of the threads. The ultimate tensile strengths and bulk

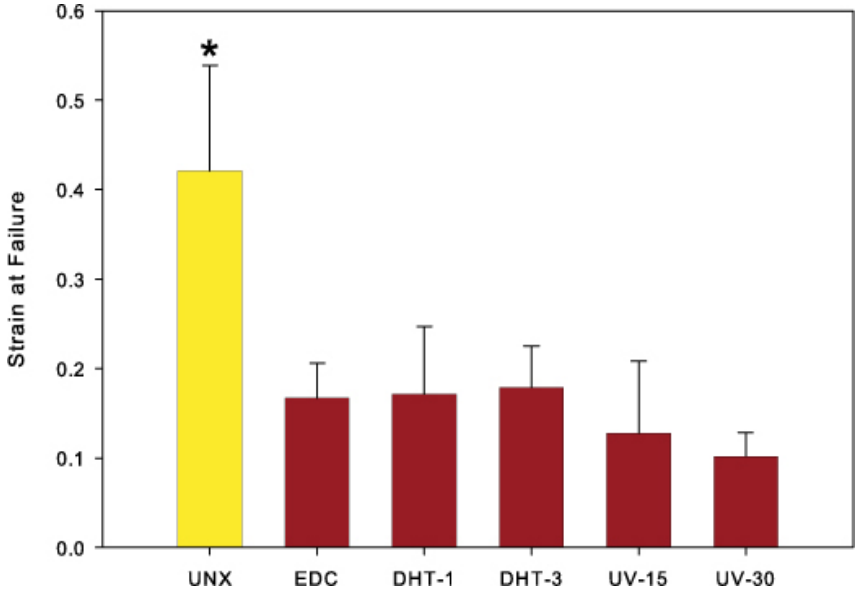

Figure 4.4: Strain to failure values of self-assembled collagen threads with crosslinking. Uncrosslinked controls were stistically greater than all crosslinke conditions by one-way ANOVA.

moduli of EDC crosslinked threads were significantly lower than threads crosslinked by other crosslinking methods in this study. The strains at failure for threads crosslinked by all of the methods in this study were similar to each other and significant less the strains at failure for uncrosslinked threads (Figure 4.4, pg. 68).

4.3.2 Crosslink Densities Correlate with Ultimate Tensile Strengths of Threads

To establish a relationship between the mechanical properties of the collagen threads and structural properties of the crosslinked and uncrosslinked scaffolds, the effective crosslink densities of the materials were calculated from the volumetric swelling ratios of the hydrated scaffolds.[9, 11] Cross-sectional areas of dry threads from each group were not statistically different from each other (Figure 4.5, pg. 69). After rehydration, uncrosslinked threads swelled to more than 12 times their dry cross-sectional area with swelling ratios averaging close to 4 times greater than those of any UV or DHT crosslinked threads. EDC crosslinked threads swelled significantly more than threads crosslinked by other methods in this study (Figure 4.5, pg. 69). From the Flory-Rehner equation, these swelling ratios were used to approximate values for the molecular weights between crosslinks and the effective crosslink densities of the different collagen threads (Table 4.2), similar to those seen in collagen membranes. [16] A plot of the ultimate tensile strengths and the effective crosslink density for each of the thread types in the

study, suggests that there is a strong positive correlation between the two values. The ultimate tensile strengths of the crosslinked threads appear to increase proportionally to the scaffold's crosslink density (Figure 4.6, pg. 70).

4.3.3 Crosslinking Affects the In Vitro Enzymatic Stability of the Collagen Threads

To characterize the enzymatic stability of self-assembled collagen threads after crosslinking, we measured the relative degradation of collagen scaffolds by bacterial collagenase. The total protein content of thread solubilized after enzymatic digestion was assayed by ninhydrin reactivity. Uncrosslinked threads degraded rapidly and by 4 hours the macroscopic morphology had been completely disrupted. This complete degradation was confirmed by equivalent optical density measurements at 4 and 24 hours (Figure 4.7, pg. 71). Crosslinking significantly decreased the *in vitro* rate of degradation for all crosslinking techniques. Unlike the uncrosslinked threads, crosslinked collagen threads maintained their macroscopic morphologies at 4 hours, and absorbance values were significantly lower when compared to uncrosslinked threads at 4 hours (Figure 4.7, pg.

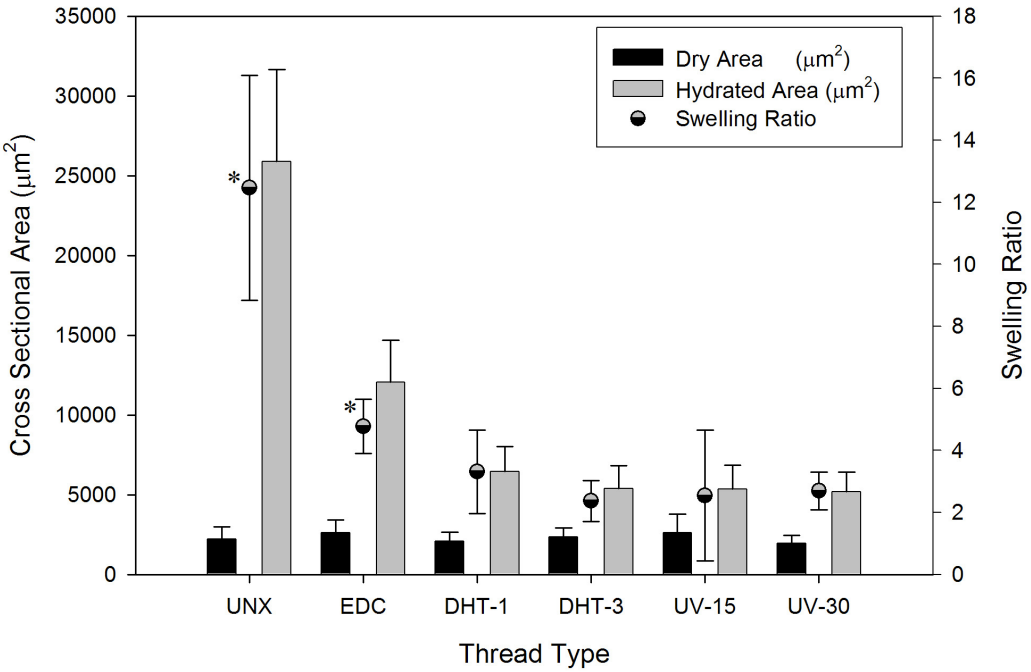

*Figure 4.5: Cross-sectional area and Swelling. The mean and standard deviations for dry and hydrated cross-sectional areas of self-assembled collagen threads are plotted against the left y-axis. Swelling ratios are plotted on top against the right y-axis. *denotes significant difference from all other swelling ratios with a one-way ANOVA*

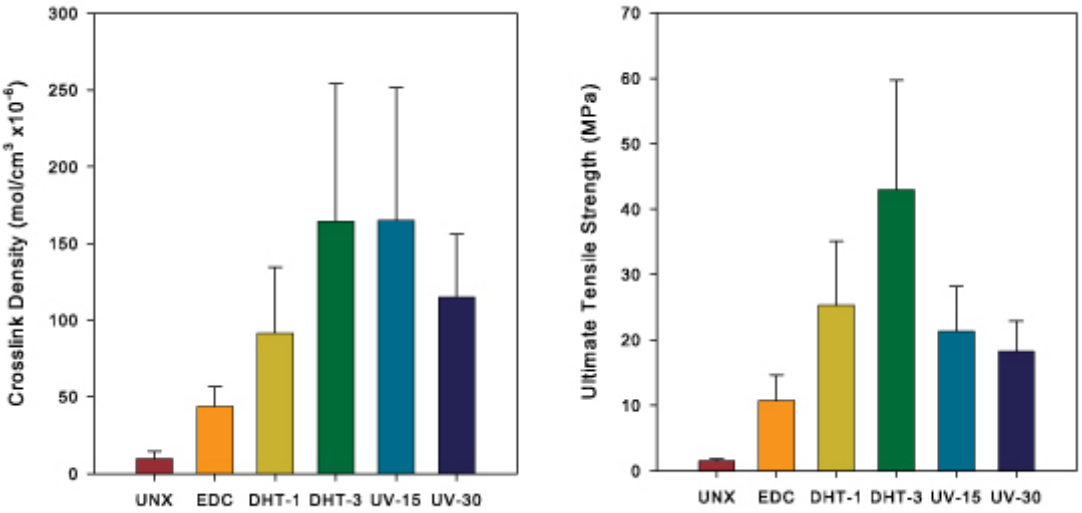

Figure 4.6: The effective crosslink density calculated from the swelling ratios of collagen thread crosslinked as specified, correlate roughly with an ultimate tensile strength.

71). By 24 hours, all crosslinked threads were significantly more degraded, relative to the 4 hour time point. Although statistical differences between crosslinked threads were not observed, EDC crosslinked threads consistently demonstrated a trend towards an increased enzymatic stability compared to threads crosslinked by other techniques.

4.3.4 Cell Outgrowth Is Decreased On Crosslinked Threads

To characterize fibroblast interaction with thread surfaces and to predict the rate of new tissue ingrowth, fibroblast outgrowth velocity was measured on self-assembled threads. Average fibroblast outgrowth velocities were significantly greater on uncrosslinked self-assembled threads than any crosslinked thread (Figure 4.8, pg. 72). When velocities on crosslinked collagen scaffolds were compared with each other, EDC crosslinked threads facilitated significantly higher average rates than all crosslinking methods, with the exception of threads that were DHT crosslinked for 1 day (DHT-1) (Figure 4.8, pg. 72). UV crosslinked threads and threads DHT crosslinked for 3 days exhibited average velocities less than half the velocity observed on uncrosslinked threads (0.86 mm/day), and approximately half the rate of EDC crosslinked threads.

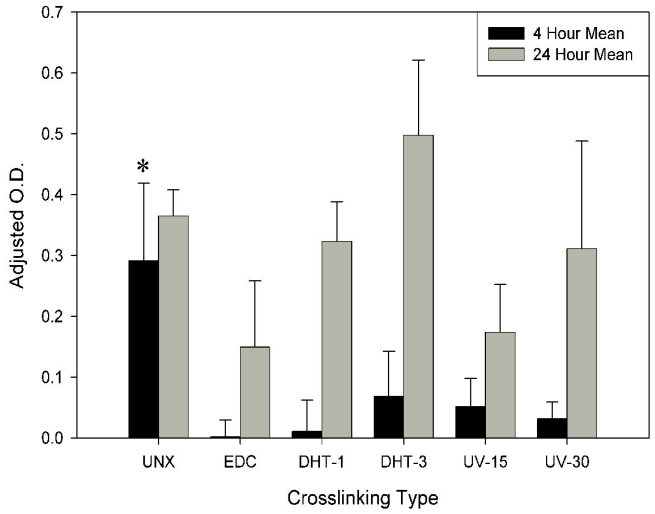

Figure 4.7: Enzymatic stability of self-assembled collagen threads Total protein content of the supernatant after degradation by bacterial collagenase was assayed by ninhydrin reactivity and reported as a measure of relative optical density (O.D.) at 4 and 24 hours. The mean (n=3) optical density of the background (collagenase only) was subtracted from the mean (n=3) of each sample type to calculate relative optical density. Uncrosslinked threads were completely degraded by 4 hours and not significantly different from threads assayed after 24 hours. (-indicates significant difference from all other thread types at 4 hours)*

4.3.5 Fibronectin Adsorption to Collagen Threads is Dependent on Crosslinking Technique

To assess protein binding affinity on the surfaces of crosslinked collagen threads, fluorescently labeled fibronectin was adsorbed to the scaffolds. Fluorescent images of fibronectin-coated threads indicate that the protein binds uniformly to the surfaces of uncrosslinked and EDC crosslinked threads (Figure 4.9, pg. 73). In contrast, fibronectin adsorption to DHT crosslinked threads appeared to be non-uniform, with irregular striations and banding regions that suggest inhomogeneous protein adsorption (Figure 4.9, pg. 73).

4.4 DISCUSSION

The goal of this study was to investigate physical and chemical crosslinking techniques that can enhance the bulk mechanical properties of self-assembled collagen threads without decreasing the outgrowth velocity on their surfaces. In a previous study, we described a technique to create self-assembled collagen threads with mechanical properties and fibrillar substructure comparable to native tendon tissue.[4] A limitation of this technique is that the threads must be physically or chemically crosslinked to impart the strength and stiffness necessary to withstand the high tensile load demands of a ligament tissue. Until now, cellular responses to crosslinked self-assembled collagen threads had yet to be characterized. In the present study, self-assembled collagen threads were stabilized with one of two physical crosslinking methods or a chemical crosslinking method. Uniaxial tensile tests showed that all of the crosslinking techniques significantly increased the strengths and stiffnesses of the threads (Figure 4.2 and Figure 4.3, pg. 65

and 67) and decreased the enzymatic degradation rates of the scaffolds (Figure 4.7, pg. 71). While each crosslinking technique also decreased the rate of fibroblast population outgrowth, velocity across the surface of EDC crosslinked threads was significantly greater than on most physically crosslinked threads (Figure 4.8, pg. 72).

In developing a functional construct to regenerate damaged tendon and ligament tissues, researchers must create scaffolds that can withstand the immediate high tensile load bearing environment of the tissue while rapidly integrating with the surrounding tissue to promote new tissue ingrowth and complete regeneration of the damaged tissue. Self-assembled collagen threads are a promising material for regenerating tendons and ligaments because of their biochemistry and structural homology to native tissue constructs. In previous model systems, it was suggested that physical and chemical crosslinking techniques may limit the performance of collagen scaffolds by decreasing the cell outgrowth.[2]

The results of this work confirm that the collagen crosslinking techniques examined in this study differentially attenuate fibroblast outgrowth velocity on the surfaces of the

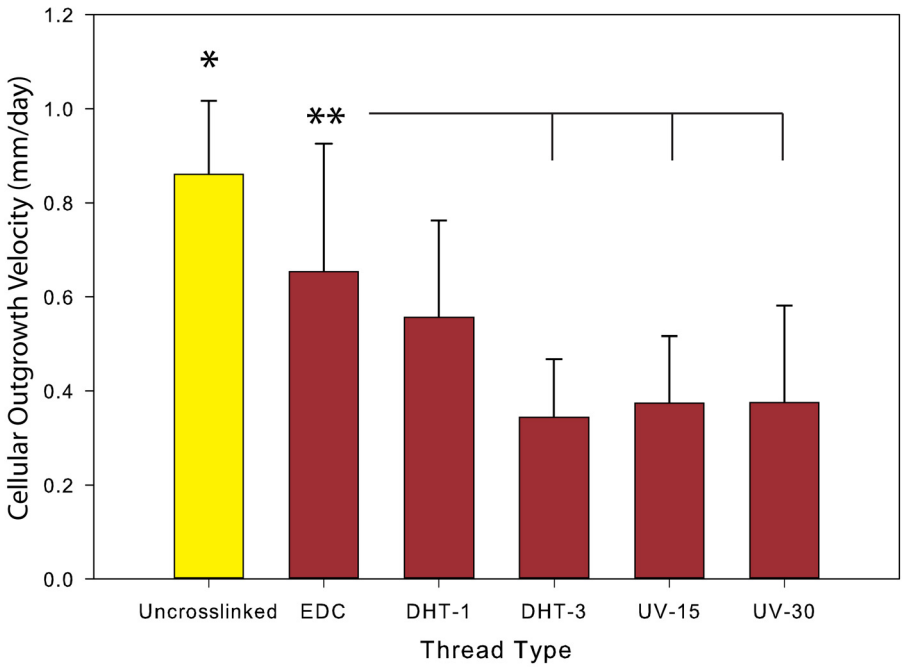

*Figure 4.8: Fibroblast Cell Outgrowth Is Decreased By Crosslinking. Plot showing means (n=12) and standard deviations of fibroblast cell outgrowth velocities measured from days 3-10 of culture for each crosslinking technique. *Denotes significant difference from all other conditions. **Denotes significant difference from other conditions as indicated.*

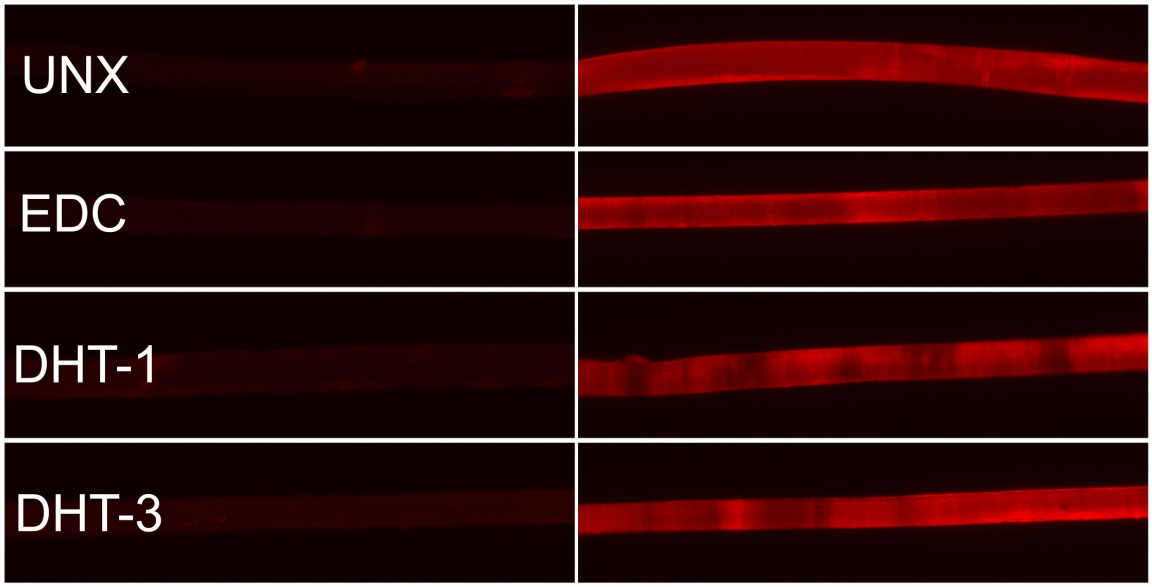

Figure 4.9: FN Attachment is Non-Uniform. Fluorescently labeled fibronectin (FN) was adsorbed to the surface of collagen threads (right), compared with no FN controls (left). The FN adsorbed to the surface of crosslinked threads was non-uniform and inconsistent.

scaffolds. The relationship between strength with crosslinking and cellular outgrowth velocity is described in Figure 4.10, page74. Cellular outgrowth velocity was plotted against ultimate tensile strength and fit with standard linear regression (R=0.94). Using a Spearman Rank Order Correlation, a correlation coefficient of -0.829 was calculated with a $p < 0.0583$. This correlation coefficient quantifies the strength of the association between the variables where a value of -1 would indicate a strong negative relationship between the two variables, with one always decreasing as the other increases. In this case, the p value is greater than 0.05 and therefore not strong enough to statistically correlate the two parameters, but ultimate tensile strength and cellular outgrowth velocity can still be considered reasonable related.

Interestingly, chemically crosslinking self-assembled collagen threads with EDC did not increase the strength or stiffness of the scaffolds to the same extent as the physically crosslinked threads; however, fibroblast migration was faster on the EDC crosslinked threads. Furthermore, EDC crosslinked threads swelled to more than 4 times their dry cross-sectional area and to a significantly greater extent than physically crosslinked threads upon rehydration (Figure 4.5, pg. 69). This increased swelling suggests that the EDC crosslinked threads have a lower crosslink density and more hydrophilic surface properties than physically crosslinked threads. Hydrophilic surfaces have been shown to enhance the biological activity of fibronectin, a key protein associated with cell

attachment, proliferation, and migration[17, 18] and cells more readily deposit endogenous fibronectin these surfaces.[19] In this study, we found that EDC crosslinked threads allowed for more consistent fibronectin binding than seen on DHT crosslinking threads as well (Figure 4.9, pg. 73). DHT crosslinking may alter the surface biochemistry in a manner that changes the surface wettability and protein conformations critical for fibroblast interactions with these surfaces. Our findings are also consistent with studies suggesting that physical crosslinking techniques such as UV or DHT denature collagen by unwinding the triple-helix[7, 20] and mask fibroblast integrin binding sites ($\alpha 1\beta 1$ and $\alpha 2\beta 1$) that are dependent on maintenance of the triple-helical conformation of collagen.[21, 22] It is also unclear whether factors such as variations in matrix stiffness or surface topography play a role in modulating cell-matrix interactions on surfaces as discussed in Chapter 3. We plan to investigate these factors in future studies.

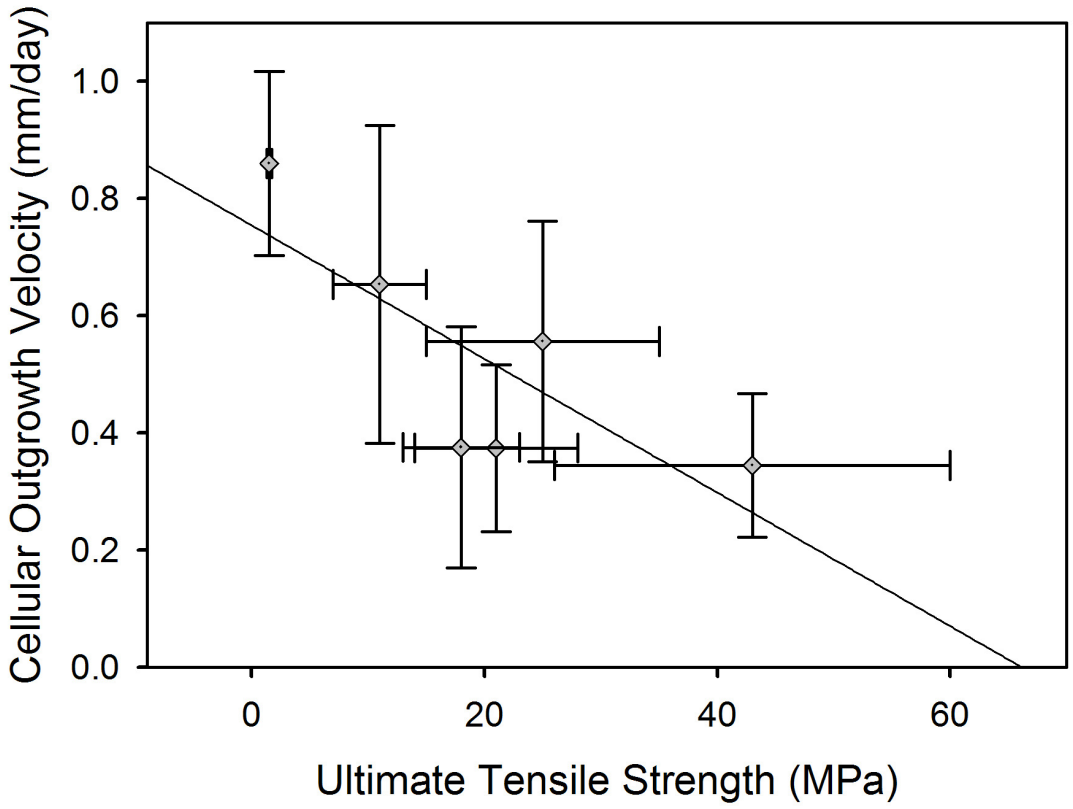

Figure 4.10: UTS Correlates to Cell Outgrowth - Cellular outgrowth velocity was plotted as function of ultimate tensile strength and fit with standard linear regression. A Spearman rank on correlation factor was calculated of -0.829 with $p<0.0583$. The two parameters are inversely correlated but not strongly.

REFERENCES

[1] Vunjak-Novakovic G, Altman G, Horan R & Kaplan DL. Tissue engineering of ligaments. *Annu Rev Biomed Eng* **6**: pp. 131-156. (2004).
[2] Dunn MG, Liesch JB, Tiku ML & Zawadsky JP. Development of fibroblast-seeded ligament analogs for acl reconstruction. *J Biomed Mater Res* **29**: pp. 1363-1371. (1995).
[3] Pins G & Silver F. A self-assembled collagen scaffold suitable for use in soft and hard tissue replacement. *Materials Science and Engineering:C* **3**: pp. 101-107. (1995).
[4] Pins GD, Christiansen DL, Patel R & Silver FH. Self-assembly of collagen fibers. influence of fibrillar alignment and decorin on mechanical properties. *Biophys J* **73**: pp. 2164-2172. (1997).
[5] George D. Pins, Eric K. Huang, David L. Christiansen, Frederick H. Silver. Effects of static axial strain on the tensile properties and failure mechanisms of self-assembled collagen fibers. *J Appl Polym Sci* **63**: pp. 1429-1440. (1997).
[6] Elsdale T & Bard J. Collagen substrata for studies on cell behavior. *J Cell Biol* **54**: pp. 626-637. (1972).
[7] Weadock KS, Miller EJ, Bellincampi LD, Zawadsky JP & Dunn MG. Physical crosslinking of collagen fibers: comparison of ultraviolet irradiation and dehydrothermal treatment. *J Biomed Mater Res* **29**: pp. 1373-1379. (1995).
[8] Gentleman E, Lay AN, Dickerson DA, Nauman EA, Livesay GA & Dee KC. Mechanical characterization of collagen fibers and scaffolds for tissue engineering. *Biomaterials* **24**: pp. 3805-3813. (2003).
[9] Baier Leach J, Bivens KA, Patrick CWJ & Schmidt CE. Photocrosslinked hyaluronic acid hydrogels: natural, biodegradable tissue engineering scaffolds. *Biotechnol Bioeng* **82**: pp. 578-589. (2003).
[10] Flory P, Rehner J. Statistical mechanics of cross-linked polymer networks. *Journal of Chemical Physics* **11(11)**: pp. 521-526. (1943).
[11] Flory P. Principles of polymer chemistry. : . (1953).
[12] Bohidar H & Jena S.. Kinetics of sol-gel transition in thermoreversible gelation of gelatin. *Journal of Chemical Physics* **98**: pp. 8970-8977. (1993).
[13] Huglin MB, Rehab M & Zakaria M. Thermodynamic interactions in copolymeric hydrogels. *Macromolecules* **19**: pp. 2986-2991. (1986).
[14] Fischer H, Polikarpov I & Craievich AF. Average protein density is a molecular-weight-dependent function. *Protein Sci* **13**: pp. 2825-2828. (2004).
[15] Starcher B. A ninhydrin-based assay to quantitate the total protein content of tissue samples. *Anal Biochem* **292**: pp. 125-129. (2001).
[16] Charulatha V & Rajaram A. Influence of different crosslinking treatments on the physical properties of collagen membranes. *Biomaterials* **24**: pp. 759-767. (2003).
[17] Grinnell F & Feld MK. Adsorption characteristics of plasma fibronectin in relationship to biological activity.. *J Biomed Mater Res* **15**: pp. 363-381. (1981).
[18] Grinnell F. Fibronectin and wound healing.. *J Cell Biochem* **26**: pp. 107-116. (1984).
[19] Grinnell F & Feld MK. Fibronectin adsorption on hydrophilic and hydrophobic surfaces detected by antibody binding and analyzed during cell adhesion in serum-containing medium.. *J Biol Chem* **257**: pp. 4888-4893. (1982).
[20] Gorham SD, Light ND, Diamond AM, Willins MJ, Bailey AJ, Wess TJ & Leslie NJ. Effect of chemical modifications on the susceptibility of collagen to proteolysis. ii. dehydrothermal crosslinking. *Int J Biol Macromol* **14**: pp. 129-138. (1992).
[21] Grab B, Miles AJ, Furcht LT & Fields GB. Promotion of fibroblast adhesion by triple-helical peptide models of type i collagen-derived sequences. *J Biol Chem* **271**: pp. 12234-12240. (1996).

[22] Kuhn K & Eble J. The structural bases of integrin-ligand interactions. *Trends Cell Biol* **4**: pp. 256-261. (1994).
[23] Karageorgiou V, Meinel L, Hofmann S, Malhotra A, Volloch V & Kaplan D. Bone morphogenetic protein-2 decorated silk fibroin films induce osteogenic differentiation of human bone marrow stromal cells. *J Biomed Mater Res A* **71**: pp. 528-537. (2004).
[24] Hollinger JO, Schmitt JM, Buck DC, Shannon R, Joh SP, Zegzula HD & Wozney J. Recombinant human bone morphogenetic protein-2 and collagen for bone regeneration. *J Biomed Mater Res* **43**: pp. 356-364. (1998).
[25] Dunn MG, Avasarala PN & Zawadsky JP. Optimization of extruded collagen fibers for acl reconstruction. *J Biomed Mater Res* **27**: pp. 1545-1552. (1993).
[26] Wasserman AJ, Kato YP, Christiansen D, Dunn MG & Silver FH. Achilles tendon replacement by a collagen fiber prosthesis: morphological evaluation of neotendon formation. *Scanning Microsc* **3**: p. 1183-97; discussion 1197-200. (1989).

CHAPTER 5: FIBRIN MICROTHREADS:
DEVELOPMENT OF NOVEL FIBRIN MICROTHREADS WITH COMPARABLE PROPERTIES TO COLLAGEN THREADS

5.1 INTRODUCTION

While self-assembled collagen threads structurally and biochemically mimic native tendon and ligament, the studies in the previous chapters of this thesis suggest that when crosslinked, collagen threads may not elicit a response that dynamically regulates the spatially and temporally complex process of tissue regeneration. While type I collagen is the basic structural protein of the extracellular matrix in healthy ligament, it is typically not the structural component immediately after injury. During the initial stages of wound healing and tissue regeneration, a fibrin provisional matrix is deposited to fill the wound space and to promote fibroblast infiltration from the wound margin (see Chapter 2.4.1). This fibrin extracellular matrix regulates cell migration, proliferation, and gene expression through integrin signaling[1-3] and localization of matrix bound signaling proteins.[4, 5] Since the ECM plays an important role in the regulation of wound healing and tissue regeneration (see Chapter 2.3.2), we hypothesize that the limitations of collagen thread-based matrices can be overcome through the addition of the early wound healing structural protein, fibrin.

Fibrin is polymerized enzymatically *in vivo* as part of the natural wound healing cascade. Initially fibrinogen, found in blood plasma at a concentration of 3 mg/ml, is modified by the enzyme thrombin to expose binding sites in the central portion of the elongated protein.[6, 7] The fibrinogen monomers then assemble laterally in an end-to-middle ½-staggered overlap pattern, forming long fibers. These fibers further aggregate laterally and branch into complex networks that constitute the fibrin matrix.[6, 7]

Similarly, these processes are duplicated *in vitro* for the development of biomaterials. Unfortunately, traditional fibrin biomaterials lack the strong mechanical properties demanded by high load bearing applications such as ligament regeneration. The structural properties can be modified, most significantly, by altering the initial fibrinogen concentration. For example, fibrin hydrogels are produced at low fibrinogen concentrations and have been widely studied for engineering applications ranging from cardiovascular grafts[8-11] to bioengineered cartilage.[12-14] However, like most gels, these materials are of limited mechanical strength. Higher fibrinogen concentrations are commercially available in adhesive sprays or glues used as sealants to control bleeding during surgery[15-18] and have recently been investigated for cell delivery.[19-21] To take advantage of the wound healing cell-signaling capabilities of fibrin and to compensate for its lack of mechanical strength, cells have been seeded in fibrin gels onto a polymer mesh[22] for cardiovascular[23] and orthopedic applications.[24, 25]

Fibrin matrices or scaffolds synthesized with a thread morphology would theoretically benefit from the structural and mechanical advantages of fiber or thread-based structures. Most notably, cylindrical substrata with diameters less than 100 μm facilitate contact guidance, the natural alignment and orientation of cells.[26] Particularly in a highly aligned connective tissues such as the ACL (See Chapter 2.1.1.1), aligned fibroblasts will lead to aligned matrix deposition and ultimately improved strength and regeneration. Secondly, fibrin threads will likely possess elevated mechanical strengths and stiffnesses for improved handling and manipulation for assembly into macro-structures. We theorized that a fibrin fiber could be produced by beginning with high concentration fibrinogen[27] and by using extrusion technologies similar to those for collagen thread production.[28] Threads produced in this manner should attain sufficient mechanical stability to allow for integration with other thread scaffolds while concurrently promoting the cell alignment and aligned ECM deposition seen on fiber scaffolds.

Therefore, the second goal of this thesis was to develop fibrin microthreads with comparable morphology to collagen threads that can be combined with other matrices for ligament tissue regeneration, to ultimately guide wound healing spatially and temporally, through aligned regeneration, growth factor delivery, and variable matrix signaling.

This chapter will focus on the manufacturing and production development of fibrin microthreads, while Chapter 6 will investigate the cell response to these optimized threads. Fibrin microthread production parameters were investigated for tensile properties in order to quantify and maximize mechanical integrity. Subsequently, these optimized microthreads were probed for their morphological similarities to collagen threads.

5.2 Materials and Methods

5.2.1 Fibrin Microthread Manufacturing

5.2.1.1 Material Preparation

Fibrin microthreads were co-extruded from solutions of fibrinogen and thrombin using extrusion techniques similar to methods described previously (Chapter 4,5 Methods). Fibrinogen from bovine plasma (Sigma, St. Louis, MO F4753) was dissolved in HEPES Buffered Saline (HBS, 20 mM HEPES, 0.9% NaCl, pH 7.4) at 70 mg/mL and stored at -20 ^{o}C. Thrombin from bovine plasma (Sigma, St. Louis, MO T4648) was stored frozen as a stock solution at a concentration of 40 U/mL in HBS. A working solution of thrombin was diluted from the stock to a final concentration of 6 U/mL in 40 mM $CaCl_2$ solution. Both the fibrinogen and thrombin solutions were warmed to 37 ^{o}C and placed into separate 1 mL syringes and were inserted into a blending applicator tip (Micromedics, Inc., St. Paul, MN). The blending applicators luer lock to the two syringes through individual bores and mix in a needle that luer locks to the tip. The solutions were combined and extruded through polyethylene tubing (BD, Sparks, MD) with an inner diameter of 0.38 mm into a bath of 10 mM HEPES (N-[2-Hydroxyethyl]piperazine-N'-[2-ethanesulfonic acid]) in a Teflon® coated pan.(Figure 5.1, pg. 80)

5.2.1.2 Coextrusion

The solutions were coextruded with variable parameters using an automated extrusion device (See appendix B for more detail). The custom-designed device consists

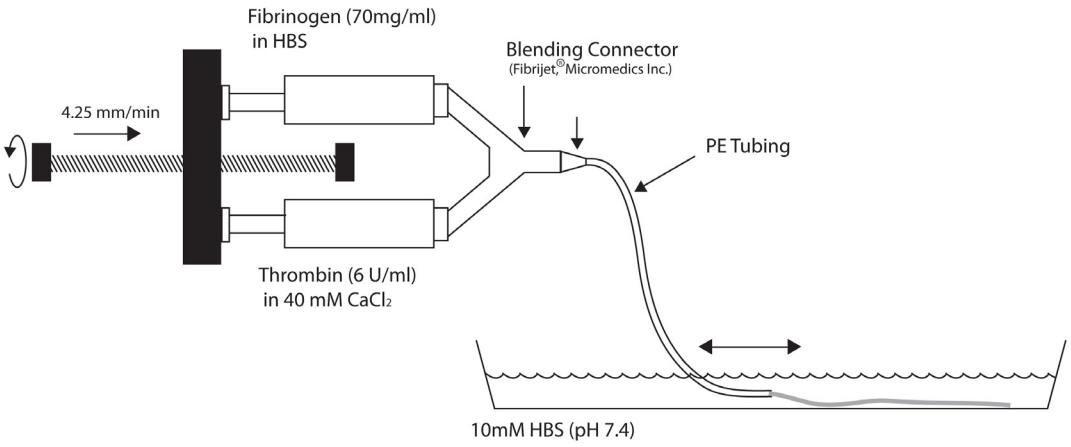

Figure 5.1: Schematic Drawing of Co-extrusion System. Fibrin microthreads were co-extruded at a crosshead speed of 4.25 mm/min from solutions of fibrinogen and thrombin in 1ml syringes through a blending connector and into a buffered bath. The threads were hand drawn through the bath at a rate approximately matching the flow rate of polymerizing solution from the tubing.

of motorized 2-D plotter, controlled with Labview software (National Instruments, Austin, TX) for spatial control of extrusion tubing tip and a stabilized crosshead on a threaded rod for control of extrusion fluid volume and rates (See Appendix A).

To characterize the effects of varying the extrusion rate and crosshead speed, microthreads were extruded at a range of syringe pump extrusion rates (0.125, 0.250, 0.500 ml/min) and with varying speed through the bath (550, 1100, 2200 mm/min). Therefore, with a tubing diameter of 0.38mm, the calculated velocities ranged from 1.84 – 7.35 cm/s for both the plotter and the flow. During data analysis, it became clear that the speed of the tubing through the bath (plotter velocity) and the speed of the fibrin solution out of the tubing (flow velocity) were directly and inversely correlated. Therefore, to more accurately represent the results, these data were compiled and described in the results as a rate ratio defined as:

$$rate\ ratio = \left(\frac{\text{flow velocity}}{\text{plotter velocity}} \right)$$

As such, a reported rate ratio of 2 has a mean flow velocity twice as fast as the tubing tip moves through the bath. At rate ratios below 1, cohesive threads could not be formed and were therefore not investigated further.

The pH and temperature of the extrusion solution were also varied and investigated for their affect on fibrin microthread tensile properties. The 10 mM HEPES solution was either heated to body temperature (37^{o}C) or left at room temperature (20^{o}C) and the pH of the bath was adjusted to either low (6.0), body (7.4), and high (8.0) values.

Finally, threads were removed from the bath, air dried under the tension of their own weight, and stored at room temperature in a desiccator until use.

5.2.2 Microthread Material Characterization

5.2.2.1 Scanning Electron Microscopy (SEM)

Fibrin microthreads were imaged with a scanning electron microscope to characterize thread morphology and surface topography. Air dried fibrin threads were mounted on aluminum stubs (Ted Pella, Inc., Redding, CA) coated with double-sided carbon tape and sputtered coated with a thin layer of gold-palladium for 30 seconds. Images were acquired at 15kV using a JSM-KLG scanning electron microscope.

5.2.2.2 Thread Swelling

Qualitative volumetric analyses based on the swelling ratio of fibrin threads were performed using methods described previously.[28] The cross-sectional area of each thread was calculated from an average of three diameter measurements along its length, assuming cylindrical thread geometry. The diameters were measured both dry and after hydration for at least 30 minutes in phosphate buffered saline (PBS) using a 20x objective on a Nikon Eclipse E400 microscope fitted with a calibrated reticule. The swelling ratio was calculated as the ratio of the wet cross-sectional area to the dry cross-sectional area for each discrete thread.

5.2.2.3 Mechanical Properties

Microthreads were hydrated and mechanically loaded in uniaxial tension to obtain stress-strain curves. Individual threads were mounted vertically with adhesive (Silastic Silicone Type A, Dow Corning) on vellum frames with precut windows that defined the region of loading. For tensile testing, the samples in the vellum frames were clamped into a custom designed micromechanical testing unit (See Appendix B) consisting of a horizontal linearly actuated crosshead and a fixed 150g load cell. Test unit operations and data acquisition were controlled with LabView software (National Instruments, Austin, TX). An initial gauge length of 20 mm was defined as the distance between adhesive spots across the precut window in the vellum frame. Threads were hydrated for

at least 30 minutes prior to testing, but were not tested submerged. After loading into the testing apparatus, the edges of each frame were cut leaving the thread intact. The threads were then loaded to failure at a 50% strain rate (10 mm/min). Curves of the 1st Piola Kirchhoff stress versus Green's Strain were calculated from the load displacement data assuming a cylindrical cross-sectional area of each thread and calculating cross-sectional area based on thread diameter measurements as described above for swelling ratio. Post-processing of the mechanical data considered a strain of zero to be when a thread was minimally loaded to a nominal threshold of 0.01 grams, or less than 1% of the ultimate load for the weakest uncrosslinked thread. Ultimate tensile strength (UTS), strain at failure (SAF), and the max tangent modulus or stiffness (E) were calculated from the stress-strain curves. The stiffness was defined as the maximum value for a tangent to the stress-strain curve over an incremental strain of 0.03.

5

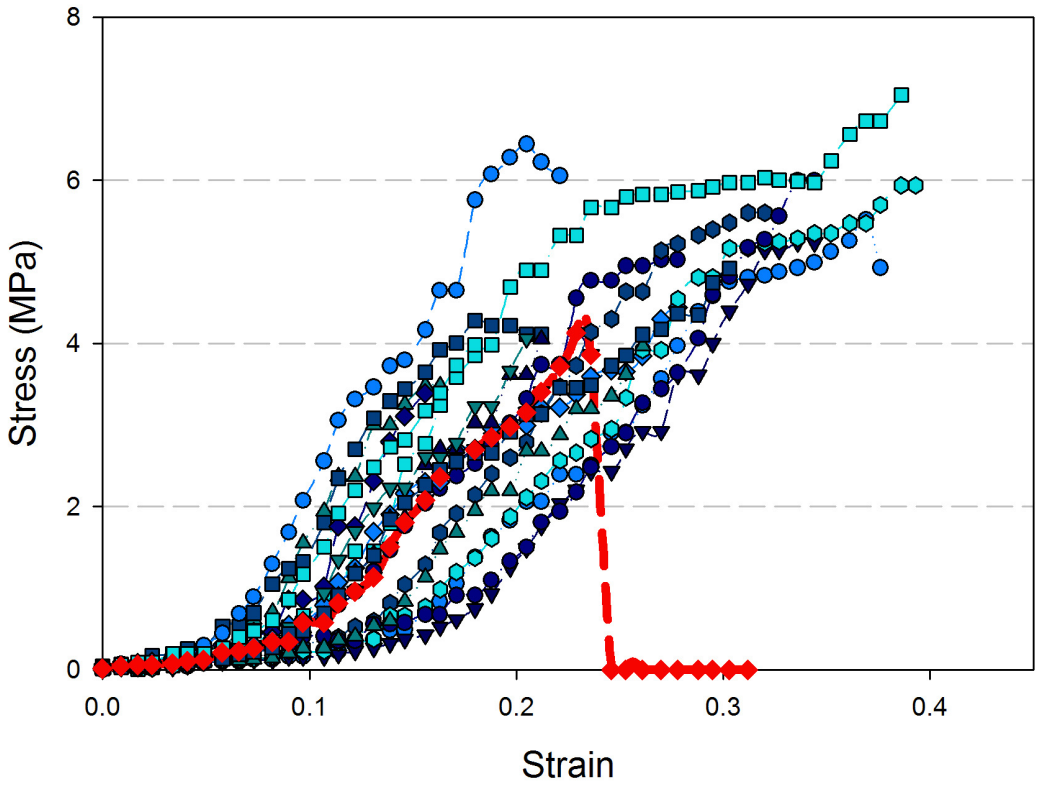

Figure 5.2: Characteristic Stress-Strain Curves. Plots of stress (MPa) versuse strain (dimensionless) are reported for hydrated fibrin microthreads (blue points, N=19) under optimized production conditions. The red curve represents an average characteristic stress-strain curve with a toe region exhibiting low stress, followed by a roughly linear higher modulus region until ultimate failure.

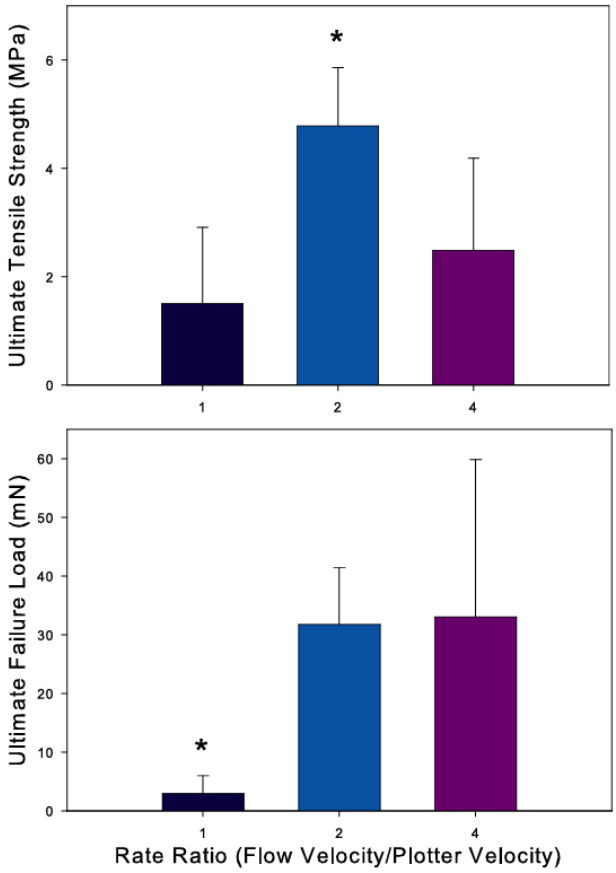

Figure 5.3: Tensile Properties With Varied Rate Ratio. Fibrin microthreads coextruded at a rate ratio of 1 demonstrated low failure tensile strength and failure loads. The ultimate tensile strength was maximized at a ratio of 2 to 1, flow velocity to plotter velocity.

Statistical differences between means of the data were conducted by one-way ANOVA with pairwise multiple comparisons (Holm-Sidak method) using SigmaStat (Systat Software Inc., Point Richmond, CA). Values reported are means and standard deviations unless otherwise stated. A $p < 0.009$ indicated a significant difference between experimental groups.

5.3 RESULTS

Fibrin microthreads were coextruded from solutions of fibrinogen and thrombin into an aqueous buffer and formed largely at the bottom of the bath. Upon removal from the bath, the threads stretched and elongated to approximately twice their length while thinning considerably in cross-sectional diameter. All the feasible process parameters were varied when possible. The fibrinogen concentration was maximized, by design, and therefore not varied. Altering the thrombin concentration led to no cohesive thread or clogging of the tubing and was therefore excluded from later analyses. However, the rate ratio, bath temperature and bath pH were scalable vectors and did alter the overall microthread mechanical properties as described in the appropriate sections below.

Hydrated fibrin microthreads were tensile tested until failure and the resulting force-displacement data were graphed as stress versus strain. In general, the tensile data collected demonstrated similar characteristic stress-strain plots. Samples typically began with toe region exhibiting low stress, followed by a high strain region of increasing

elongation roughly correlating with the expulsion of water from the microthread interior as visualized during experimentation. This was followed by a roughly linear, higher modulus region that continued until ultimate failure. Stress strain curves for what was eventually determined to be optimized production parameters are displayed in Figure 5.2, page 82, with an average characteristic curve highlighted in red.

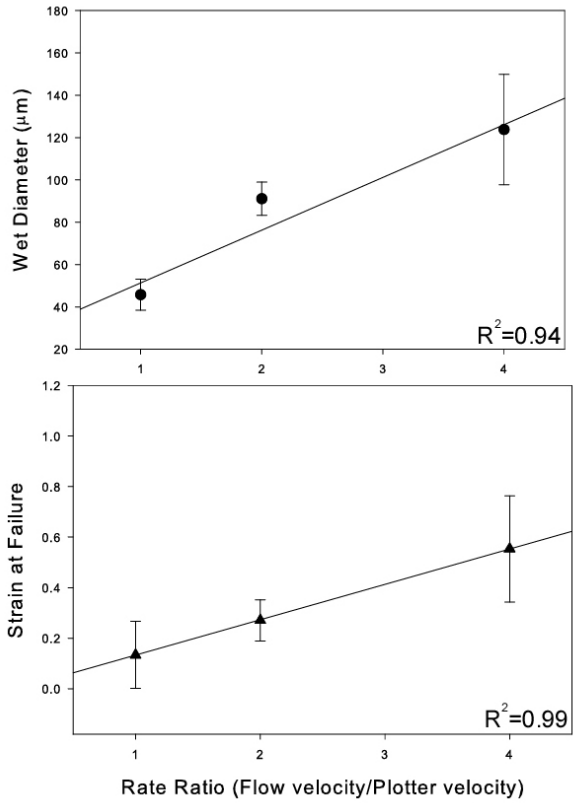

Figure 5.4: Diameter and Strain to Failure With Rate Ratio. The wet diameter and ultimate failure strain increased linearly with increasing rate ratio although linear regression correlations are not strong when fitting less than 5 data points.

5.3.1 Effect of Rate Ratio Variation

The ratio of the flow velocity to the plotter velocity was varied and investigated for its effects on microthread diameter and tensile properties. The ultimate tensile strength averaged 4.78 MPa for a rate ratio of 2 while ratios either above or below 2 resulted in statistically lower tensile strength (Figure 5.3, pg. 83). However, the load to failure for rate ratios 2 and 4 were similar and both load values were greater than at a rate ratio of 1 (Figure 5.3, pg. 83). Furthermore, increasing the rate ratio increased both the wet diameter (Figure 5.4, pg. 84) and the strain to failure (Figure 5.4, pg. 84) in a roughly linear fashion.

5.3.2 Effect of Bath pH and Temperature

The temperature and pH of the 10mM HEPES bath solution was varied to determine the effect on microthread tensile properties. At a relatively neutral pH (7.4) and at a higher pH (8.5), the microthread tensile strength was significantly higher than at lower pH (6.0) (Figure 5.5, pg. 85). However the maximum strength was attained at pH 7.4, which is roughly the pH of the human body in which fibrin formation typically occurs. Finally, the tensile strength of microthreads produced at room temperature (25 ^{o}C) was statistically greater than those produced at body temperature of 37 ^{o}C (Figure 5.5, pg. 85).

5.3.3 Fibrin Microthread Morphology

The morphology of coextruded fibrin microthreads was evaluated with scanning electron microscopy. Fibrin microthreads were consistently and repeatably cylindrical in shape throughout the length of the fiber (Figure 5.6, pg. 87). The surfaces of fibrin microthreads were generally smooth with limited to no surface roughness on a scale greater than 5 um. Submicron surface roughness was observed with high magnification SEM images, but was not quantitatively characterized (Figure 5.6, pg. 87).

5.4 Discussion

The goal of this chapter was to develop fibrin microthreads with a comparable morphology to collagen threads. Achieving this goal would produce threads with structural and mechanical properties sufficient for the post-manufacture manipulation and ultimate fabrication of composite thread matrices for ligament tissue regeneration. Furthermore, we sought to optimize the parameters of fibrin microthread production to ultimately achieve manufacturing practices that could repeatedly produce consistent microthreads with these optimized morphological characteristics.

As many process parameters as possible were varied so long as cohesive threads were ultimately formed. The first parameters investigated were the velocity of the tubing through the bath and the velocity of the fibrin solution flowing out of the tubing into the bath. These two values were inversely correlated, and were therefore combined into a rate ratio for improved analysis. Doubling the rate ratio resulted in close to a three fold increase in the ultimate tensile strength and a 10-fold increase in load to failure.

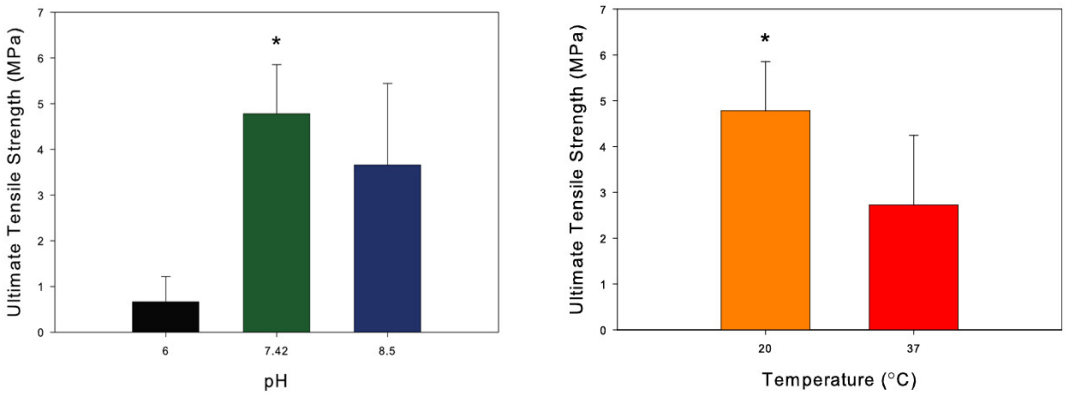

*Figure 5.5: Tensile Strength With Varied pH and Temperature. The ultimate tensile strength of fibrin microthreads was optimal at a pH close to body pH and at room temperature. *denotes significant difference from all other conditions, $p<0.05$*

Table 5.1: Side-by-side Comparison Table of Self-Assembled Collagen Threads and Fibrin Microthreads

Microthread Type	Hydrated Diameter (μm)	Strain at Failure	Tensile Strength (MPa)
Self-Assembled Collagen	72.1 ±10	0.241 ±0.164	9.05 ±2.56
Fibrin	91.1 ±7.8	0.271 ±0.082	4.78 ±1.07

However, a further increase in rate ratio resulted in similar loads at failure, but a decrease in ultimate tensile strength. These results can partially be explained by the resulting diameters and strains of the microthreads extruded at different rate ratios. With increasing rate ratio, the flow out of the tubing was faster than the rate of the tubing moving through the bath. This resulted in an excess material deposition rate and therefore increasing diameters and cross-sectional areas. Furthermore, the strain increased linearly as the microthread diameter increased. This suggests that during the stretching of failure mode testing, the Poisson's effect was more apparent in large diameter threads. This is consistent with our visual observations that during experimentation, the threads thinned before reaching a critical point of increasing load.

The pH and temperature of the fibrin assembly bath were also modified and tested for their effect on the mechanical properties of the assembled microthreads. These parameters were chosen under the hypothesis that either pH or temperature may alter the aggregation of protofibrils during fibrin assembly and ultimately alter the larger scale mechanical properties. Previous research demonstrated that the mean sub-micron fiber diameter of the fibrin architecture varied over a range of pH 6.0 to 8.5.[29] In our studies, neither increasing nor decreasing the pH of the fibrin assembly buffer increased the tensile strength of the resulting fibrin microthreads. Furthermore, optimal tensile properties were observed at neutral physiologic pH of 7.4. Lowering the temperature of the assembly buffer, from 37 ^{o}C to 25 ^{o}C, did not have dramatic effects on ultrastructural properties of fibrin microthreads. This is consistent with research suggesting that the sub-micron mean fibril diameter of fibrin did not significantly change between 0, 20, and 37 ^{o}C.[29] In fact, the tensile strength was slightly increased at 25 ^{o}C, which ultimately may simplify the need to maintain temperature during manufacture.

Fibrin microthreads can be manufactured with morphological properties comparable to those of self-assembled collagen threads (Summarized in Table 5.1, pg. 86). Optimized fibrin microthreads attained ultimate tensile strengths of approximately 4.5 +/- 1.8 MPa. These values are similar to uncrosslinked collagen threads of similar diameter and are substantially higher than the strength values of 6.0 kPa +/- 2.0 kPa, reported previously for fibrin gels[30]. These relatively high mechanical properties are not only advantageous for high load bearing applications including tendons and ligaments, but allow for the post-assembly manufacture of braided or woven fibrin scaffolds as well as composite scaffolds of fibrin and other thread matrices, especially collagen-fibrin composites. Although the amount of strain in the low stress regions is greater than that of uncrosslinked collagen, the strains to failure are not statistically different from collagen threads and the general stress strain curve shape is similar, thereby limiting stress shielding effects.

Morphologically, fibrin and collagen threads share many similar characteristics as well. Fibrin microthreads are cylindrical in shape and maintain a consistent cylindrical shape along the length of the thread. The diameters are on the same approximate size scale as collagen threads, typically ranging from approximately 80 to 100 μm when hydrated. Furthermore, the surfaces of fibrin microthreads were quite smooth with a sub-micron surface structure when imaged dehydrated using SEM. Although collagen

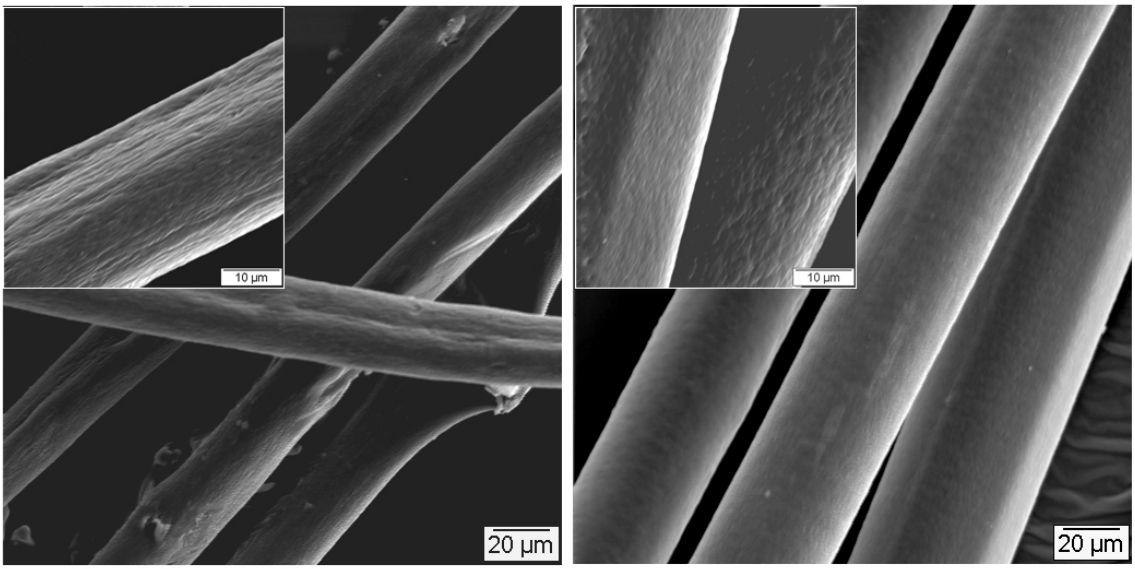

Figure 5.6: SEM of Collagen and Fibrin Biopolymer Microthreads. Scanning electron micrographs demonstrate submicron surface texture on collagen (left) and fibrin (right) microthreads. Both thread types have similar cylindrical morphology and consistent diameter.

microthreads had increased surface roughness, the texture was nominally greater that that found on fibrin microthreads.

Although the development of repeatable and consistent fibrin microthreads was successfully demonstrated, the current manufacturing process is not without limitations or need for further study. Current manufacturing utilizes a syringe pump extruding solutions through small diameter polyethylene tubing, approximately 60-80 mm in length. Given it's natural function as a clotting agent, fibrin has a propensity for polymerizing within the length of tubing, preventing further extrusion, as well as exacerbating the already high pressure generated at the junction between the large diameter syringes and the small diameter tubing. Therefore, fibrin thread assembly and polymerization must occur largely outside the confines of the tubing. This limits the ability to control certain biochemical aspects of fibrin assembly, such as rate of polymerization. The diameter and shape of fibrin microthreads are dictated in part by the diameter of the tubing, but more significantly by the manual stretching that occurs during the removal from the formation bath, as well as through gravitational loading from the threads own mass during drying.

Future studies should investigate natural crosslinking methods, material purity, and fibrin substructure. *In vivo*, fibrin networks are stabilized through crosslinks added by factor XIIIa, a transamidase of the tranglutaminase family of enzymes activated from factor XIII by thrombin and Ca^{2+}. Therefore the use of transglutaminases during fibrin polymerization could increase the strength and stiffness of fibrin microthreads. Our preliminary data found no increases in tensile strength or stiffness with the addition of transglutaminase in low doses (data not shown); however, these experiments were inconclusive and likely require further investigation of experimental techniques to acquire more conclusive results. Furthermore, the ultrastructural properties of the fibrin fibrillar networks both with and without transglutaminase were not investigated therein and need further study. In addition, the starting material used for these studies contains a significant amount of clottable protein as well as fibrinogen. Therefore other proteins may potentially be contained in the mixture including transglutaminase and fibronectin both of which have been shown to alter fibrin polymerization and cell matrix interactions, respectively.[18, 31] Future studies should investigate the effects of high purity fibrinogen preparations on mechanical properties and cellular responses.

In this study, fibrin microthreads were developed with comparable morphological and mechanical properties to self-assembled collagen threads. Fibrin microthreads

exhibited consistent cylindrical shape on a size-scale roughly equivalent to collagen threads and with a similar sub-micrometer surface roughness. The resulting threads demonstrated strengths and stiffnesses orders of magnitude greater than fibrin hydrogels suggesting that these materials have significant utility for load bearing applications. Furthermore, these materials can be sterilized, dehydrated, and manipulated by hand or machine to construct oriented, woven, or composite thread matrices.

REFERENCES

[1] Feng X, Clark RA, Galanakis D & Tonnesen MG. Fibrin and collagen differentially regulate human dermal microvascular endothelial cell integrins: stabilization of alphav/beta3 mrna by fibrin1. *J Invest Dermatol* **113**: pp. 913-919. (1999).
[2] Gailit J, Clarke C, Newman D, Tonnesen MG, Mosesson MW & Clark RA. Human fibroblasts bind directly to fibrinogen at rgd sites through integrin alpha(v)beta3. *Exp Cell Res* **232**: pp. 118-126. (1997).
[3] Xu J & Clark RA. Extracellular matrix alters pdgf regulation of fibroblast integrins. *J Cell Biol* **132**: pp. 239-249. (1996).
[4] Sahni A, Odrljin T & Francis CW. Binding of basic fibroblast growth factor to fibrinogen and fibrin. *J Biol Chem* **273**: pp. 7554-7559. (1998).
[5] Sahni A, Sporn LA & Francis CW. Potentiation of endothelial cell proliferation by fibrin(ogen)-bound fibroblast growth factor-2. *J Biol Chem* **274**: pp. 14936-14941. (1999).
[6] Clark RA. Fibrin and wound healing. *Ann N Y Acad Sci* **936**: pp. 355-367. (2001).
[7] Mosesson MW, Siebenlist KR & Meh DA. The structure and biological features of fibrinogen and fibrin. *Ann N Y Acad Sci* **936**: pp. 11-30. (2001).
[8] Jockenhoevel S, Zund G, Hoerstrup SP, Chalabi K, Sachweh JS, Demircan L, Messmer BJ, et al.. Fibrin gel -- advantages of a new scaffold in cardiovascular tissue engineering. *Eur J Cardiothorac Surg* **19**: pp. 424-430. (2001).
[9] Long JL & Tranquillo RT. Elastic fiber production in cardiovascular tissue-equivalents. *Matrix Biol* **22**: pp. 339-350. (2003).
[10] Ross JJ & Tranquillo RT. Ecm gene expression correlates with in vitro tissue growth and development in fibrin gel remodeled by neonatal smooth muscle cells. *Matrix Biol* **22**: pp. 477-490. (2003).
[11] Swartz DD, Russell JA & Andreadis ST. Engineering of fibrin-based functional and implantable small-diameter blood vessels. *Am J Physiol Heart Circ Physiol* **288**: p. H1451-60. (2005).
[12] Fussenegger M, Meinhart J, Hobling W, Kullich W, Funk S & Bernatzky G. Stabilized autologous fibrin-chondrocyte constructs for cartilage repair in vivo. *Ann Plast Surg* **51**: pp. 493-498. (2003).
[13] Hunter CJ, Mouw JK & Levenston ME. Dynamic compression of chondrocyte-seeded fibrin gels: effects on matrix accumulation and mechanical stiffness. *Osteoarthritis Cartilage* **12**: pp. 117-130. (2004).
[14] Sims CD, Butler PE, Cao YL, Casanova R, Randolph MA, Black A, Vacanti CA, et al.. Tissue engineered neocartilage using plasma derived polymer substrates and chondrocytes. *Plast Reconstr Surg* **101**: pp. 1580-1585. (1998).
[15] Clark RA. Fibrin sealant in wound repair: a systematic survey of the literature. *Expert Opin Investig Drugs* **9**: pp. 2371-2392. (2000).
[16] Silver FH, Wang MC & Pins GD. Preparation and use of fibrin glue in surgery. *Biomaterials* **16**: pp. 891-903. (1995).
[17] Spotnitz WD & Prabhu R. Fibrin sealant tissue adhesive--review and update. *J Long Term Eff Med Implants* **15**: pp. 245-270. (2005).
[18] Amrani DL, Diorio JP & Delmotte Y. Wound healing. role of commercial fibrin sealants.. *Ann N Y Acad Sci* **936**: pp. 566-579. (2001).

[19] Gorodetsky R, Clark RA, An J, Gailit J, Levdansky L, Vexler A, Berman E, et al.. Fibrin microbeads (fmb) as biodegradable carriers for culturing cells and for accelerating wound healing. *J Invest Dermatol* **112**: pp. 866-872. (1999).
[20] Wechselberger G, Russell RC, Neumeister MW, Schoeller T, Piza-Katzer H & Rainer C. Successful transplantation of three tissue-engineered cell types using capsule induction technique and fibrin glue as a delivery vehicle. *Plast Reconstr Surg* **110**: pp. 123-129. (2002).
[21] van Griensven M, Zeichen J, Tschernig T, Seekamp A & Pape H. A modified method to culture human osteoblasts from bone tissue specimens using fibrin glue. *Exp Toxicol Pathol* **54**: pp. 25-29. (2002).
[22] Hokugo A, Takamoto T & Tabata Y. Preparation of hybrid scaffold from fibrin and biodegradable polymer fiber. *Biomaterials* **27**: pp. 61-67. (2006).
[23] Mol A, van Lieshout MI, Dam-de Veen CG, Neuenschwander S, Hoerstrup SP, Baaijens FPT & Bouten CVC. Fibrin as a cell carrier in cardiovascular tissue engineering applications. *Biomaterials* **26**: pp. 3113-3121. (2005).
[24] Ameer GA, Mahmood TA & Langer R. A biodegradable composite scaffold for cell transplantation. *J Orthop Res* **20**: pp. 16-19. (2002).
[25] Lee CR, Grad S, Gorna K, Gogolewski S, Goessl A & Alini M. Fibrin-polyurethane composites for articular cartilage tissue engineering: a preliminary analysis. *Tissue Eng* **11**: pp. 1562-1573. (2005).
[26] Rovensky Y & Samoilov V. Morphogenetic response of cultured normal and transformed fibroblasts, and epitheliocytes, to a cylindrical substratum surface. possible role for the actin filament bundle pattern. *J Cell Sci* **107 (Pt 5)**: pp. 1255-1263. (1994).
[27] Sierra DH, Eberhardt AW & Lemons JE. Failure characteristics of multiple-component fibrin-based adhesives.. *J Biomed Mater Res* **59**: pp. 1-11. (2002).
[28] Pins GD, Christiansen DL, Patel R & Silver FH. Self-assembly of collagen fibers. influence of fibrillar alignment and decorin on mechanical properties. *Biophys J* **73**: pp. 2164-2172. (1997).
[29] Weisel JW. Fibrin assembly. lateral aggregation and the role of the two pairs of fibrinopeptides. *Biophys J* **50**: pp. 1079-1093. (1986).
[30] Billiar KL, Throm AM & Frey MT. Biaxial failure properties of planar living tissue equivalents. *J Biomed Mater Res A* **73**: pp. 182-191. (2005).
[31] Lorand L. Factor xiii: structure, activation, and interactions with fibrinogen and fibrin.. *Ann N Y Acad Sci* **936**: pp. 291-311. (2001).

CHAPTER 6: CELLULAR INTERACTIONS ON FGF-LOADED FIBRIN MICROTHREADS:

EFFECT OF COEXTRUDED FGF-FIBRIN THREADS ON FIBROBLAST ALIGNMENT, PROLIFERATION, AND MIGRATION

6.1 INTRODUCTION

Fibrin microthreads represent a novel biopolymer material composed of the natural structural protein of healing tissues but in the conformation of a mechanically robust thread matrix that can be assembled into aligned bundles for tissue regeneration. Chapter 5 of this thesis demonstrated the development and characterization of these fibrin microthreads with with similar morphology to collagen threads. However, the power of fibrin microthreads lies in their potential interactions with cells and growth factors.

The fibrin matrix that assembles *in vivo* to seal the wound bed acts as a sink for growth factors and cytokines while promoting the migration and proliferation of fibroblasts from the wound margin (See Chapter 2.4). In particular, fibrin has a high binding affinity for fibroblast growth factor-2 (FGF-2) which has been implicated as key example in the matrix bound localization of this signaling protein to promote wound healing.[1, 2] FGF-2 specifically binds and saturates both fibrinogen and polymerized

fibrin with low Kd values ranging from 1.3 nM for high affinity sites to 260 nM for low affinity binding sites.[1] Therefore, in normal plasma concentrations, all FGF-2 should be bound to fibrinogen[1] and *in vivo,* FGF is likely stored in a bound state, becoming functionally available upon release[3]. FGF-2 binding to fibrin prevents proteolytic degradation [4] and has the potential to facilitate the aggregation of growth factor and integrin receptors to promote signal integration.[5] Integrin $\alpha_v\beta_3$ and FGFR1 colocalize when both fibrinogen and FGF-2 are present [6] within the focal adhesion complex.[7] Together, fibrin and FGF-2 potentiate cell proliferation[2] in a manner not seen with FGF-1,[5] and to do so, requires the integrin $\alpha_v\beta_3$.[6, 8] Additionally, fibrin acts as a cofactor with FGF-2 in regulating gene expression of proteins involved in pericellular matrix degradation.[9] Combined, this data suggests that the matrix aids in the spatial regulation of FGF-2, integrins, and signaling to direct wound healing.

Specifically, the effects of FGF-2 have been investigated on tendon and ligament during both *in vitro* and *in vivo* experiments and most typically demonstrating increased wound healing characteristics.[10] *In vitro*, FGF-2 increases proliferation[11, 12] as well as migration of tendon fibroblasts in a wound closure model[12] while upregulating the expression of integrins $\alpha_v\beta_3$ and $\alpha_5\beta_1$, which are important for angiogenesis and tendon healing.[8] *In vivo*, after injection into healing tendons, FGF-2 increased type III collagen content as well as tenocyte proliferation.[13] Using an *in vivo* canine ligament model, addition of FGF-2 increased the healing response marked by enhanced neovascularization.[14] Similarly, early wound healing was enhanced with the addition of FGF-2 in a fibrin gel to a defect MCL model.[15]

Additionally, fibrin matrices synthesized with a thread morphology would benefit from the structural and mechanical advantages of fiber or thread-based structures. Most notably, cylindrical substrata with diameters less than 100 μm facilitate contact guidance, the natural alignment and orientation of cells.[16] Particularly in a highly aligned connective tissues such as the ACL (See Chapter 2.1.1.), aligned fibroblasts lead to aligned matrix deposition and ultimately improved strength and regeneration.[17, 18]

Therefore the goal of this chapter was to demonstrate the potential of fibrin biopolymer microthreads to regenerate torn ligaments by delivering FGF-2 to promote migration and proliferation while simultaneously promoting fibroblast alignment in a physiologically relevant manner.

This chapter will investigate the cell response to the optimized fibrin microthreads developed in Chapter 5 as the control material compared to fibrin threads loaded with increasing concentrations of FGF-2. The effect of FGF-2, loaded in the threads during assembly, was determined on attachment, proliferation, and migration as well as fibroblast alignment and cytoskeletal orientation.

6.2 Materials and Methods

6.2.1 Fibrin Microthread Manufacture

Fibrin microthreads were co-extruded from solutions of fibrinogen and thrombin using extrusion techniques described in Chapter 5.2.1. Fibrinogen from bovine plasma (Sigma, St. Louis, MO F4753) was dissolved in HEPES Buffered Saline (HBS, 20 mM HEPES, 0.9% NaCl) at 70 mg/mL and stored at -20 ^{o}C. Thrombin from bovine plasma (Sigma, St. Louis, MO T4648) was stored frozen as a stock solution at a concentration of 40 U/mL in HBS. A working solution of thrombin was diluted from the stock to a final concentration of 6 U/mL in 40 mM $CaCl_2$ solution. Human, recombinant, basic fibroblast growth factor (FGF-2) (Calbiochem, La Jolla, CA) was diluted to 5 μg/mL in phosphate buffered saline and 0.1% bovine serum albumin, aliquotted, and stored frozen at -80 ^{o}C.

Fibrinogen, thrombin and FGF solutions were warmed to 37 ^{o}C and placed into separate 1 mL syringes which were inserted into a blending applicator tip (Micromedics, Inc., St. Paul, MN). The blending applicator luer locks to the two syringes through individual bores and mix in a needle that luer locks to the tip of the applicator. The solutions were combined and extruded through polyethylene tubing (BD, Sparks, MD) with an inner diameter of 0.38 mm into a bath of 10 mM HEPES (N-[2-Hydroxyethyl]piperazine-N'-[2-ethanesulfonic acid]) in a Teflon® coated pan. For threads incorporating growth factor, 40 μl aliquots of FGF-2 stock solution were added to the fibrinogen solution to reach the desired final concentration and vortexed immediately prior to extrusion.

Finally, threads were removed from the bath, air dried under the tension of their own weight, and stored at room temperature in a desiccator until use.

6.2.2 Cell Culture

Human dermal fibroblasts isolated from neonatal foreskins as previously described (Chapter 3.2.3) were used for all experiments. For the cell outgrowth assay, fibroblasts were modified to overexpress GFP as previously described (Chapter 3.2.4). GFP modified and non-modified fibroblasts were cultured in Dulbecco's Modified Eagles Medium (DMEM; Gibco BRL, Gaithersburg, MD) supplemented with 10% fetal bovine serum (FBS; Atlanta Biologicals, Lawrenceville, GA) and penicillin/streptomycin (100 U/ 100 μg per mL) (Gibco BRL, Gaithersburg, MD)). Fibroblasts were incubated at 37 ^{o}C in 10% CO_2. GFP fibroblasts (P10-13) were used for the cell outgrowth bioassay and non-modified fibroblasts (P7-12) were used for all other assays.

6.2.3 Attachment and Proliferation

6.2.3.1 Thread Bundle Seeding and Culture

To quantify attachment, fibroblasts were seeded onto bundles of normal and FGF-loaded fibrin microthreads. To facilitate handling, bundles composed of 10 threads were adhered to stainless steel rings (ID: 0.750 in, OD: 1.188 in, thickness: 0.005 in, Seastrom, Twin Falls, ID) with Silastic medical adhesive (Silicone type A, Dow Corning, Midland, MI). Bundles were placed individually into wells of a six-well plate containing a 1cm square of Thermanox® tissue culture plastic (Nalge Nunc, Rochester, NY) adhered to the center of the well. Plates were dessicated overnight allowing the silicone to cure. The bundles were sterilized in the wells with 70% isopropyl alcohol, rinsed 3 times with sterile PBS and air dried overnight. Fibroblasts were seeded at a concentration of 300,000 cells/mL onto fibrin threads suspended over the Thermonox® square, in a 100 μL bolus of DMEM containing 10% FBS and incubated under normal cell culture conditions. After 30 minutes, 2 mL of DMEM containing 2% FBS was added to each well and returned to the incubator.

After 4 hours of attachment, fibrin microthread bundles were transferred to new wells retaining only cells attached to the bundles. For determination of attachment, bundles were immediately processed for image acquisition as described below. For proliferation, 2 mL of DMEM containing 2% FBS was added to each well and the plate were returned to normal incubation conditions for a duration of 2, 5, or 7 days.

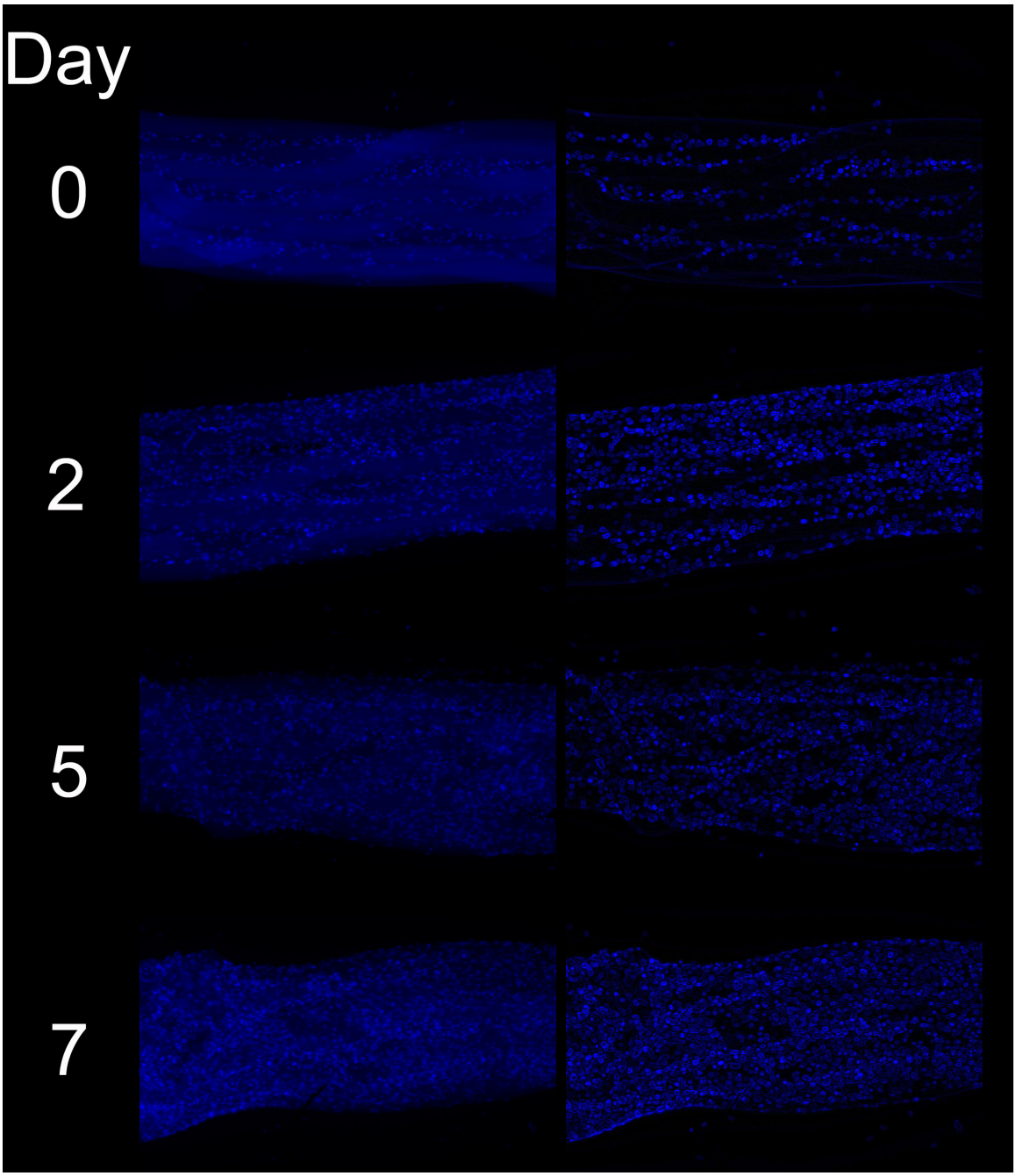

Figure 6.1: Proliferation Quantification. Example of 1 of 5 images taken along the length of thread bundles at each time point (left). Fibroblasts nuclei were stained with Hoechst nuclear dye and images were acquired at 4x magnification (left). These images were processed with edge detection software to clarify nuclei (right), then these nuclei were counted with a particle analysis algorithm.

For quantification, bundles were imaged and cell nuclei counted for determination of the total number of attached fibroblasts. Fibrin thread bundles were rinsed once with sterile PBS, and incubated with 17mM Hoechst nuclear reagent in PBS (Molecular Probes, Eugene, OR) for 15 minutes at room temperature. Bundles were then rinsed in PBS to clear excess stain, removed from the attachment rings, and placed on slides with coverslips for viewing and image acquisition. For each thread bundle, 5 images were acquired covering the end to end length of the bundle at 4x magnification (Figure 6.1, pg. 95). The total count for each image was summed for the 5 images of the bundle to acquire a total cell count. Images were processed and cell quantity determined using ImageJ software (open source software, NIH). Images were processed with edge detection and converted to binary optimized for cell density (Figure 6.1, pg. 95). Nuclei were counted using a particle detection algorithm assuming particles sizes greater than 10 pixels. This process was repeated on three separate bundles for each condition, giving a sample size of 3 for each condition.

6.2.4 Cell Outgrowth

Cell outgrowth was determined using the assay developed in Chapter 3. Briefly, raised rectangular platforms (0.5 cm X 5 cm) of Thermanox® tissue culture plastic were elevated 1.5 mm above the surface of rectangular one-well plates (Nalge Nunc International, Rochester, NY). Microthreads were suspended across the raised platforms spaced 1 cm apart, and the thread ends attached to the tissue culture plates with Silastic® medical adhesive (Dow Corning, Midland, MI). The systems were sterilized with 70% isopropanol overnight and rinsed 3 times in sterile PBS. The systems were air dried in a laminar flow hood prior to seeding.

To seed cell migration assays, 0.5-mL aliquots of fibroblast-populated collagen lattice were placed onto each platform. These lattices were produced by mixing 3.0 mL of 5×10^5 cells/mL subconfluent GFP transduced fibroblasts with 2.4 mL of type I collagen (2.5 mg/mL) and 0.6 mL 5 × DMEM. After the gels were allowed to set at room temperature for 1 hr, the one-well plates were filled with 20 mL of DMEM supplemented with 2% FBS to a height just above the platforms and threads. Every 24 hours, the threads were visualized with a Nikon Eclipse TS100 inverted epifluorescent microscope coupled with a SpotRT CCD Camera (Diagnostic Instruments, Sterling Heights, MI). Measurements of the distance to the furthest cell on the thread from the edge of the platform as the cells migrated out of the gel onto the threads were taken using a calibrated reticule in the eyepiece of the microscope. The average migration rates reported are

averages of values measured daily between days 3-6. The sample size was determined from the number of viable microthread-platform intersection sites. Individual threads were randomly placed in the system, and the experimenter was blinded to the identities until measurements were complete.

6.2.5 Fixing and Staining

For determination of fibroblast alignment and orientation, bundles of fibrin microthreads were seeded with cells, fixed, and stained. Bundles of 10 microthreads of each type were assembled and seeded as described (Section 6.2.3.1, pg 94). After 4 hours of attachment, bundles were rinsed twice in PBS and fixed in 4% formaldehyde (Ted Pella, Redding, CA) and 0.2% Triton (Sigma, St. Louis, MO). Samples were rinsed 2 times in a PBS and incubated for 15 minutes in PBS and 1%BSA. Samples were then stained with 165 nM Alexaflour 488 phalloidin (Molecular Probes, Eugene, OR) and 17mM Hoechst nuclear reagent (Molecular Probes, Eugene, OR) for 45 minutes.

For imaging of attachment and proliferation, as well as determining viability, bundles of fibrin microthreads stained with a live/dead stain. Bundles of 10 microthreads were assembled and seeded as described (Section 6.2.3.1, pg 94). After 4 hours of attachment, bundles were removed from the seeding wells and transferred to a new well for staining. Half of these samples were immediately stained, while the remaining were cultured for 7 days under normal culture as indicated previously. Bundles were incubated after removal of media, in 1.5 mL of a 4 μM ethidium homodimer-1 and 2 μM calcein AM solution (Molecular Probes, Eugene, OR). Bundles were incubated at room temperature for 30 minutes. Calcein (green, Ex/em 495nm/515 nm) is retained in living cells while ethidium (red, Ex/em 495nm/635 nm) is excluded by intact plasma membrane, but enters damaged membranes where it can fluoresce upon binding to nucleic acid. Thread bundles were then cut from attachment rings and placed on slides for fluorescent imaging. Images were then acquired on a Nikon Eclipse E400 microscope.

6.2.6 Scanning Electron Microscopy (SEM)

For SEM, samples were fixed either after seeding as previously described (Section 6.2.3.1, pg 94) or after cell outgrowth during 5 days in the bioassay, cultured as previously described (Section 6.2.4, pg 96). Reagents for SEM were purchased from Ted Pella, Redding, CA unless otherwise stated. The media was removed and samples were fixed in a modified Karnovsky fixative of 2% gluteraldehyde, 4% formaldehyde, 0.1M

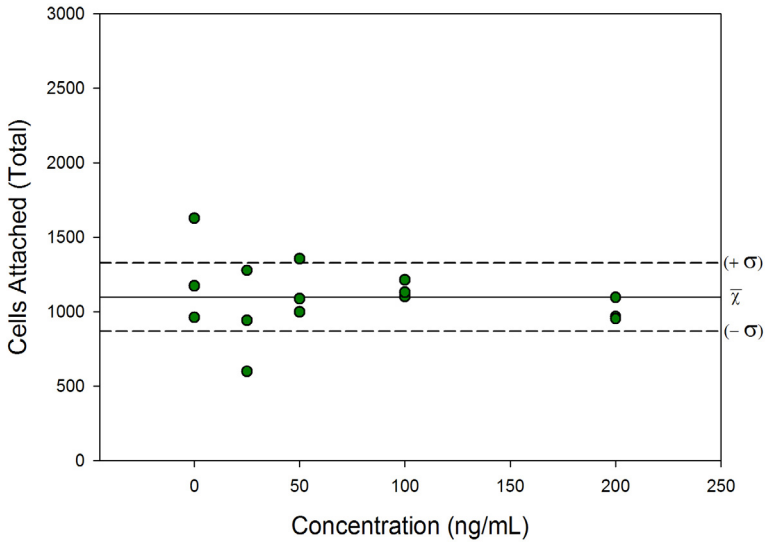

Figure 6.2: FGF-2 Incorporation Did Not Alter Fibroblast Attachment. The total number of fibroblasts attached to fibrin bundles with varying concentrations of FGF-2 were not significantly different from each other or control (0 ng/mL) after 4 hours of fibroblast attachment. (reference lines are the mean ± standard deviation of all data points)

cacodylate and 4mM $CaCl_2$ (Sigma, St. Louis, MO) for 90 minutes. Samples were then washed twice in 0.1M cacodylate and 1.5mM $CaCl_2$ before a secondary fixative of 1% osmium tetraoxide in 0.1M cacodylate and 1.5mM$CaCl_2$ for 1 hour. Next, samples were washed twice in 0.1M cacodylate, then replaced with 50% ethanol, followed by a block stain in 2% uranyl acetate in 50% ethanol for 1 hour. Finally samples were dehydrated in increasing concentrations of ethanol up to 100% and dried in a critical point drier.

Cell-seeded fibrin microthreads were then imaged with a scanning electron microscope. Thread were mounted on aluminum stubs (Ted Pella, Inc., Redding, CA) coated with double-sided carbon tape and sputtered coated with a thin layer of gold-palladium for 30 seconds. Images were acquired at 15kV using a JSM-KLG scanning electron microscope.

6.2.7 Statistical Analyses

Statistical analyses were performed using SigmaStat 3.1 software (Systat Software, Inc., San Jose, CA). All experiments results were statistically evaluated using one-way analysis of variance (ANOVA) with an overall significance of $P < 0.05$. In most cases, a Holm-Sidak pairwise multiple comparison tests were performed on the results to determine significant difference between groups. In certain cases where indicated, a Holm-Sidak multiple comparison versus the control group was performed to determine significant difference between samples and the control.

6.3 RESULTS

6.3.1 Attachment

Fibroblast attachment to bundles of fibrin microthreads containing various quantities of FGF-2 was measured by quantifying the total number of adhered cells after 4 hours. The number of fibroblasts attaching to control threads averaged 1200 cells. The mean attachment value for FGF-2 loaded microthreads was not significantly different from controls and did not change with increasing concentrations of FGF-2 (Figure 6.2, pg. 98).

6.3.2 Proliferation

Cell proliferation was quantified on days 2, 5, and 7 for control fibrin microthreads and threads loading with varying amounts of FGF-2. Fibroblasts proliferated readily on both FGF-2 loaded and control fibrin microthreads. Total cell numbers were 3-4 times

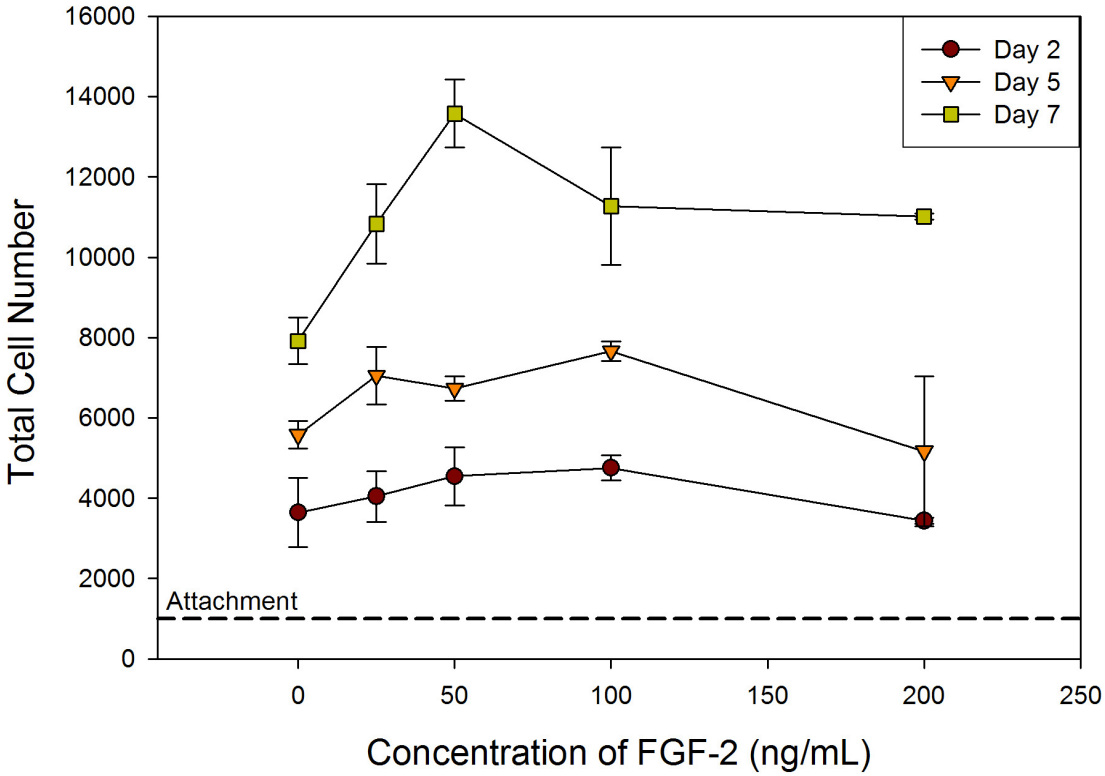

Figure 6.3: Cell Proliferation with Time and Concentration of FGF-2. Fibroblasts proliferated on threads with or without FGF-2 loaded. FGF-2 increased proliferation over unloaded controls, and the effect of this increase is more dramatic as time in culture increased.

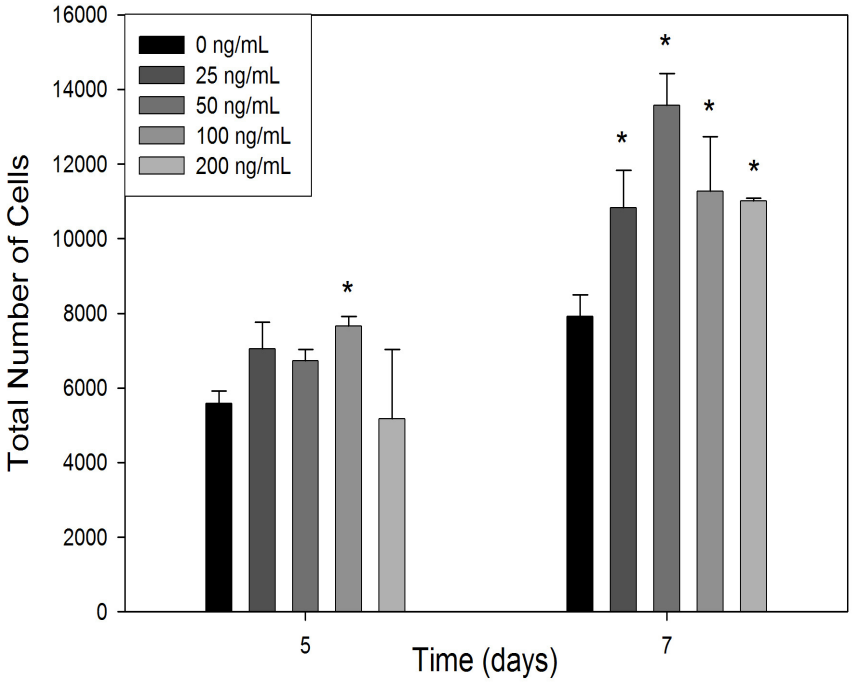

*Figure 6.4: Cell Proliferation Increased with FGF-2 Incorporation. At day 5, total cell numbers on FGF-2 were higher than controls, and by day 7, total cell numbers were significantly greater than controls. (*denotes significant difference by one-way ANOVA, $p > 0.05$)*

greater by day 2 than after initial attachment and increased over the length of the experiment for all conditions. Total cell numbers increased with the addition of FGF-2 loaded in the fibrin microthreads; however this phenomenon was most pronounced at later time points (Figure 6.3 and Figure 6.4, pg. 99, 100). Regardless of time point analyzed, the proliferation versus FGF-2 concentration dose-response curves demonstrated a general arching trend; increasing FGF-2 concentrations increased proliferation with lower levels of FGF-2, but typically plateaued and decreased by the highest levels of FGF-2 (Figure 6.3, pg. 99). By day 7, despite low sample sizes, all FGF-2 loaded threads had statistically greater total cell numbers than unloaded controls (Figure 6.4, pg. 100). When normalized to the average number of cells attached for each experimental condition, the fold increase on FGF-2 loaded threads by day 7 was almost twice that of unloaded controls (Figure 6.5, pg. 101).

6.3.3 Cell Outgrowth

The cell outgrowth on the surface of fibrin microthreads either loaded with increasing concentrations of FGF-2 or unloaded were measured using the discrete thread

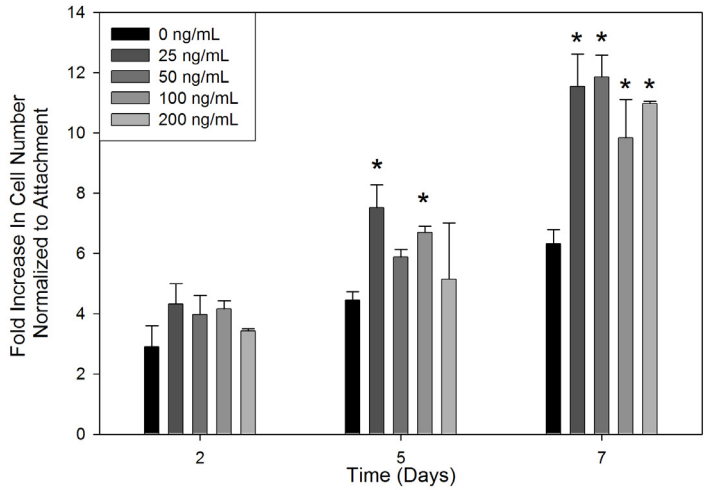

*Figure 6.5: FGF-2 Incorporation Increases Proliferation On Fibrin Microthreads. The fold increase in cell number on fibrin microthreads was determined by measure the total cell number and normalizing to value to the average cell number attached for each FGF-2 concentration. Proliferation was greater on FGF-2 loaded threads by day 2 of culture and by day 7 were all significantly greater than unloaded controls. (*denotes significant difference from control by one-way ANOVA, p > 0.05)*

method of characterization developed in Chapter 3 of this thesis. The cell outgrowth rate for control fibrin microthreads was 0.34 ± 0.11 mm/day. However, the addition of FGF-2 into fibrin microthreads significantly increased the cell outgrowth rate to nearly double the rate of control threads (Figure 6.6, pg. 101). The concentration of FGF-2 loaded into the fibrin threads did not significantly change the cell outgrowth velocity.

6.3.4 Cell and Cytoskeletal Alignment

Fibroblast alignment on fibrin microthreads was investigated both on discrete threads after culture during studies of cell outgrowth as well as when combined into aligned bundles of microthreads. Fibroblasts readily align along the long axis of fibrin microthreads both on aligned bundles (Figure 6.7B, pg. 102) as well as on individual fibers (Figure 6.8, pg. 103) and maintained their alignment during culture. Fibroblasts on individual microthreads fixed and imaged

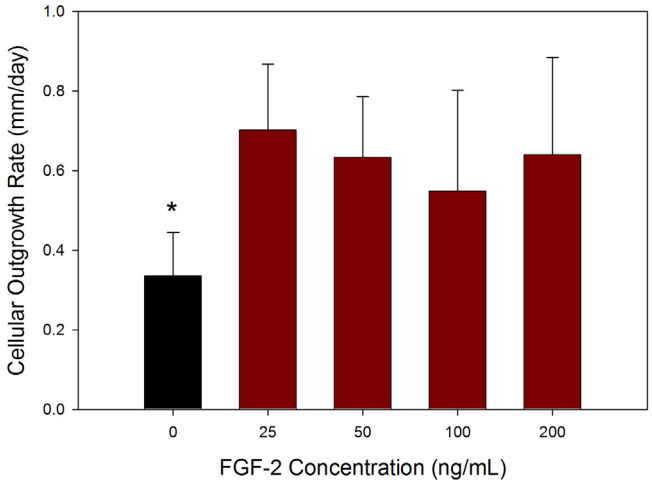

Figure 6.6: Effect of FGF-2 on Cell Outgrowth. The cell outgrowth rate on the surface of fibrin microthreads was measured on threads with increasing quantities of FGF-2 loaded into the thread substructure. The cell outgrowth rate was significantly higher upon inclusion of FGF-2, but was not effected by FGF-2 quantity. (denotes siginficant difference from all other conditions by one-way ANOVA, p> 0.05)*

with SEM demonstrated elongation parallel to the long axis of threads in both areas containing many cells as well as in areas containing few cells (Figure 6.8, pg. 103). When seeded onto bundles of aligned fibrin microthreads, the fibroblasts initially tended to align and aggregate in the grooves between adjacent threads, forming an extremely thin and elongated morphology (Figure 6.7, pg. 102).

The cytoskeletal organization of fibroblasts on fibrin microthreads was clearly distinguishable from that under standard 2-D tissue culture conditions. On standard tissue culture treated plastic, the visualized cytoskeletal components demonstrated no preferential direction (Figure 6.7A, pg. 102), while filamentous actin bundles stained with phalloidin were noticeably oriented in parallel aligned bundles down the length the fibrin threads when cultured on microthreads (Figure 6.7C, pg. 102).

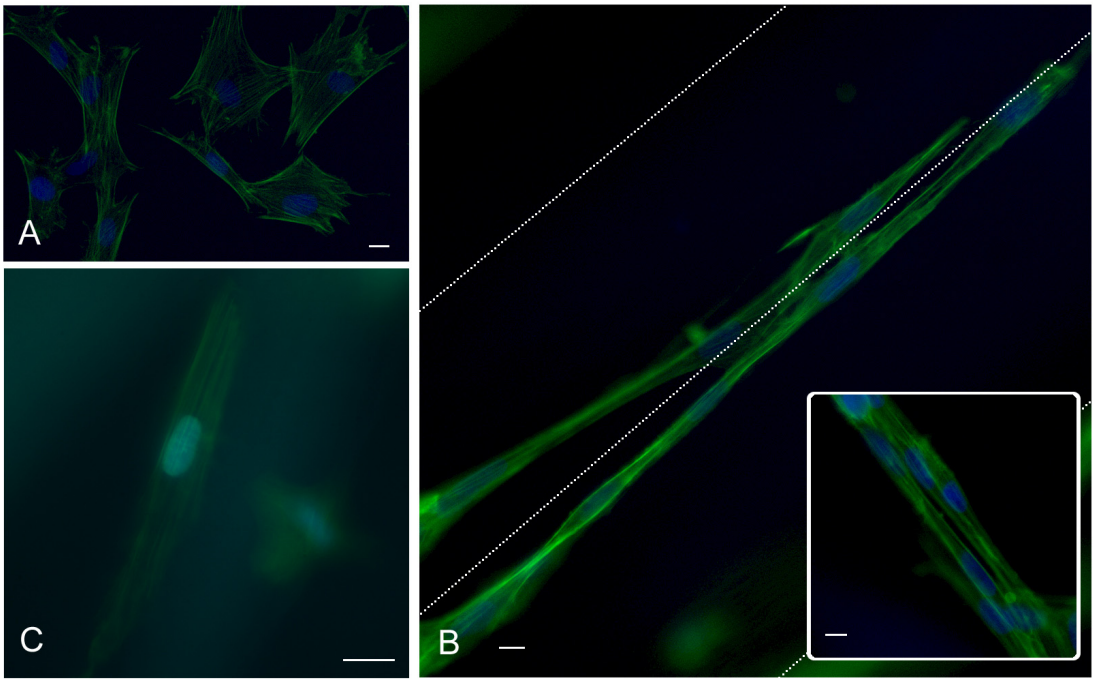

Figure 6.7: Cell and Cytoskeletal Alignment on Fibrin Microthreads. Fibroblasts seeded on bundles of fibrin microthreads were stained for filamentous actin (Phalloidin, green) and nucleic acid (Hoechst, blue) after 4 hours of attachment. (A) Control fibroblasts on tissue culture plastic showed now preferential alignment or orientation. (B) Fibroblasts on fibrin threads aligned along the long axis of the fibers (highlighted white dashed line) particularly in the grooves between fibers (inset shown without drawn thread boundary line). (C) Fibroblast actin is oriented in parallel arrays along the long axis of fibrin microthread. [scale bars = 5 μm]

6.4 Discussion

Overall, fibroblasts readily attach, proliferate, and migrate on fibrin microthreads, therefore representing viable scaffolds for ACL regeneration. Fibroblasts attached to the surface of fibrin microthreads after seeding, remaining greater than 99% viable for the duration of culture as indicated by viability staining and imaging (Figure 6.9, pg. 104). Furthermore, fibroblasts exhibited substantial proliferation during seven days of culture leading to complete encapsulation of threads within a layer of aligned fibroblasts (Figure 6.10, pg. 105).

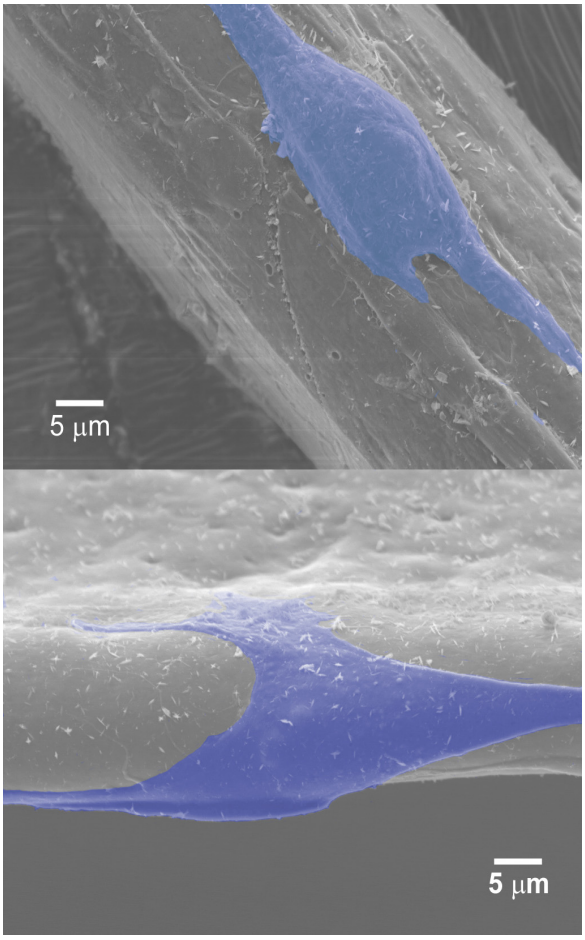

Figure 6.8: Cell Alignment on Individual Fibrin Microthreads. Samples were taken during the late stages of the cell outgrowth assay (Day 7), fixed, and dehydrated for imaging with SEM. Individual cells can be seen aligned along the long axis of the microthread (blue highlighting added for emphasis during analysis, post-acquisition).

FGF-2 was added to the substructure fibrin matrix during fabrication signaling an increased cellular response in fibroblasts. FGF-2 is not only considered a potent mitogenic and chemotactic growth factor, but has also been implicated as a matrix bound co-factor in regulating wound healing gene expression. Although no effect was seen on fibroblast attachment (Figure 6.2, pg. 98), incorporation of FGF-2 into the fibrin microthread matrix resulted in significant increases in migration (Figure 6.6, pg. 101) and proliferation (Figure 6.5, pg. 101). Particularly by day 7 of culture, addition of FGF-2 into the matrix significantly increased proliferation over control threads, in a varied manner dependent on FGF-2 quantity (Figure 6.4, pg. 100). While increasing FGF-2 concentration at low levels increased proliferation, total cell numbers eventually plateaued (Figure 6.3, pg. 99). At high concentrations of FGF-2, the total cell numbers were typically lower than at low concentration (Figure 6.3, pg. 99). Dose dependent effects are not uncommon with growth factors including FGF-2, although these findings

are typically cell dependent as well. In tenocytes, FGF-2 stimulated type I and type III collagen production at low levels, but suppressed it at high values.[11] In periodontal ligament cells, FGF-2 downregulated the gene expression of col I and upregulated the gene expression of MMP-1.[19] The results of our study demonstrate similar trends suggesting that sub-maximal concentrations of FGF-2 may be optimal to direct cell-mediated matrix synthesis.

The cell outgrowth was increased on all thread types loaded with FGF-2; however, little variation was seen with increasing concentrations of FGF-2 within the matrix (Figure 6.6, pg. 101). This may in effect be a result of the quantity of growth factor present on the surface of the fibrin microthreads and control of growth factor exposure by degradation. As fibroblasts reach a profibrotic phenotype in the later stages of the proliferation assay and as fibrin/FGF-2 stimulates MMP production, more fibrin matrix is broken down, exposing more FGF-2. This could account for the increasing response to FGF-2 apparent during later time points in the proliferation experiment and the relative non-stimulatory effect above baseline with increasing FGF-2 during cell outgrowth studies.

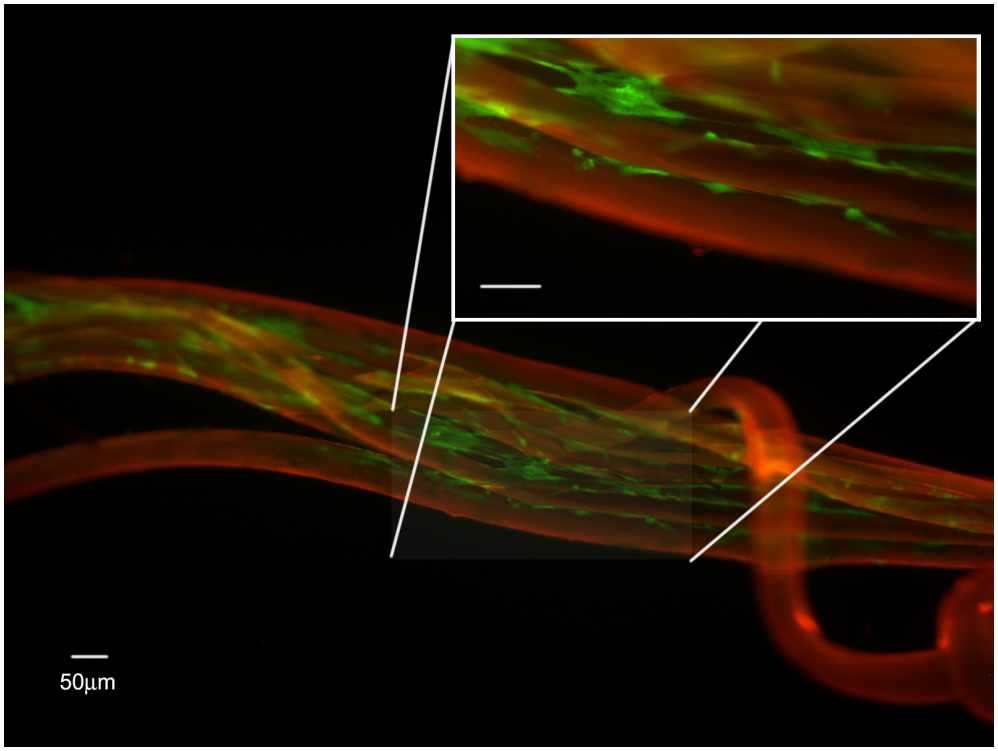

Figure 6.9: Attachment Imaging. After seeding bundles of fibrin microthreads with fibroblasts, the bundles were imaged with calcein, a stain of viable cells (green). [Error bars 50 µm]

Fibroblasts align along the long axis of fibrin microthreads regardless of growth factor presence. In particular, the fibroblasts preferentially aggregated and attached in the grooves between adjacent microthreads and subsequently aligning the actin cytoskeletal components (Figure 6.7 and Figure 6.8, pg. 102 and 103). The cytoskeleton has been shown to play a role in the coordination of ECM deposition in tendon fibroblasts.[20] This occurs through a mechanism where aligned actin filaments orient collagen fibrils within the finger-like projects of the cell membrane that eventually deposit the fibril in the ECM.[20] Therefore, fibroblast alignment ultimate leads to aligned matrix depostion. We hypothesize that using fibrin microthreads could lead to decreasing the disorganization of normal wound healing matrix by producing more aligned and ordered wound ECM. A more aligned collagen matrix would also likely have increased tensile properties due to the improved biomechanical protein interactions. Furthermore, aligned fibroblasts more closely mimic the spindle-like cell morphology of native ligament fibroblasts lending a more biomimetic cell shape and therefore cell function.

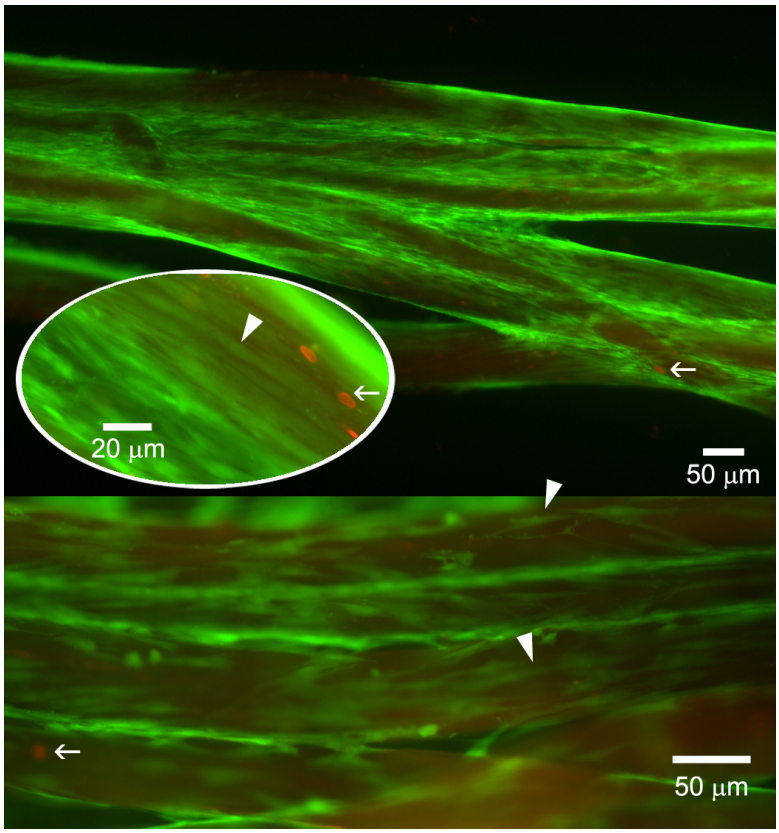

Figure 6.10: Proliferation Imaging. By day 7, fibroblasts completely encapsulated fibrin microthreads as visualized, where viable cells stained green (arrow heads) and dead cell nuclei stained red (arrows)

REFERENCES

[1] Sahni A, Odrljin T & Francis CW. Binding of basic fibroblast growth factor to fibrinogen and fibrin. *J Biol Chem* **273**: pp. 7554-7559. (1998).
[2] Sahni A, Sporn LA & Francis CW. Potentiation of endothelial cell proliferation by fibrin(ogen)-bound fibroblast growth factor-2. *J Biol Chem* **274**: pp. 14936-14941. (1999).
[3] Sahni A & Francis CW. Plasmic degradation modulates activity of fibrinogen-bound fibroblast growth factor-2. *J Thromb Haemost* **1**: pp. 1271-1277. (2003).
[4] Sahni A, Baker CA, Sporn LA & Francis CW. Fibrinogen and fibrin protect fibroblast growth factor-2 from proteolytic degradation. *Thromb Haemost* **83**: pp. 736-741. (2000).
[5] Sahni A, Altland OD & Francis CW. Fgf-2 but not fgf-1 binds fibrin and supports prolonged endothelial cell growth. *J Thromb Haemost* **1**: pp. 1304-1310. (2003).
[6] Sahni A & Francis CW. Stimulation of endothelial cell proliferation by fgf-2 in the presence of fibrinogen requires alphavbeta3. *Blood* **104**: pp. 3635-3641. (2004).
[7] Plopper GE, McNamee HP, Dike LE, Bojanowski K & Ingber DE. Convergence of integrin and growth factor receptor signaling pathways within the focal adhesion complex. *Mol Biol Cell* **6**: pp. 1349-1365. (1995).
[8] Harwood FL, Goomer RS, Gelberman RH, Silva MJ & Amiel D. Regulation of alpha(v)beta3 and alpha5beta1 integrin receptors by basic fibroblast growth factor and platelet-derived growth factor-bb in intrasynovial flexor tendon cells.. *Wound Repair Regen* **7**: pp. 381-388. (1999).
[9] Sahni A, Sahni SK, Simpson-Haidaris PJ & Francis CW. Fibrinogen binding potentiates fgf-2 but not vegf induced expression of u-pa, u-par, and pai-1 in endothelial cells. *J Thromb Haemost* **2**: pp. 1629-1636. (2004).
[10] Hsu C & Chang J. Clinical implications of growth factors in flexor tendon wound healing. *J Hand Surg [Am]* **29**: pp. 551-563. (2004).
[11] Takahashi S, Nakajima M, Kobayashi M, Wakabayashi I, Miyakoshi N, Minagawa H & Itoi E. Effect of recombinant basic fibroblast growth factor (bfgf) on fibroblast-like cells from human rotator cuff tendon.. *Tohoku J Exp Med* **198**: pp. 207-214. (2002).
[12] Chan BP, Chan KM, Maffulli N, Webb S & Lee KK. Effect of basic fibroblast growth factor. an in vitro study of tendon healing.. *Clin Orthop Relat Res* : pp. 239-247. (1997).
[13] Chan BP, Fu S, Qin L, Lee K, Rolf CG & Chan K. Effects of basic fibroblast growth factor (bfgf) on early stages of tendon healing: a rat patellar tendon model.. *Acta Orthop Scand* **71**: pp. 513-518. (2000).
[14] Kobayashi D, Kurosaka M, Yoshiya S & Mizuno K. Effect of basic fibroblast growth factor on the healing of defects in the canine anterior cruciate ligament.. *Knee Surg Sports Traumatol Arthrosc* **5**: pp. 189-194. (1997).
[15] Fukui N, Katsuragawa Y, Sakai H, Oda H & Nakamura K. Effect of local application of basic fibroblast growth factor on ligament healing in rabbits.. *Rev Rhum Engl Ed* **65**: pp. 406-414. (1998).
[16] Rovensky Y & Samoilov V. Morphogenetic response of cultured normal and transformed fibroblasts, and epitheliocytes, to a cylindrical substratum surface. possible role for the actin filament bundle pattern. *J Cell Sci* **107 (Pt 5)**: pp. 1255-1263. (1994).
[17] Glass-Brudzinski J, Perizzolo D & Brunette DM. Effects of substratum surface topography on the organization of cells and collagen fibers in collagen gel cultures.. *J Biomed Mater Res* **61**: pp. 608-618. (2002).
[18] Manwaring ME, Walsh JF & Tresco PA. Contact guidance induced organization of extracellular matrix.. *Biomaterials* **25**: pp. 3631-3638. (2004).
[19] Palmon A, Roos H, Edel J, Zax B, Savion N, Grosskop A & Pitaru S. Inverse dose- and time-dependent effect of basic fibroblast growth factor on the gene expression of collagen type i and matrix metalloproteinase-1 by periodontal ligament cells in culture.. *J Periodontol* **71**: pp. 974-980. (2000).
[20] Canty EG, Starborg T, Lu Y, Humphries SM, Holmes DF, Meadows RS, Huffman A, et al.. Actin filaments are required for fibripositor-mediated collagen fibril alignment in tendon.. *J Biol Chem* **281**: pp. 38592-38598. (2006).

CHAPTER 7: DISCUSSION AND FUTURE WORK:
BIOPOLYMER MICROTHREADS

7.1 OVERVIEW

This thesis describes the development of a cell outgrowth metric, the use of that metric to analyze cellular responses to material properties, and the creation of a novel biomaterial designed to improve on the current material limitations elucidated during our initial studies. I developed a novel *in vitro* method of characterizing fibrous thread matrices by probing their ability to promote tissue ingrowth from a wound margin as a measure of their ability to promote repopulate and regeneration. This method is useful in the optimization of thread scaffolds, and is sensitive enough to distinguish between subtle variations in biopolymer chemistry and organization. Furthermore, I used this method to characterize the effects of crosslinking on the cell outgrowth and correlated the findings with the mechanical properties of collagen threads. The results suggest that crosslinking is required to achieve sufficient mechanical properties for high stress applications such as ACL replacement, but regardless of technique, crosslinking will attenuate the tissue ingrowth properties of the threads. To improve the regenerative capacity of these scaffolds, I developed novel fibrin microthread matrices with a similar morphology to collagen threads and sufficient mechanical strength to be incorporated in composite thread scaffold systems. These fibrin microthreads can be loaded with FGF-2, a potent mitogen and chemotactic agent that works synergistically with fibrin in

regulating cell signaling and gene expression. I successfully demonstrated increases in fibroblast migration and proliferation in FGF-2-loaded fibrin threads with the concomitant promotion of oriented, aligned, spindle-like fibroblast morphology. These results suggest that fibrin-FGF-2 microthreads have distinct advantages as a biomaterial for the rapid regeneration of injured tissues with an increased wound healing response.

7.2 Biopolymer Threads for ACL Regeneration

Overall, collagen and fibrin biopolymer microthreads are promising materials for the regeneration of torn anterior cruciate ligaments (ACL). Being assembled from the native structural proteins of ligaments and provision matrix respectively, both materials are biomimetic on multiple levels. Each retain a biochemistry that mimics the extracellular matrix, while being assembled into microthreads and bundles that structurally replicate aligned soft connective tissue such as tendons and ligaments. These ECM cues are what distinguish biopolymer threads from synthetic polymers and what make them attractive for applications in tissue regeneration.

Thread-based matrices are not new to bioengineered ACL research. Synthetic polymer thread matrices were manufactured extensively for ACL replacements, but were limited by extremely high failure rates caused by poor integration, stress shielding, and fatigue failure[1]. Researchers are investigating more traditional braided or woven degradable materials such as poly L-lactic acid (PLLA)[2, 3]; however, it is unclear how these polymers will support tissue ingrowth or regeneration, particularly given the increase in concentration of acidic byproducts at the wound site during degradation. Biologically inspired fibers of silk[4, 5] from spider cocoons or chitosan/alginate fibers[6, 7] made from sea shells and seaweed both offer degradable alternatives to synthetic polymers. However, these materials are still foreign bodies and ultimately cannot be expected to elicit matrix signaling or cellular responses that direct tissue regeneration.

Both collagen and fibrin biopolymer microthreads are composed of the natural structural proteins of healthy and healing ligament tissue. These materials remodel and degrade under normal wound healing pathways, maintain robust mechanical properties, and can regulate gene expression through integrin signaling in a biologically predictable manner. Specifically, collagen thread matrices have been widely investigated as a degradable scaffold for many years and demonstrated moderate success *in vivo* (Chapter 2.2.2.1). Yet to attain strength and degradation rates required for load bearing

applications such as ligament regeneration, these threads must be physically or chemically crosslinked. Numerous methods have been investigated (Chapter 2.2.2.1 - Collagen Crosslinking) and the results of this thesis quantitatively confirm that most commonly employed crosslinking techniques reduce cell outgrowth on the threads. While collagen is an advantageous biomaterial for many of the previously stated reasons, overcoming this limitation will require a novel strategy for promoting tissue ingrowth.

Incorporating fibrin biopolymer microthreads into a composite matrix with collagen threads would be a simple, yet elegant solution to improving the tissue ingrowth and remodeling characteristics of these acellular ligament scaffolds. Fibrin has been shown to differentially alter cell function through integrin mediated interactions [8-11]. In contrast, collagen attenuates collagen production as part of the dynamic reciprocity of matrix signaling, a mechanism not seen on fibrin, which promotes migration as well as matrix synthesis [8]. By combining collagen and fibrin thread matrices, an acellular graft can be assembled that uses fibrin to promote migration and matrix synthesis during early regeneration and crosslinked self-assembled collagen for strength and long term stability.

7.3 Method of Characterization

This thesis describes a novel *in vitro* model system for quantitatively measuring tissue ingrowth onto discrete biopolymer thread matrices that closely mimics ACL tissue regeneration. In this system, we maintain a structurally and biochemically relevant 3-D contextual environment, but in a system that closely mimics the mechanisms of cellular repopulation that occurs during ACL replacement surgery with acellular matrices. Results of studies using this bioassay determined that threads composed of collagen showed a significantly greater outgrowth velocity than synthetic threads. Although crosslinking decreased this velocity, these lowest values were still almost twice that of synthetic threads.

While designed originally for the investigation of collagen threads, this model system has wide ranging applications for the *in vitro* investigation of tendon and ligament regeneration as well as in the development of engineered fiber-based biomaterials. Simple modifications to the methods described would allow for the quantitative evaluation of tissue regeneration capacity for any particular cell lineage. For example, researchers have suggested that fibroblasts isolated from the MCL and ACL of the knee have slightly different phenotypes.[12-16] Their inherent capacity for for tissue regeneration can be measured in the selection of an appropriate cell line for tissue

engineering of ACL. Furthermore, the bioassay can systematically probe modifications to surface biochemistry or topography. Specifically in this thesis, the bioassay was used to evaluate the addition of FGF-2 to fibrin microthreads and confirmed not only the presence of FGF-2 in the matrices but the maintenance of biological activity. This concept could be extended to investigate the effects of other signaling cues that regulate migration and proliferation, such as IGF-1,[17] on cell outgrowth.

Although current testing included only measurement of the cell outgrowth metric, numerous other measurements could be generated from this system. The total number of cells on threads could be quantified to improve the validity of the cell outgrowth metric. Once the cells have reached confluence on the threads and begin the remodeling phase, these cell-seeded threads could be excised and assayed for synthesis of collagens, tenascins, MMPs, or other important matrix molecules. Furthermore, at a range of time points during both the ingrowth and the remodeling phases, the mRNA could be extracted and quantified with reverse transcriptase polymerase chain reaction (rtPCR) to investigate any number of regenerative markers or signals. Utilizing these additional measurements would further improve understanding of the model system while opening future possibilities for asking different questions about cell matrix interactions in a 3-D biologically relevant context.

While generally successful, the method for quantifying tissue ingrowth is not without limitation. Current methods for quantifying population density were suboptimal due to poor image contrast, cell delineation detail, and limited imaging field of view. Improvements were clearly seen when daily Fura-2 staining protocols were replaced by the use of a GFP-expressing fibroblast cell line; however, using fibroblasts modified to express GFP sequestered to the nucleus only, rather than the cytoplasm, could allow for simple quantification of cell number using image analysis software. Measuring percent confluence or population density would aid in modeling the cell outgrowth on threads and allow for a more accurate representation of collected data. Furthermore, the entire system could be improved by tracking cells in real time to reduce the day to day variations and experimental error. Additionally, the current system works well as metric for determining differences *in vitro*, but the direct correlation between *in vitro* results and *in vivo* response has yet to be systematically investigated.

Overall, the *in vitro* bioassay of tissue ingrowth is a useful tool for the investigation fiber biomaterials and the regeneration of soft connective tissues including tendon and ligament. In the future, this *in vitro* bioassay will enable us to identify parameters to

optimize the rate of cell outgrowth for the development of constructs for soft tissue regeneration, as well as to determine fine variations in the cell-matrix interactions as a function of matrix materials and surface biochemistries.

7.4 Fibrin Biopolymer Microthreads

Fibrin microthreads represent a novel biopolymer material composed of the natural structural protein of healing tissues but in the conformation of a mechanically robust thread matrix that can be assembled into aligned bundles for tissue regeneration. Under normal culture conditions, fibroblasts attached, remained viable, and exhibited substantial proliferation during seven days of culture leading to complete encapsulation of fibrin threads within a layer of aligned fibroblasts. Fibroblasts align along the long axis of fibrin microthreads individually and in bundles, preferentially aggregating in the grooves between adjacent microthreads. This alignment mimics the cell morphology of ligament fibroblasts and has implications for the control of cell function. Cell alignment subsequently orients actin cytoskeletal components that have been shown to play a role in the coordination of ECM deposition in tendon fibroblasts.[18] We hypothesize that using fibrin microthreads could lead to increasing the organization of normal wound healing matrix by producing more aligned and ordered wound ECM.

FGF-2 was added in the substructure of fibrin thread matrix during manufacture to signal an increased wound healing response in fibroblasts. FGF-2 is not only considered a potent mitogenic and chemotactic growth factor, but has also been implicated as a fibrin matrix bound co-factor in regulating wound healing gene expression. While FGF-2 did not increase attachment, FGF-2 loaded fibrin microthreads promoted increased cell outgrowth and proliferation. While clearly responding to the addition of FGF-2, it is equivocal whether this response is the simple result of FGF-2 signaling or a more complex co-regulatory response to fibrin and FGF-2. Regardless, fibrin microthreads are a promising biomaterial for tissue regeneration particularly for their matrix signaling capabilities particularly when combined with matrix bound growth factors such as FGF-2.

Fibrin microthreads are mechanically robust thread material, but alone do not attain sufficient tensile properties for high load bearing situations such as ligament tissue regeneration. *In vivo*, fibrin networks are naturally crosslinked by factor XIIIa, a member of the transgultaminase family of enzymes. Transgultaminases have been previously been isolated and investigated in fibrin and collagen materials, demonstrating increased

strength and stiffness in both[19-23]. My initial investigations demonstrated no differences in strength with the addition of transglutaminase (data not shown), but these findings were incomplete and require a more thorough investigation of techniques and methods to be conclusive. Other crosslinking methods such as exposure to ultraviolet light and EDC crosslinking chemistry that were investigated for collagen threads may be equally successful in altering the magnitude of fibrin strength and stiffness, but these techniques would likely result in similar impedance of cell matrix interactions[24].

Other benefits of these novel fibrin microthread scaffolds is that they can be made from autologous materials and ultimately be designed to reverse-engineer the wound healing milieu. Fibrinogen can be readily isolated from a patient's own blood for the development of autologous graft materials, thereby making immunological rejection negligible. Fibrinogen can be further purified during isolation, but this may not be necessary. Using starting materials containing fibrinogen as well as plasma-derived cytokines and growth factors could lead to a autologous fibrin microthread that maintains both fibrin and growth factor signaling capabilities in a mechanically strong morphology. Regardless, fibrin microthreads can be readily assembled with growth factors and cytokines in a controlled manner that will ultimately allow for the reverse-engineering of granulation tissue matrix in aligned and oriented mechanically stable grafts.

7.5 Future Work

Future research involving collagen and fibrin microthreads should focus on three vital areas including biomaterial development, cell-matrix interactions, and application diversification. Biomaterial investigations should include further characterization of degradation, development of composite fibrin/collagen thread scaffolds, and *in vivo* implantation studies. Studies of cell-matrix interactions could delve into the comparative integrin signaling mechanisms between collagen and fibrin microthreads. The final area of future study would include investigation of microthread matrices, particularly fibrin, for applications in the regeneration of tissues other than ligament.

7.5.1 Biomaterial Development

Results of this thesis suggest that collagen and fibrin microthreads are promising materials for the regeneration of torn ACL tissue, meriting future consideration and investigation. As previously discussed, some combination of crosslinked collagen threads and growth factor loaded fibrin threads may make for the ideal composite scaffold for ACL regeneration. Future investigations should focus on combinatoric ratios

of collagen and fibrin threads to optimize both strength and cell outgrowth. Furthermore, biomaterial composite modeling techniques may be useful in the prediction of functional outcomes such as tensile strength of composite collagen/fibrin microthread matrices. A significantly useful next step would include implantation studies designed to investigate the short and medium term outcomes of fibrin, fibrin/FGF, and composite fibrin/collagen microthreads for scaffold remodeling and new tissue synthesis.

While collagen thread matrices have been widely investigated (Chapter 2..2.2.1), the novel fibrin microthread matrices developed in this thesis require further characterization. Fibrin thread matrices remain largely intact during seven days of standard culture conditions during testing, but their *in vitro* and *in vivo* degradation characteristics remain largely undetermined. To be a truly viable candidate for tissue regeneration applications, fibrin microthreads must maintain structural stability and degrade at a rate matching new tissue synthesis. Studies investigating the degradation characteristics should look to determine these rates as well as controlling them through crosslinking with factor XIIIa [22, 23], transglutaminases [22], or carbodiimides.

Further fibrin microthread material modifications could include alterations to thread size or incorporation of additional growth factors and function peptides. The diameter of fibrin threads investigated herein is dependent on both the diameter of the extrusion head as well as the magnitude of pre-stretching that occurs during removal from the aqueous buffer and subsequent drying under the weight of gravity. The microthread diameter could theoretically be reduced by mechanical stretching while hydrated. While the current radius of curvature supports fibroblast alignment and orientation, fibrin threads with smaller diameters may allow for more spatial regulation of cytoskeletal components, focal adhesions, and ultimately cell function. Beyond simple mechanical alterations, fibrin had been molecularly modified to incorporate bifunctional bioactive peptides, such as RDG sequences.[25] Furthermore, fibrin materials have been modified for the controlled release of growth factors including BMP-2 [26, 27], β–NGF [28], VEGF [29], and other heparin binding growth factors[30, 31]. In brief, a host of fibrin modifications are available for future investigations to further control cell function for tissue regeneration applications.

7.5.2 Cell-Matrix Interactions

Future work is necessary to acquire a more thorough understanding of the mechanisms involved in regulating cell-matrix interactions on collagen and fibrin thread matrices. The ECM is more than a simple structural material. It acts as a regulator of

cell function through integrin-meditated mechanisms and the localization of cytokines and growth factors.[32] On collagen and fibrin, cells demonstrate matrix dependent expression of integrins [9, 11] and response to growth factors[8, 11]. A more direct comparison between collagen and fibrin threads could elucidate the existence of a similar response, confirming previous findings and translating them to more mechanically stable regeneration template. Furthermore, these results may assist in explaining the insufficient tissue ingrowth and regeneration experienced with collagen thread matrices during *in vivo* implantation studies[33]. Investigating signaling pathways on collagen and fibrin threads, when compared with collagen and fibrin hydrogels, could improve the understanding of how cell morphology and alignment alter signaling in biologically relevant 3-D matrices. Tests directly comparing collagen and fibrin signaling could lay the groundwork for the control of wound regeneration through the temporal direction of cell function by the collagen and fibrin ECM and spatial direction of regeneration dictated by the alignment and orientation of thread matrices.

7.5.3 Alternative Applications

Although initially developed to manufacture robust composite thread matrices with collagen for ligament regeneration, fibrin microthreads have applications well beyond that singular tissue. In cross-hatch or weave patterns, fibrin thread fabrics could be used as patches for dermal regeneration or plastic surgery. The morphology of scar tissue is different from normal skin due to more parallel oriented collagen fiber bundles [34]. Using a cross-hatch pattern could ideally prevent the uni-axial fibroblast alignment that leads to parallel oriented collagen bundle formation prevalent during dermal scar tissue formation.

Fibrin biomaterials have also shown promise as supporting scaffolds for nerve regeneration.[35] Autologous fibrin glue has been shown to increase axonal regeneration in a rabbit peroneal nerve defect.[36] The authors of this research suggest that this response may be the combined result of the fibrinogen network as well as growth factors present in or trapped by the glue.[36] Heparin binding peptides have been incorporated into fibrin gels to enhance neurite extension for nerve tissue engineering.[30] These designer matrices can be used to control the release of growth factors such as nerve growth factor[28], neurotrophin-3[37], and other heparin binding growth factors[31]. Furthermore, neurite alignment can be controlled with oriented fibrin fibril alignment[38]. These results suggest that fibrin biopolymer threads could similarly control neurite extension, especially given the morphological homology to bundles of nerve ganglia. Future fibrin microthreads research could investigate incorporating neural

growth factors and controlling neurite extension for the repair of peripheral and spinal nerve injuries.

While fibrin hydrogel matrices have been suggested for cardiovascular tissue engineering applications[39, 40], the authors themselves have suggested that the low stiffness and stability of fibrin hyrdogels are a significant limitation of their use. Fibrin microthreads alone or in combination with additional cell seeded fibrin hydrogels could alleviate the initial stability issues, while simultaneously promoting aligned collagen deposition and matrix regeneration. Furthermore, Jockenhoevel et al. suggest that scaffold contraction in fibrin hydrogel matrices makes the formation of tissue engineered hydrogel constructs difficult, while preventing this contraction by border fixation promotes collagen production [39]. This phenomenon is similar to the effects seen in fixed and floating collagen gels, where fibroblasts in unconstrained collagen gels are quiescent and apoptotic, while fibroblasts in constrained gels are activated, proliferative, and collagen producing.[41] Fibroblasts did not significantly contract fibrin microthread matrices during initial one weeks seeding experiments and could therefore reduce gel contraction issues by allowing a semi-rigid structure for attachment and proliferation of myofibroblasts for cardiac applications. In an interesting twist on cardiovascular applications, fibrin microthreads wrapped sequentially around a mandrel could be cultured in layers with cells in the development of bioengineered blood vessels, expanding on the use of fibrin gels for tissue engineered small diameter blood vessels[42, 43]. Due to their robust mechanical properties, fibrin threads can be manipulated to develop structurally stable 3-D environments for the control of oriented aligned tissue engineering scaffolds in a natural biochemical environment that simulates the native wound provisional matrix.

7.6 CONCLUSIONS

The primary goal of this thesis was to develop and investigate biopolymer microthread technologies for repair of injured anterior cruciate ligaments. An *in vitro* method of characterizing tissue ingrowth on collagen thread scaffolds was designed and successfully used to probe cell function on polymer and biopolymer thread matrices. The results of these studies demonstrated an increased ingrowth on biopolymer threads over synthetic polymers, but an attenuation in fibroblast ingrowth when collagen biopolymer threads were crosslinked. Since crosslinking of self-assembled collagen threads is necessary *in vivo* to increase strength and decrease the otherwise rapid degradation rate, an alternative biopolymer thread technology based on fibrin was developed. These fibrin

biopolymer microthreads have drastically increased mechanical strength properties over fibrin hydrogels, possess the ability of fiber matrices to organize and align cells, and can readily incorporate matrix bound growth factors for increased migration and proliferation. The ultimate goal of these novel fibrin biopolymer microthreads is to improve the wound healing cell-signaling capability of acellular thread matrices to increase tissue ingrowth, scaffold remodeling, and tissue synthesis.

A secondary, but equally important, conclusion of this thesis is the underlying importance that surface-protein interactions play in dictating outcome of cell-fate process and cell function on thread matrices. This reoccurring theme was part of both the rationale and outcomes of this biomaterials research, from justifying the use of biopolymer matrices to helping explain the variations in cell outgrowth seen with crosslinking. Collagen was initially chosen for threads because of the structural and biochemical homology of the protein to native tissues. Cells adhere and respond differently to the naturally derived protein than to foreign materials like plastics. We hypothesize that crosslinking alters the ability of serum proteins to adsorb to the surface of collagen threads, and subsequently reduces the ability of cells to attach and migrate on the surface. Fibrin was selected as a protein for thread assembly because of its favorable protein interactions, including its ability to act as a sponge for growth factors and cytokines as well as it's differential, integrin-mediated signaling capabilities. The high binding affinity and the possible role in matrix co-localization made FGF-2 and fibrin a prosperous combination. The results of the studies in this thesis strongly suggest that cell-protein-biomaterial interactions play a crucial part in the future of bioengineered materials for ligament regeneration and should not be overlooked.

In conclusion, collagen and fibrin biopolymer microthreads are promising acellular materials for the regeneration of torn anterior cruciate ligaments. Future *in vitro* and *in vivo* studies should continue to investigate the material properties of composite fibrin and crosslinked collagen scaffolds, while further characterizing the degradation of fibrin thread scaffolds as well as the differential integrin-mediated signaling capabilities of collagen and fibrin microthreads that direct cell-based ligament regeneration.

REFERENCES

[1] Guidoin MF, Marois Y, Bejui J, Poddevin N, King MW & Guidoin R. Analysis of retrieved polymer fiber based replacements for the acl. *Biomaterials* **21**: pp. 2461-2474. (2000).
[2] Laurencin CT & Freeman JW. Ligament tissue engineering: an evolutionary materials science approach. *Biomaterials* **26**: pp. 7530-7536. (2005).

[3] Lu HH, Cooper JAJ, Manuel S, Freeman JW, Attawia MA, Ko FK & Laurencin CT. Anterior cruciate ligament regeneration using braided biodegradable scaffolds: in vitro optimization studies. *Biomaterials* **26**: pp. 4805-4816. (2005).
[4] Altman GH, Horan RL, Lu HH, Moreau J, Martin I, Richmond JC & Kaplan DL. Silk matrix for tissue engineered anterior cruciate ligaments. *Biomaterials* **23**: pp. 4131-4141. (2002).
[5] Altman GH, Diaz F, Jakuba C, Calabro T, Horan RL, Chen J, Lu H, et al.. Silk-based biomaterials. *Biomaterials* **24**: pp. 401-416. (2003).
[6] Majima T, Funakosi T, Iwasaki N, Yamane S, Harada K, Nonaka S, Minami A, et al.. Alginate and chitosan polyion complex hybrid fibers for scaffolds in ligament and tendon tissue engineering. *J Orthop Sci* **10**: pp. 302-307. (2005).
[7] Funakoshi T, Majima T, Iwasaki N, Yamane S, Masuko T, Minami A, Harada K, et al.. Novel chitosan-based hyaluronan hybrid polymer fibers as a scaffold in ligament tissue engineering. *J Biomed Mater Res A* **74**: pp. 338-346. (2005).
[8] Clark RA, Nielsen LD, Welch MP & McPherson JM. Collagen matrices attenuate the collagen-synthetic response of cultured fibroblasts to tgf-beta. *J Cell Sci* **108 (Pt 3)**: pp. 1251-1261. (1995).
[9] Feng X, Clark RA, Galanakis D & Tonnesen MG. Fibrin and collagen differentially regulate human dermal microvascular endothelial cell integrins: stabilization of alphav/beta3 mrna by fibrin1. *J Invest Dermatol* **113**: pp. 913-919. (1999).
[10] Greiling D & Clark RA. Fibronectin provides a conduit for fibroblast transmigration from collagenous stroma into fibrin clot provisional matrix. *J Cell Sci* **110 (Pt 7)**: pp. 861-870. (1997).
[11] Xu J & Clark RA. Extracellular matrix alters pdgf regulation of fibroblast integrins. *J Cell Biol* **132**: pp. 239-249. (1996).
[12] Woo SL, Niyibizi C, Matyas J, Kavalkovich K, Weaver-Green C & Fox RJ. Medial collateral knee ligament healing. combined medial collateral and anterior cruciate ligament injuries studied in rabbits. *Acta Orthop Scand* **68**: pp. 142-148. (1997).
[13] Geiger MH, Green MH, Monosov A, Akeson WH & Amiel D. An in vitro assay of anterior cruciate ligament (acl) and medial collateral ligament (mcl) cell migration. *Connect Tissue Res* **30**: pp. 215-224. (1994).
[14] Nagineni CN, Amiel D, Green MH, Berchuck M & Akeson WH. Characterization of the intrinsic properties of the anterior cruciate and medial collateral ligament cells: an in vitro cell culture study. *J Orthop Res* **10**: pp. 465-475. (1992).
[15] Lyon RM, Akeson WH, Amiel D, Kitabayashi LR & Woo SL. Ultrastructural differences between the cells of the medical collateral and the anterior cruciate ligaments. *Clin Orthop Relat Res* : pp. 279-286. (1991).
[16] Wiig ME, Amiel D, Ivarsson M, Nagineni CN, Wallace CD & Arfors KE. Type i procollagen gene expression in normal and early healing of the medial collateral and anterior cruciate ligaments in rabbits: an in situ hybridization study. *J Orthop Res* **9**: pp. 374-382. (1991).
[17] Molloy T, Wang Y & Murrell G. The roles of growth factors in tendon and ligament healing. *Sports Med* **33**: pp. 381-394. (2003).
[18] Canty EG, Starborg T, Lu Y, Humphries SM, Holmes DF, Meadows RS, Huffman A, et al.. Actin filaments are required for fibripositor-mediated collagen fibril alignment in tendon.. *J Biol Chem* **281**: pp. 38592-38598. (2006).
[19] Chen R, Ho H & Sheu M. Characterization of collagen matrices crosslinked using microbial transglutaminase.. *Biomaterials* **26**: pp. 4229-4235. (2005).
[20] McDermott MK, Chen T, Williams CM, Markley KM & Payne GF. Mechanical properties of biomimetic tissue adhesive based on the microbial transglutaminase-catalyzed crosslinking of gelatin.. *Biomacromolecules* **5**: pp. 1270-1279. (2004).
[21] Sun Y, Giraudier O & Garde VL. Rheological characterization and dissolution kinetics of fibrin gels crosslinked by a microbial transglutaminase.. *Biopolymers* **77**: pp. 257-263. (2005).
[22] Greenberg CS, Birckbichler PJ & Rice RH. Transglutaminases: multifunctional cross-linking enzymes that stabilize tissues.. *FASEB J* **5**: pp. 3071-3077. (1991).

[23] Lorand L. Factor xiii: structure, activation, and interactions with fibrinogen and fibrin.. *Ann N Y Acad Sci* **936**: pp. 291-311. (2001).
[24] Cornwell K & Pins G. Discrete crosslinked fibrin microthread scaffolds for tissue regeneration. *J Biomed Mater Res A* **accessible online**: . (2007).
[25] Schense JC & Hubbell JA. Cross-linking exogenous bifunctional peptides into fibrin gels with factor xiiia.. *Bioconjug Chem* **10**: pp. 75-81. (1999).
[26] Schmoekel HG, Weber FE, Hurter K, Schense JC, Seiler G, Ryrz U, Spreng D, et al.. Enhancement of bone healing using non-glycosylated rhbmp-2 released from a fibrin matrix in dogs and cats.. *J Small Anim Pract* **46**: pp. 17-21. (2005).
[27] Schmoekel HG, Weber FE, Schense JC, Grätz KW, Schawalder P & Hubbell JA. Bone repair with a form of bmp-2 engineered for incorporation into fibrin cell ingrowth matrices.. *Biotechnol Bioeng* **89**: pp. 253-262. (2005).
[28] Sakiyama-Elbert SE & Hubbell JA. Controlled release of nerve growth factor from a heparin-containing fibrin-based cell ingrowth matrix.. *J Control Release* **69**: pp. 149-158. (2000).
[29] Zisch AH, Schenk U, Schense JC, Sakiyama-Elbert SE & Hubbell JA. Covalently conjugated vegf--fibrin matrices for endothelialization.. *J Control Release* **72**: pp. 101-113. (2001).
[30] Sakiyama SE, Schense JC & Hubbell JA. Incorporation of heparin-binding peptides into fibrin gels enhances neurite extension: an example of designer matrices in tissue engineering.. *FASEB J* **13**: pp. 2214-2224. (1999).
[31] Sakiyama-Elbert SE & Hubbell JA. Development of fibrin derivatives for controlled release of heparin-binding growth factors.. *J Control Release* **65**: pp. 389-402. (2000).
[32] Nathan C & Sporn M. Cytokines in context.. *J Cell Biol* **113**: pp. 981-986. (1991).
[33] Dunn MG, Liesch JB, Tiku ML & Zawadsky JP. Development of fibroblast-seeded ligament analogs for acl reconstruction. *J Biomed Mater Res* **29**: pp. 1363-1371. (1995).
[34] van Zuijlen PPM, Ruurda JJB, van Veen HA, van Marle J, van Trier AJM, Groenevelt F, Kreis RW, et al.. Collagen morphology in human skin and scar tissue: no adaptations in response to mechanical loading at joints.. *Burns* **29**: pp. 423-431. (2003).
[35] Novikova LN, Novikov LN & Kellerth J. Biopolymers and biodegradable smart implants for tissue regeneration after spinal cord injury.. *Curr Opin Neurol* **16**: pp. 711-715. (2003).
[36] Choi B, Han S, Kim S, Zhu S, Huh J, Jung J, Lee S, et al.. Autologous fibrin glue in peripheral nerve regeneration in vivo.. *Microsurgery* **25**: pp. 495-499. (2005).
[37] Taylor SJ, McDonald JW3 & Sakiyama-Elbert SE. Controlled release of neurotrophin-3 from fibrin gels for spinal cord injury.. *J Control Release* **98**: pp. 281-294. (2004).
[38] Dubey N, Letourneau PC & Tranquillo RT. Neuronal contact guidance in magnetically aligned fibrin gels: effect of variation in gel mechano-structural properties.. *Biomaterials* **22**: pp. 1065-1075. (2001).
[39] Jockenhoevel S, Zund G, Hoerstrup SP, Chalabi K, Sachweh JS, Demircan L, Messmer BJ, et al.. Fibrin gel -- advantages of a new scaffold in cardiovascular tissue engineering. *Eur J Cardiothorac Surg* **19**: pp. 424-430. (2001).
[40] Ye Q, Zund G, Jockenhoevel S, Hoerstrup SP, Schoeberlein A, Grunenfelder J & Turina M. Tissue engineering in cardiovascular surgery: new approach to develop completely human autologous tissue. *Eur J Cardiothorac Surg* **17**: pp. 449-454. (2000).
[41] Grinnell F. Fibroblast biology in three-dimensional collagen matrices. *Trends Cell Biol* **13**: pp. 264-269. (2003).
[42] Swartz DD, Russell JA & Andreadis ST. Engineering of fibrin-based functional and implantable small-diameter blood vessels. *Am J Physiol Heart Circ Physiol* **288**: p. H1451-60. (2005).
[43] Yao L, Swartz DD, Gugino SF, Russell JA & Andreadis ST. Fibrin-based tissue-engineered blood vessels: differential effects of biomaterial and culture parameters on mechanical strength and vascular reactivity. *Tissue Eng* **11**: pp. 991-1003. (2005).

Appendix A: Automated Extrusion Device

Introduction

To improve the consistency and repeatability, an automated 2-axis thread extrusion device was constructed for the assembly of biopolymer thread matrices. Design of this device was undertaken and advised in conjunction with the 4 undergraduate students as part of the fulfillment of their Major Qualify Project, entitled "Designing an Extrusion System to Optimize the Production of Self-Assembled Collagen Microthreads", by William Bishop, Diana Camire, Ngoc Chau Duong, Jason Robinson.[1] This project received the 2005 Provost's MQP Award in the WPI Department of Biomedical Engineering.

Threads extruded from solutions of type I collagen have been widely investigated as biomaterials for the regeneration of soft connective tissue, particularly tendons and ligaments (Chapter 2.1.1.1). The extrusion process as described requires the pumping of collagen solutions through small diameter tubing and into a fiber formation buffer, using methods modified largely from Pins et al.[2][3][4] As the pumped solution flows out of the tubing, the tubing end is carefully manually drawn slowly through the bath at a rate approximately matching the flow rate of solution exiting the tubing. This hand-drawn procedure was not only laborious, but generally inconsistent with poor repeatability. *Hence, the goal of the project was to develop an thread extrusion device with automated features to more accurately control the positional coordination of the tubing exit orifice, thereby increasing thread consistency while reducing batch-to-batch variation.*

Device

The final device design consisted of two motor/controller integrated stepper motors, each controlling 1-axis of motion. The stepper motors (LIN Engineering, Santa Clara, CA) had integrated motor controller and driver allowing for full programming through serial port attachments to a computer with the addition of RS485-R232 converters. These motors turn pulley/belts systems that translocate suspended carriages in a vehicle system (Figure A1). The suspended carriage contains a tubing attachment rod for local guidance of the tubing at the extrusion tip and off-axis tilt of the carriage is limited by the use of two stabilizing stainless steel track-rods in each axis. The vehicle system is inverted and placed on stainless steel legs, elevated above the temperature controlled extrusion bath. Tubing, extending from the end of a syringe in a syringe pump is threaded through the top of the vehicle system, attached to the tubing attachment rod, and guided through the bath solution. Motion of the motors was controlled using a Labview (National Instruments, Austin, TX) program described below.

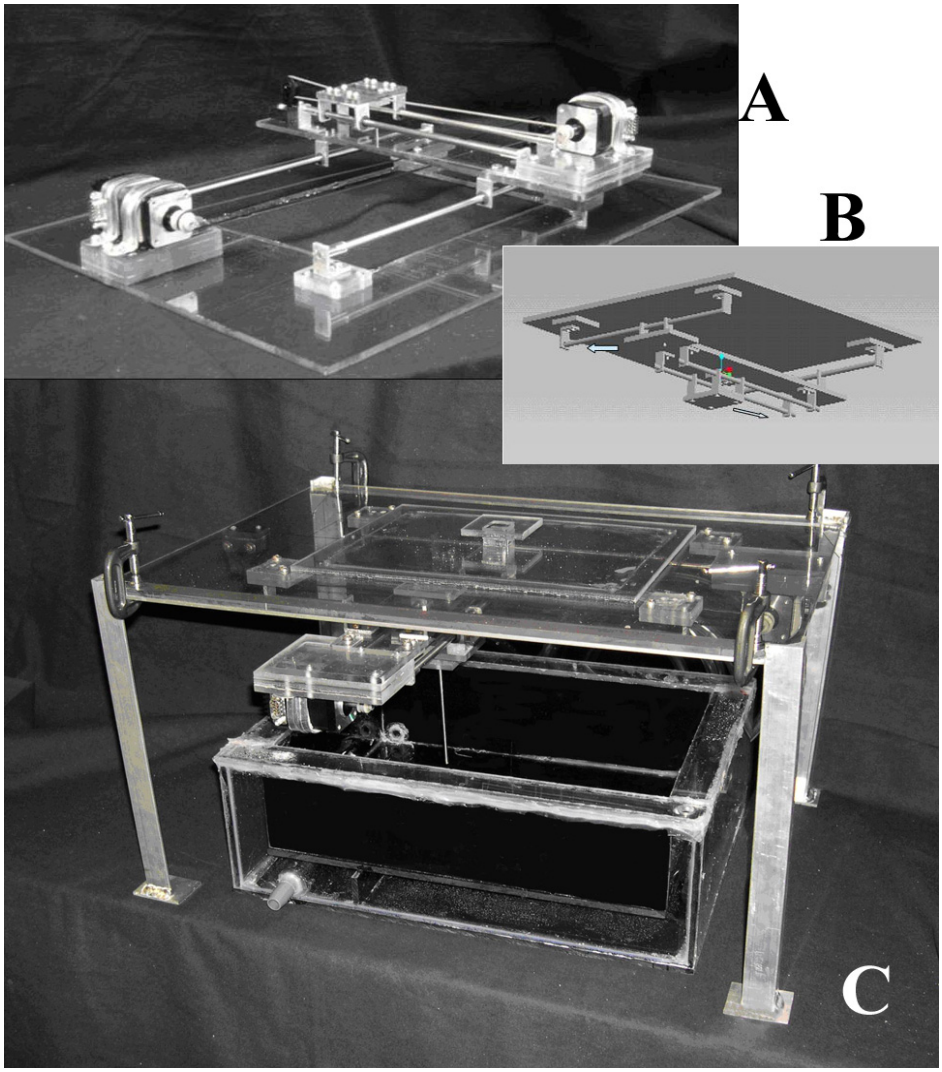

Figure A1: Image of inverted carriage vehicle system (A) and CAD drawing of the same in operational orientation (B). Image of full setup automated extrusion device including carriage vehicle system elevated on stainless steel supports and a temperature controlled water bath (C). (Device has a 3′ by 2′ footprint)

Testing and Results

Diameter and tensile tests were performed to analyze and compare the fibers produced automatically with the manually extruded fibers. The results showed that the fibers produce with the automated extrusion device exhibit more uniform structural and mechanical properties than those produced manually. The average value for the unhydrated fiber diameter was 70 µm with a standard deviation of only 0.5 µm. Fibers produced using the manual extrusion method were 53 ± 7.6 um. Fibers extruded using the automated device clearly demonstrate smaller variation compared to those fibers extruded via the currently system (Figure A2). The tensile strength for the automated and

manually extruded fibers were 0.7 ± 0.05 and 1.5 ±0.2 MPa respectively. Hydrated fiber diameters were 350 ± 6.8 and 140 ±19 microns, and strain at failure were 0.80 ± 8 and 0.42 ± .12 for automated extrusion and manually extruded threads respectively. Further results can be seen in table A1 below.

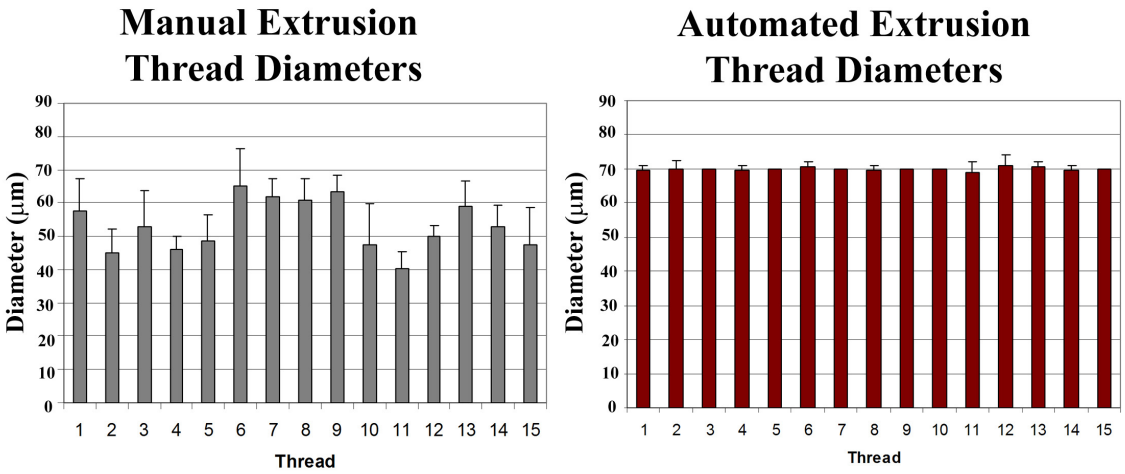

Figure A2: Increased consistency with automated extrusion. Diameter measurements in microns along the length of threads either manually drawn (left) or autoextruded (right). Variation both along the length of threads as well as between threads is minimal with autoextrusion.

Parameters	Automated Extrusion System	Manual Extrusion System
Fiber Production/Min	10	1
Fiber Production/Bath	30	20
Dry Fiber Diameter (μm)	70 ± 0.05	53 ± 7.6
Hydrated Fiber Diameter (μm)	350 ± 6.8	140 ± 19
Maximum Load (mN)	0.07 ± 0.01	0.04 ± 0.01
Ultimate Tensile Strength (MPa)	0.7 ± 0.05	1.5 ± 0.2
Strain	0.80 ± 0.8	0.42 ± 0.12

Table A1. Side-by-side comparison of automated and manual extrusion

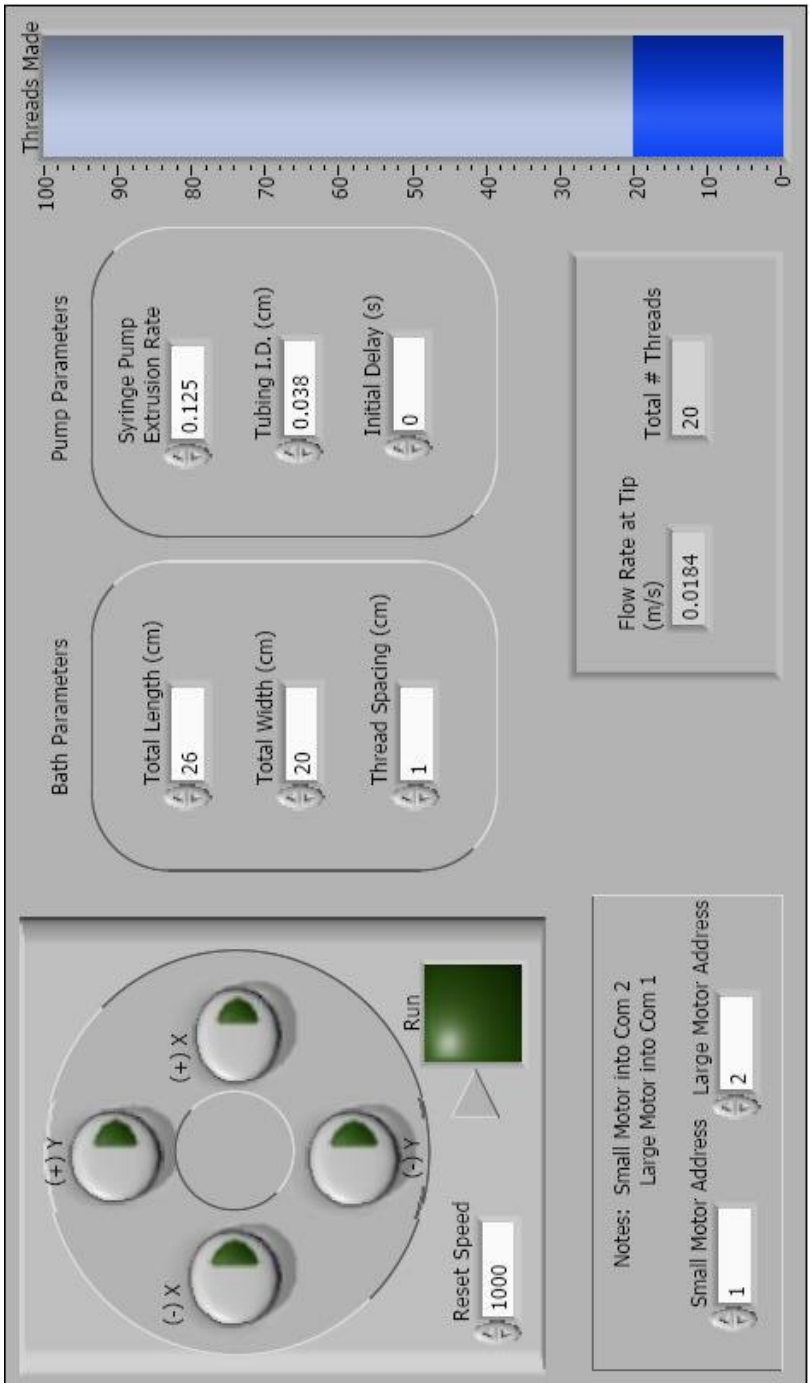

Figure A3. Graphical user interface of the 2-axis automated thread extrusion device displayed rotated 90 degrees.

Labview Interface

Labview was used control the motors for the 2-axis automated thread extrusion device (Figure A4, A5). The program was designed in two parts. The first allows the user to manually manipulate the extrusion tip through the bath in the x-direction and y-direction using the large buttons on the raised upper left panel (Figure A3). The portions not on the raised panel let the user set the specification for the automated extrusion process (Figure A3). These settings include bath parameters, that dictate the size of the extrusion path and distance between threads, as well as the syringe pump parameters. The syringe pump parameters should ideally match those input on the syringe pump, and are used in the calculation of volumetric flow rates to extrude at a rate twice the speed of the extrusion head through the bath. These settings are preset based on optimized results of fibrin thread extrusion discussed in Chapter 5. Once the user clicks the large green, 'Run' icon, the program will actuate the motors to translocate the extrusion tip in straight line patterns, the full length of the bath input parameters, with line spacing as specified in the input parameters. As the program runs, the current flow rate at the tip is displayed while the number of threads produced is sequentially incremented and displayed.

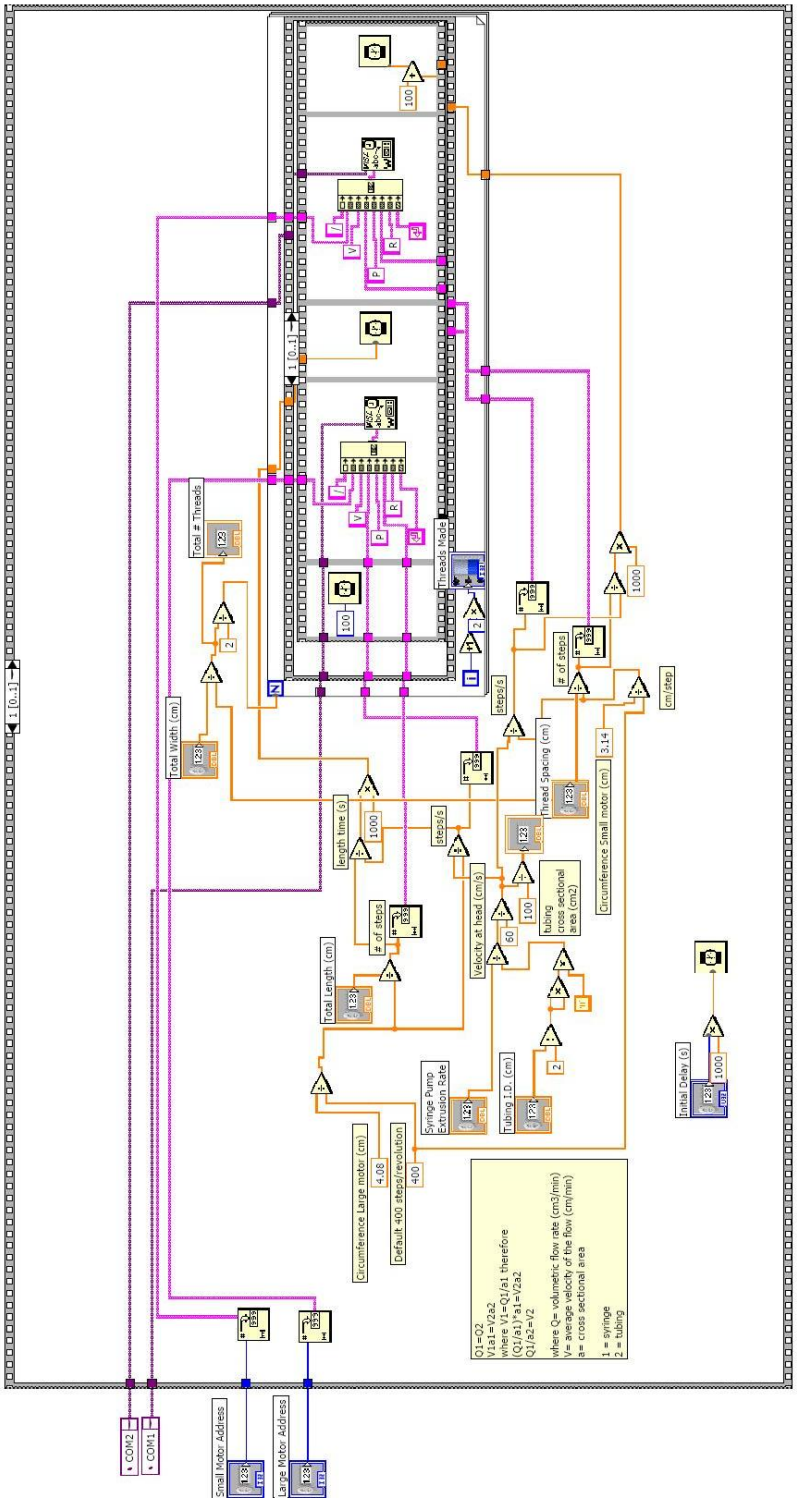

Figure A4. Block diagram of the Labview code for the automated extrusion device (sequential 0) displayed rotated 90 degrees.

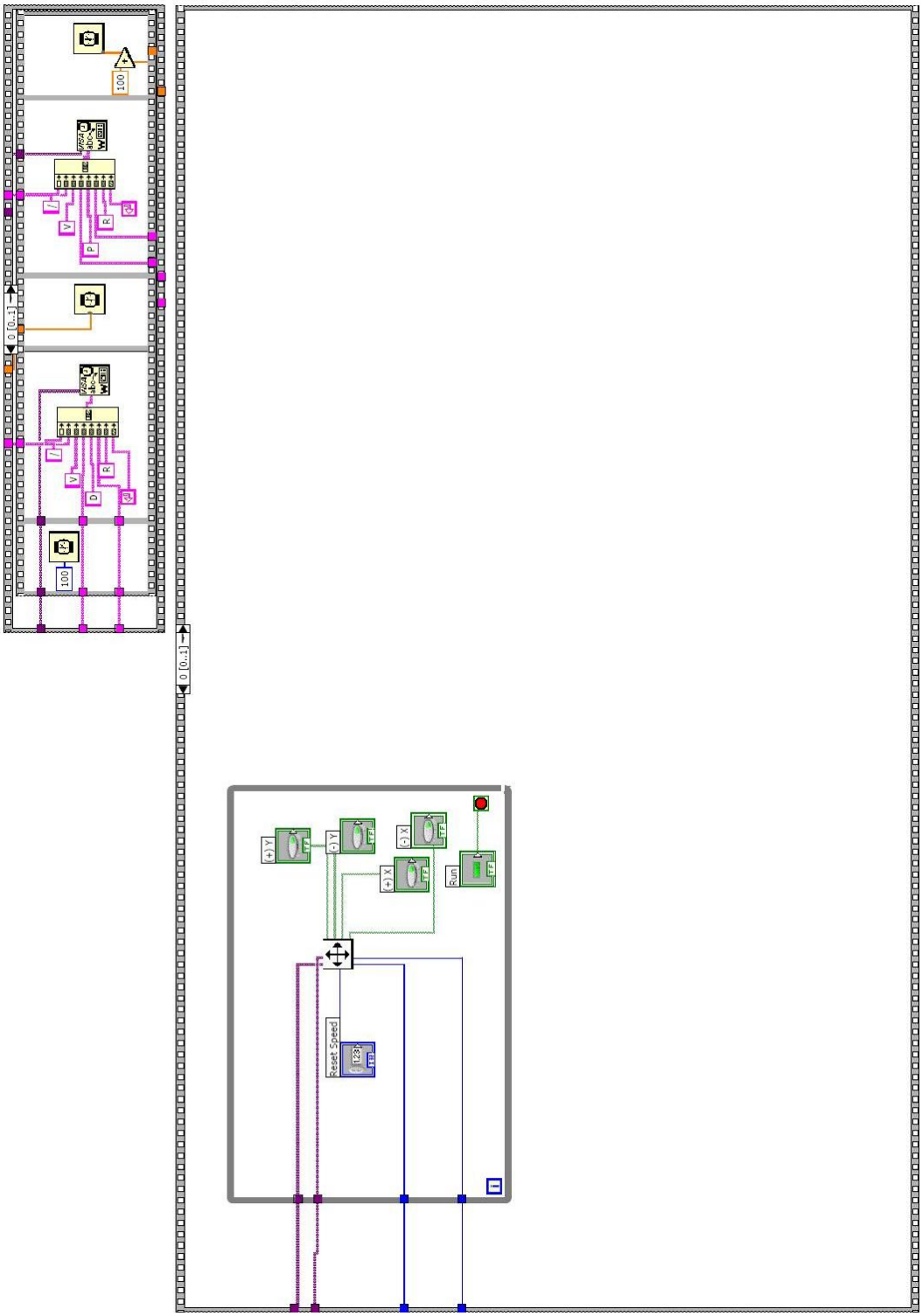

Figure A5. Block diagram of the Labview code for the automated extrusion device (sequential 1) displayed rotated 90 degrees (hidden from view behind sequential 1 in figure A4)

Ultimately, the automated 2-axis thread extrusion device developed increases the consistency and drastically reduces the batch-to-batch variation in production of collagen threads. Furthermore, this device was successfully adapted to control the extrusion process of fibrin biopolymer microthreads discussed in Chapters 5 and 6.

References

[1] Bishop W, Camire D, Duong ND & Robinson JR. Design of an extrusion system to optimize the production of self-assembled collagen microthreads. MQP. Worcester Polytechnic Institute (GXP-0508). 2005-6.

[2] Pins G & Silver F. A self-assembled collagen scaffold suitable for use in soft and hard tissue replacement. *Materials Science and Engineering:C* **3**: pp. 101-107. (1995).

[3] Pins GD, Christiansen DL, Patel R & Silver FH. Self-assembly of collagen fibers. influence of fibrillar alignment and decorin on mechanical properties. *Biophys J* **73**: pp. 2164-2172. (1997).

[4] George D. Pins, Eric K. Huang, David L. Christiansen, Frederick H. Silver. Effects of static axial strain on the tensile properties and failure mechanisms of self-assembled collagen fibers. *J Appl Polym Sci* **63**: pp. 1429-1440. (1997).

Appendix B: Micromechanical Testing Device

Introduction

In order to analyze the mechanical properties of collagen and fibrin biopolymer microthreads, a micromechanical testing device was manufactured in house for a small fraction of the estimated $75,000 cost of a professional mechanical testing apparatus. The device is designed for controlled uni-axial tensile testing of small diameter, limited strength polymers.

Device

The micromechanical tester consists of a loading frame, force transducer, and linear actuator (Figure B1). The linear actuator is a syringe pump (KDScientific, Holliston, MA), which acts as simple bar on a threaded rod to pull the sample at a controlled speed. The loading frame includes two, custom-machined, stainless-steel platforms which are secured separately to the crosshead and the force transducer. The force transducer (kindly lent by Peter Grigg, Ph.D. at the University of Massachusetts Medical School)

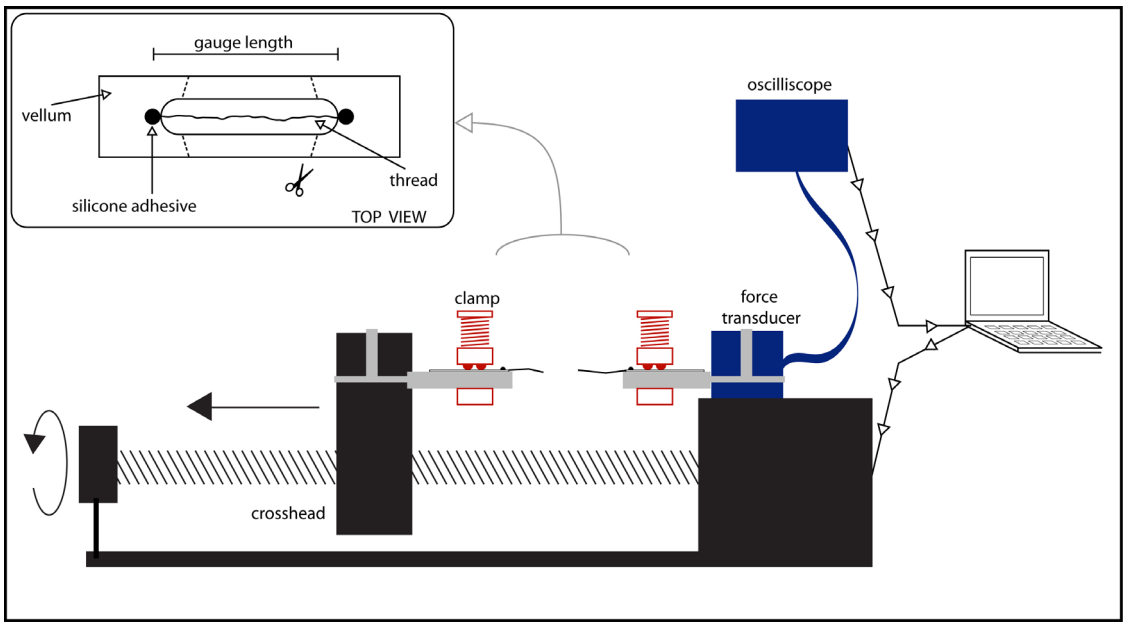

Figure B1. Schematic of the micromechanical tester. Samples are adhered to vellum frames which define the initial gauge length (upper left inset). Samples are then clamped in place, the edges of the frame cut leaving only the thread, and pulled to failure at a constant strain rate. A Labview program on a computer controls the linear actuation and the resulting voltages from the load cell are transmitted to the computer. Although images are schematic and not to scale, the gauge length is 2cm.

reports a voltage linearly with force in the 0-150 gram loading range and is securely attached to a fixed portion of the syringe pump. Both the linear actuator (syringe pump) and the force transducer (via an oscilloscope, Tektronix, Model TDS2000, Beaverton, OR) are controlled with Labview software (NI, Austin, TX).

Testing Procedure

Individual thread samples are adhered to vellum frames, precut with windows to the defined gauge length (Figure B1 inset). Samples are then hydrated for 30 minutes in phosphate buffered saline. After reaching swelling equilibrium, the diameters of each thread are measured in three locations along the length of the thread using a calibrated reticle in the eyepiece of a microscope. These diameters are later used for the calculation of initial cross-sectional area, need for the determination of tensile strength. Once the diameter measurements are complete, vellum test frames are then clamped into the tester on horizontal platforms, and the edges of the test frame are cut to leaving only the thread remaining between the actuator and the load cell (Figure B1 inset). Finally, using the associated Labview program, the sample is pulled to failure at a constant (50%) strain rate.

Labview Interface

The graphical user interface (GUI) for this program is shown below (Figure B2). The program is started and stopped with the ON/OFF button in the upper left corner (lit green when running). There is only one main input for the program allowing the user to set the strain rate in mm/min. Other settings including channel and port selection are available to match hardware settings on the oscilloscope and computer. The test/reset toggle switch changes between testing mode and return to origin mode. In test mode, pressing the green go button runs a test at the desired strain rate until the sample breaks. Clicking stop then brings up a prompt to save the data to the computer hard drive. In reset mode, pressing go will return the actuator to its original position to begin an new test. During test mode, the interface displays the current load in grams.

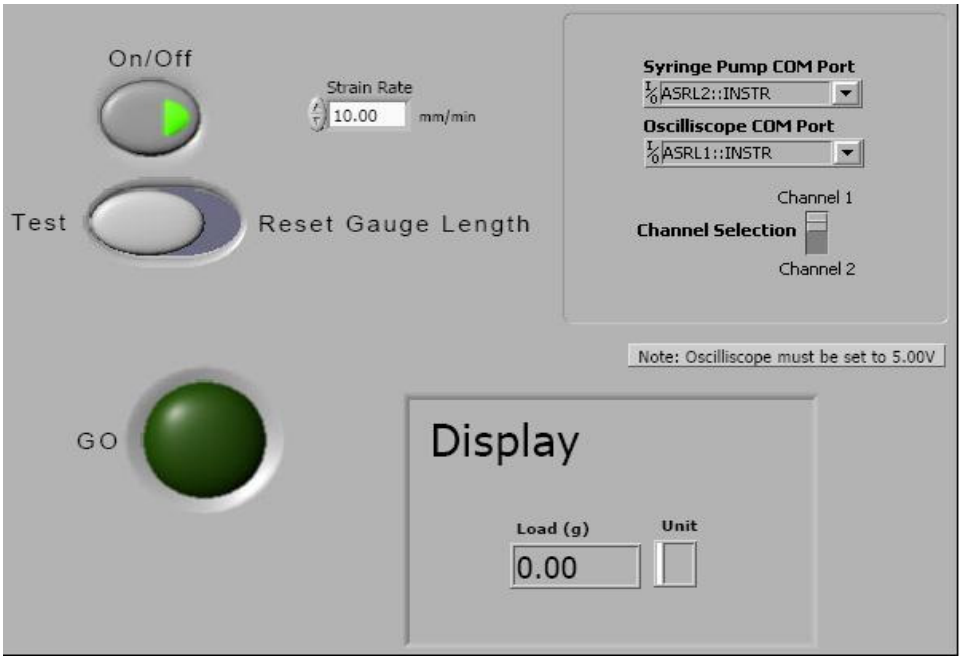

Figure B2. Labview graphical user interface of the micromechanical testing apparatus.

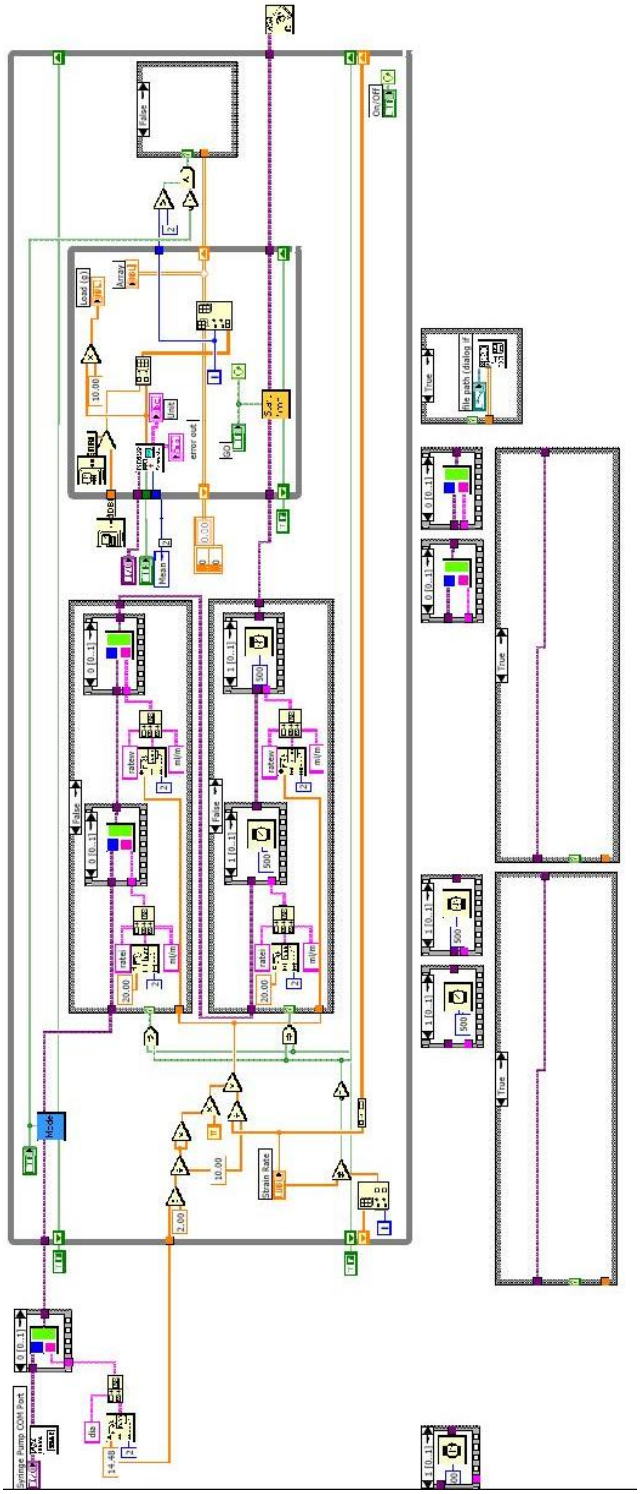

Figure B3. Block diagram of the Labview code for the micromechanical tester displayed rotated 90 degrees.

List of SubVIs and Express VIs with Configuration Information

mode.vi
Custom VI - controls alternating of crosshead direction (infusion/withdrawal)

write.vi
Custom VI - controls sending of text commands to crosshead (syringe pump)

TKTDS2XX Example1.vi
Oscilliscope Manufacturer's VI (Tektronix, Model TDS) used to receive transducer input

Write To Spreadsheet File.vi
C:\Program Files\National Instruments\LabVIEW 7.1\vi.lib\Utility\file.llb\Write To Spreadsheet File.vi

startstop.vi
Custom VI - controls the starting and stopping of syringe pump motion

VISA Configure Serial Port
C:\Program Files\National Instruments\LabVIEW 7.1\vi.lib\Instr_visa.llb\VISA Configure Serial Port

VISA Configure Serial Port (Instr).vi
C:\Program Files\National Instruments\LabVIEW 7.1\vi.lib\Instr_visa.llb\VISA Configure Serial Port (Instr).vi

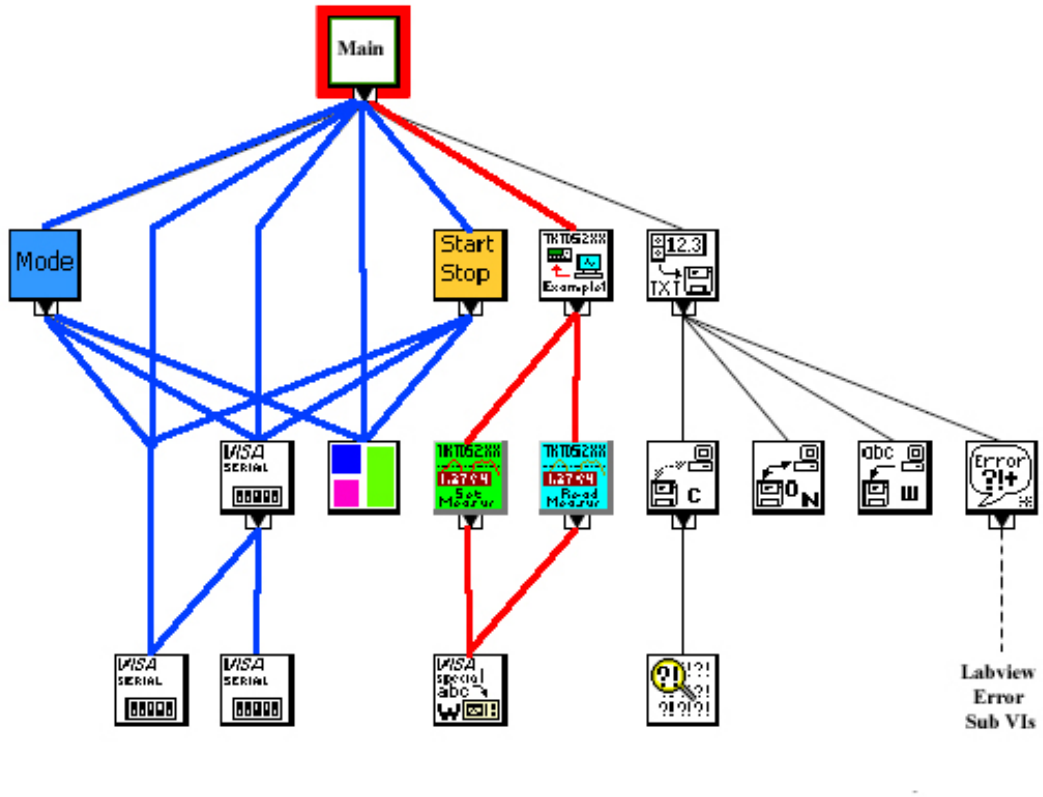

Figure B4. List of labview sub VIs called in the micromechanical testing software including custom VIs, Labview VIs, and device manufacturers VIs (top). Heirarchy of the sub VIs necessary for program function including custom (blue) and manufacturers (red) Vis (bottom).